



HAL
open science

Nanosensors for sustainable cities - From fundamentals to deployments

Bérengère Lebental

► **To cite this version:**

Bérengère Lebental. Nanosensors for sustainable cities - From fundamentals to deployments. Micro and nanotechnologies/Microelectronics. Université Paris-Saclay/Université Paris-Sud, 2016. tel-01798285

HAL Id: tel-01798285

<https://hal.science/tel-01798285v1>

Submitted on 23 May 2018

HAL is a multi-disciplinary open access archive for the deposit and dissemination of scientific research documents, whether they are published or not. The documents may come from teaching and research institutions in France or abroad, or from public or private research centers.

L'archive ouverte pluridisciplinaire **HAL**, est destinée au dépôt et à la diffusion de documents scientifiques de niveau recherche, publiés ou non, émanant des établissements d'enseignement et de recherche français ou étrangers, des laboratoires publics ou privés.

UNIVERSITE PARIS SUD
UFR SCIENCES

HABILITATION À DIRIGER DES RECHERCHES

DOSSIER PRESENTE PAR **BERENGERE LEBENTAL**

Nanosensors for sustainable cities

From fundamentals to deployments

Soutenu le 19 Octobre 2016, devant le jury compose de

BAILLARGEAT Dominique	HDR, Professeur, XLIM, Directeur	Rapporteur
GABRIEL Jean -Christophe	HDR, CEA, Programme Nanosciences, Directeur Adjoint	Rapporteur
HAPPY Henri	HDR, Professeur, IEMN, Equipe Carbone, Directeur	Rapporteur
BONDAVALLI Paolo	HDR, Thales Research & Technology, Responsable Transverse Nanomatériaux	Examineur
DOLLFUS Philippe	HDR, DR, C2N, Equipe Nanoélectronique Computationnelle, Directeur	Examineur
LEFEUVRE Elie	HDR, Professeur, C2N, Laboratoire MINASYS	Examineur
OLARD François	HDR, Eiffage Infrastructure, Directeur Recherche & Innovation	Examineur

Abstract

In the current context of environmental urgency amplified by climate changes, optimizing the workings of urban ecosystems in terms of resource preservation and quality of life is on the critical path toward a sustainable future. To achieve this, the massive monitoring of urban spaces via the so-called “internet of sensors” is proving its worth, guiding decision-making at every level, from global policies to individual actions. However, progresses are slowed by determining hardware, software and usage bottlenecks, such as power autonomy, network resilience or protection of privacy.

Nanotechnologies have long been proposed as key-enabling technologies to overcome the hardware bottlenecks of the Internet of Sensors, notably for improved sensing capabilities at lower cost and lower energy consumption. But concrete examples of real-life applications are few and far in between. This work investigates two of the main hurdles for actual deployments of nanosensors, namely reproducibility and reliability.

It reports notably on the development of a repertoire of nanocarbon-based sensors for strain, humidity and chemical sensing. In view of achieving real-life applications, a strong focus is placed on the topic of reproducibility as the key to both mechanisms understanding and subsequent electronic integration. Highly reproducible carbon nanotubes strain sensors were successfully deployed in the field for durability monitoring in concrete materials.

The concept of nanoreliability is also introduced as a mean to predict and optimize lifetime of nanodevices in their actual conditions of use with the development of nanodevice-compatible modelling and characterization tools. Namely, an experimental platform for multiphysic loadings under in-situ characterizations is now available to determine fatigue behavior of nanodevices and identify at the microscale weak spots that foster ageing. High resolution characterization tools complemented with data processing tools are used to further understand the nanoscale mechanisms of operation and of ageing. The outputs of both approaches are gathered to build accurate device models, which will be later use to predict lifetime.

Overall, the reported results strongly support the worth of nanosensors for urban applications. The industrial transfer of nanocarbon-based sensors is now at a one-to-three year horizon. Nanosensors will actually get disseminated into the civil society in the near future, contributing to a more sustainable approach to urbanization.

As a direct consequence, the scientific community needs to ensure that the benefits of nanosensors in terms of sustainability are not overcome by the health and environmental risks nanoparticles may present. Toward this goal, the development and application of a methodological framework for nanosensor life cycle analysis is proposed.

Content

Abstract	2
Acknowledgments	6
Part 1 - Curriculum	8
1. Curriculum vitae	8
Current position	8
Previous positions	8
Diploma	8
2. Research activities	9
Summary	9
Collaborative projects	9
International collaborations	10
Expertise actions	10
Administrative functions	11
3. Teaching and student supervision	12
Summary	12
Teaching activities	12
PhDs	12
Post-docs	13
Engineers and apprentice	13
Part 2 – Body of work	14
1. Introduction	14
1.1. Solving urban challenges requires intensive urban evaluation	14
1.2. The “internet of sensors”, the next stage for urban assessment	21
1.3. Nanosensors: a key-enabling technology for urban monitoring	32
1.4. Outline of the manuscript	34
2. Nanocarbon-based sensors: from design to deployment	36
2.1. Nanocarbon-based sensors: state of the art	36
2.2. A repertoire of carbon nanotubes and graphene sensors	39
2.3. The state of the art in reproducibility for sensors based on CNT networks	44
2.4. Deployment of nanosensors for embedded monitoring of construction materials	45
2.5. Conclusions	47
3. Reliability assessment of nanodevices by multiscale characterizations	48
3.1. The challenge: to improve the reliability of nanodevices	48

3.2.	PLATINE in-situ characterization bench for fatigue behavior under complex loadings	50
3.3.	Ex-situ characterization to identify the nanoscale causes for failure	53
3.4.	From in-situ and ex-situ characterization to nanodevice modelling: a key to understanding operation and failure mechanisms	56
4.	Conclusion and prospects.....	62
4.1.	Reproducibility and reliability of nanosensors: from the nanoparticle up to deployment level	62
4.2.	What about nanosensors for greener cities?	63
4.3.	Personal Roadmap for the future.....	64
5.	Bibliography.....	66
Appendices		76
Appendix 1: Personal bibliography, August 2016		76
Appendix 2: State of the art on carbon nanotube sensors		82
Appendix 3: State of the art of reproducibility in carbon nanotube network-based sensors		92
Appendix 4: Michelis et al., Carbon 2015 (95) 1020-1026		98
Appendix 5: Loisel et al., Scientific Reports 2016 (6) 26224.		110

Acknowledgments

None of the story told in this manuscript could have happened without strong research partnerships, heavy supports from my bosses and, most importantly, intense efforts from my students.

My gratitude goes first to the late Olivier Coussy, who convinced Armel de la Bourdonnaye - at the time head of research at ENPC - that it was a good idea to let me engage in a PhD on nanosensors for civil engineering. Then to Frédéric Bourquin, Anne Ghis and Jean-Marie Caussignac, my PhD directors and advisers, who supported this research from scratch, before there actually was anything to believe in. Each in your own manner, you shaped (hopefully for the better) the way I do research now.

Fortunately for me, Hélène Jacquot-Guimbal and Henri Van Damme both accepted to pursue this risky story by recruiting me at IFSTTAR at the end of my PhD in 2010. Beside this, for which I am obviously thankful, you both have put a deep stamp on my work: Henri for your support of Sense-City (which probably won us the grant), for your scientific vision and, last but not least, for introducing me to Eduardo Ruiz, who in turn set me out on the nanoasphalt path; Hélène for regularly sharing out-of-the-box advice, notably on human and project management and on problem solving.

Since 2010, we have transformed Sense-City from a castle in the air into a flagship of Paris Est. For this, very special thanks go to François Derkx, who did a large part of the heavy lifting! After his retirement last year, his work has been taken over by Erick Merliot, Philippe Bruley and Pierre Perrin, who do an amazing work of turning this paper project into a real research facility.

I am also grateful to all of my colleagues at IFSTTAR (Julien Waeytens, Anne Ruas, Patrice Chatellier, Frédéric Bourquin, Nicolas Hautière, Rachida Chakir, Fatima Bouanis, Sandrine Marceau, Vincent le Cam, Jean Dumoulin) and among Sense-City partners (notably Tarik Borouina at ESIEE, Costel Cojocar and Yvan Bonnassieux at LPICM, Hervé Rivano at INRIA, Jean-Marc Laheurte at UPEM), who believed in this project and worked with me to build it into a shared scientific vision of a Smart, Sustainable City.

Bernard Drévilion and Costel Sorin Cojocar first, then Pere Roca and Yvan Bonnassieux, you opened the doors of LPICM to me and we built the NACRE research team together. I thank you all deeply for this privilege, which enabled me to keep doing advanced research on nanotechnologies while working on innovative applications at IFSTTAR. I thank you all for welcoming me in this great lab.

In 2014, I had the chance to meet Laurence Bodelot around the topic of nanoreliability. Since then, we are working together and it has been a very exciting scientific time. I am deeply grateful to you for your energy and motivation, as well as for applying your outstanding skills on our shared research. Now, it seems that the seed is taking and I am very glad that Gael Zucchi and Boris Gusarov have joined us on this adventure.

In the last few years, I have directed a lot of students, from master's students to postdocs, from Nawres Sridi and Fadi Zaki, who went on to pursue their PhD, to Alfredo Gutierrez, still in his postdoc with me. I am thankful to all of you for your efforts on the behalf of these researches. Among you, I have very special thanks to address to Fulvio Michelis and Loic Loisel. A lot of the work presented here stems from your theses and I am very proud of the work we carried out together.



Last but not least, I wish to thank collectively all my colleagues at LPICM and IFSTTAR for sharing these years with me and making all of this possible: not only the researchers and engineers (particularly Yvan Bonnassieux, Ileana Florea, Abderrahim Yassar, Denis Tondelier, Marc Chatelet, Jean-Eric Bourré, Jean-Charles Vanel, Jean Luc Maurice at LPICM; François Derkx, Erick Merliot, Julien Waeytens, Rachida Chakir, Fatima Bouanis, Frédéric Bourquin, Anne Ruas, Patrice Chatellier, Sandrine Marceau, Vincent le Cam, Jean Dumoulin, Nicolas Hautière, Dominique Siegert, Cyril Nguyen at IFSTTAR), but also all the administrative teams (especially Maddly Fremont, Séverine Somma at IFSTTAR, Laurence Corbel, Gabriela Medina at LPICM), the valorization teams (Emilie Bacchi and Dominique Fernier at IFSTTAR, Delphine Marcillac at LPICM) and the support teams (notably Jean Luc Moncel, Jérôme Charliac, Eric Paillassa at LPICM; Pierre Perrin, Juliette Renaud, Emilie Vidal, Stéphane Buttigieg, Gonzague Six, Jean-Luc Bachelier at IFSTTAR).

During these times, both good and bad, my husband and family have supported me without reservation, for which makes me very fortunate, and also very grateful ☺





Part 1 - Curriculum

1. Curriculum vitae




Current position

Since Sept. 2010 	Researcher at IFSTTAR (50%) LISIS Laboratory (Monitoring, Modelling, Scientific Computing) <i>Université Paris-Est, Cité Descartes, 77447 Marne-La-Vallée Cedex</i>
Since Sept. 2014 	Researcher at LPICM (UMR 7647 CNRS-Ecole Polytechnique) (50 %) within NACRE joint research team IFSTTAR/LPICM/LMS. Team Organic and Large Area Electronics <i>Ecole Polytechnique, Route de Saclay, 91120 Palaiseau Cedex</i>

Previous positions

Sept. 2010-Sept. 2014 	Researcher at LPICM (UMR 7647 CNRS-Ecole Polytechnique) (50 %) within NACRE joint research team IFSTTAR/LPICM. Team Nanomaterials and Devices
Oct. 2007-Sept. 2010 	PhD at IFSTTAR and CEA-LETI. Diploma from Université Paris-Est in Civil Engineering. <i>Instrumentation of cementitious materials with carbon nanotubes-based ultrasonic transducers.</i> Supervisors: Frédéric Bourquin (IFSTTAR); Anne Ghis (CEA/LETI) 2011 PhD prize from ENPC PariTech
Feb. 2007-Aug. 2007 	MSc Internship at CEA-LETI <i>Functionalizing concrete materials with micro and nanosystems : identification of the technological bottlenecks.</i> Supervisor : Anne Ghis
Apr. 2006-Aout. 2006 	Internship at IBM Almaden Research Center (San José, CA, USA) <i>Development of magnetic materials by Molecular Beam Epitaxy.</i> Supervisor: Stuart S. P. Parkin 2006 Internship prize from Physics Department at Ecole Polytechnique

Diploma

Sept. 2008-	Engineer in the Corps des Ponts, des Eaux et des Forêts ¹ (IPEF)
Sept. 2006-Aug. 2008 	Engineer-in-Training in the Corps des Ponts, des Eaux et des Forêts
Sept. 2006-Sept. 2007 	MSc of Ecole Polytechnique -MSc Sciences of Materials and Nano-objects, Paris VI University, France -MSc Condensed Matter Physics, Paris XI University, France
Sept. 2003-Sept. 2006 	Ingénieur de l'Ecole Polytechnique ; Palaiseau, France Multidisciplinary curriculum (Quantum Physics and Chemistry, Statistical physics, Solid and fluids mechanics, Applied mathematics, Economy, Humanities...) Specialization in Condensed matter physics, Electronics and Nanotechnologies

¹ IPEF (Ingénieur des Ponts Eaux et Forêts) is the second rank out of four for Civil Servant Engineers belonging to the Corps des Ponts, des Eaux et des Forêts (Corps of Bridges, Waters and Forests). It is a technical Grand Corps of the French State (grand corps de l'Etat).

2. Research activities

Summary

Nanosensors for Sustainable Cities: from fundamentals to deployments

CNU 63: Génie électrique, électronique, photonique et systems

Scientific publications: 10 peer-reviewed papers; 5 patents (4 with PCT extension); 1 book chapter; 17/23 conferences with/without proceedings (among which 2 posters, 9 invited talks)

Dissemination activities: 7 written and 3 video interviews to regional, national or specialized press; 4 articles in specialized press; 3 interventions in general public conferences

Collaborative and industrial projects, administrative work: 9 national and international collaborative projects, 4 as coordinator; 2 international collaborations; 3 industrial contracts; co-leader of 2 joined research teams; participation to 3 academic taskforces (2 as leader)

Field of research:

As a physicist specialized in the **nanoelectronics of carbon-based nanomaterials**, my research focuses on the development of **reproducible and reliable nanosensors for applications to urban sustainability**, with a focus on **micromechanical and chemical sensing**.

My work addresses the multidisciplinary fields required to **bring nano-enabled prototypes from the proof of concept (TRL 1-2-3) to the industrial market (TRL 4-5-6)**: device fabrication on Silicon and low cost substrates, with a focus on process reproducibility (microelectronics, wet process such as inkjet printing, material functionalization), advanced thin film and device characterizations (Raman, MEB, AFM, TEM, electrical, sensing performances...) with a focus on systematic data processing (including image analysis, statistical methods), device physical/electrical modelling (analytical, semi-analytical or finite element models, discrete models), device integration into sensor nodes (signal conditioning, integration into sensor node) and device deployment in lab test benches and realist scenarios (packaging, data gathering, high-level design of lab-scale and urban-scale testbed).

Collaborative projects

Since Sept. 2014 **Co-founder and Co-manager** with Laurence Bodelot (LMS) of Ecole Polytechnique PLATINE facility (Reliability of Nanosensors; project co-financed by the SESAME Paris Region program, by the Paris 2030 program and by Ecole Polytechnique)



Partners: Ecole Polytechnique (LPICM, LMS, PMC, LSI), IFSTTAR

Research actions:

- Design, realization and exploitation of an equipment platform for in-situ, multi-scale characterization of nano-enabled devices under coupled loadings
 - Development of the associated data processing and modelling tools required to build a framework for reliability assessment of nano-enabled devices
 - Application of the methodology to different types of devices via collaborative projects such as **Deflex** (DGA project on CNT network based strain sensors on polymer) or **Nanoperco** (Maturation project from CHARMMMAT Labex on nanoparticule-based strain gauges)
-

Feb. 2011-Sept. 2016 **Coordinator** of Sense-city Excellence Equipment "Equipex" Program (Prototyping and Validation of Nanosensors for Sustainable Cities, 2011-2019). <http://sense-city.ifsttar.fr/>



Partners: IFSTTAR, ESIEE, CSTB, LPICM, INRIA, UPEM

R&D Actions

- Setting of requirements for the flagship Sense-City mobile climatic chamber; implementation and follow-up of the public tender for conception/realization; the facility is to be operational by mid-2017.
- Setting of requirements, design, conception and exploitation of the 1st "communicating miniature city" (250m² of outdoor, scale one urban deployment dedicated to new technologies for sustainable cities; platform operational since March 2015) and of the 2nd miniature city (to be implemented within Sense-city climatic chamber by mid-2017).
- Design, realization and exploitation of experimental campaigns within Sense-City's "miniature cities" within the framework of collaborative projects, such as **PSPC SMARTY** and **FUI MIMESYS** on air quality, **H2020 Proteus** on water quality, **FUI CONNECTeCITY** on urban telemanagement.

Coordination and Disseminations actions:

- Scientific leadership (roadmapping, creation and fostering of synergies, creation of

dedicated taskforces, co-organization of the yearly Sense-City workshops...)

-Administrative management (consortium agreement, integration of new partners, yearly reporting, yearly project meeting...)

-Dissemination to specialized and general public (interviews, scientific and vulgarization papers, talks and roundtables at scientific and non-scientific events)

Feb. 2015-
Jan. 2018



Coordinator of H2020 ICT project PROTEUS (Reconfigurable micro- and nano-enabled sensors for water quality monitoring). <http://www.proteus-sensor.eu/>

Partners: IFSTTAR, ESIEE, EGM, Ponsel, Uninova, UI, SMAS, Wings ICT, NIPS

Research actions:

-Development, characterization and optimization of a set of Ohmic chemical sensors for liquid phase sensing based on inkjet-printed, random networks of carbon nanotubes (CNT) functionalized with dedicated conjugated polymers. The CNT sensors are co-integrated with MEMS sensors.

-Development and exploitation of a test-bench for automated performance assessment for physical and chemical water quality sensors

-Design, realization and exploitation of a scale one water network within the Sense-City facility for water sensor deployment and validation

Jun. 2015-
Apr. 2018



Leader of the Nanoasphalt project (prematuration of the Nanoasphalt technology, at Ecole Polytechnique; June 2015-May 2016), of its associated project smartR (simulation of StartUp building on Nanoasphalt invention, at HEC MBA, Entrepreneurship Track; funded by FCS Paris Saclay; Sept. 2015-Dec. 2015) and of the subsequent SmartR maturation project (maturation of Nanoasphalt technology in view of startup creation; SATT Paris Saclay; Dec. 2016-Apr. 2018). The concept was initially proposed during the FUI project SIPRIS (Systèmes Intelligents pour la Prévention des Risques Structurels, Jan. 2012-Dec. 2014) to which I participated.

International collaborations

Since 2013



Collaboration with **Nanyang Technological University (EEE School), Singapour and CINTRA (UMR Thalès, CNRS, NTU).**

-Main contacts: Beng Kang Tay, Philippe Coquet

-Topics: reliability in nanomaterials-based devices; smart cities

-2 PhD supervisions

-Involvement in joint proposals (4 submitted, 1 accepted in 2015 so far)

Since 2013



Collaboration with **Materials Science Institute Of Madrid, CSIC, Department of New Architectures in Materials Chemistry**

-Main contacts: Eduardo Ruiz, Pilar Aranda

-Topic: Exploitation of innovative carbon-based materials (synthesized by CSIC) in device applications, in particular within the SIPRIS project and now the Nanoasphalt project (1 joint patent)

Expertise actions

2014



Subcontractor of **CMI** for the writing of the “**Vademecum: Innovation and sustainable cities**” commissioned by **Advancity** and financed by the **Caisse des Dépôts et Consignations**

Task: Writing of chapter on the “**evaluation of urban demonstrators**”

2014-2015



2 successive contracts with **Engie** on **wireless sensor networks for infrastructures**

Task: Dedicated state of the art analysis; Scientific expert to project management

Administrative functions

2015-2020



Co-leader with Laurence Bodelot of the initiative “**Smart world: nanosensors and nanoreliability**”, selected by Ecole Polytechnique as one of the pillars of its ongoing fundraiser

2015-2016



Participant to the taskforce **Electronics, Spintronics** of the **Electrical, Optical and Bio Engineering Department of Université Paris-Saclay**

2013-2017



Coordinator of the internal IFSTTAR taskforce on **Sustainable Urbanization via Nanosensors**

Mai 2011-Apr.

2015



Co-founder and Co-leader of NACRE joint research team between IFSTTAR and LPICM (Nanosensors for Environmentally-aware cities).

The team was renewed in 2015 for 4 years and extended to the LMS.

2010-2014





Co-leader of CARMIN joint research team between IFSTTAR and CEA (Sensor networks for Infrastructure Monitoring).
The team was renewed in 2014 for 3 years.

3. Teaching and student supervision





Summary

Teaching	40+ hours/year at ESIEE Paris since 2011 M1/M2 level; curriculum exclusively in English
Completed supervision	3 defended PhD (2 as main advisor-70%, 1 as co-advisor-15%) 2 post-doc (18 months-100%, 12 months- 30%, 9 months-40%) 1 Engineer (3 years-70%) 10 M1/M2 students
Supervision in progress	1 PhD student defending 2018 (co-adviser-40%) 1 apprentice from IOGS (main adviser-80%) 1 engineer (main adviser-90%) 3 post-docs (2 as main adviser-90%, 1 as co-adviser-30%)







Teaching activities

 Sept. 2011-	Material Sciences <i>25h/y - M1 level - ESIEE International Master's degree (curriculum in English)</i>
	Technologies of microelectronics <i>4h/y - M1 level - ESIEE International Master's degree (curriculum in English)</i>
	Introduction to nanotechnologies <i>8-12h/y – M2 level - ESIEE International Master's degree (curriculum in English)</i>
 Sept. 2014-	Mathematics for Physicists <i>5h/y - M1 level - ESIEE International Master's degree (curriculum in English)</i>





PhDs

 Nawres Sridi Oct. 2010-Oct. 2013	Topic: Study of ultra-thin membranes for integration into ultrasonic transducer; an experimental approach. PhD supervisor: J.-C. Gabriel. Main advisor: A. Ghis. Co-advisor: B. Lebental, 15% Production: 1 peer-reviewed journal paper, 2 international conferences with proceedings
 Fulvio Michelis Oct. 2012-Oct. 2015	Topic: Wireless Nano Sensors for Embedded Durability Monitoring in Concrete. PhD supervisor: Y. Bonnassieux. Main advisor: B. Lebental, 80%. Co-advisor: L. Bodelot Production: 2 peer-reviewed journal paper (1 in prep), 3 international conferences with proceedings, 1 international conference without proceedings
 Loic Loisel Jan. 2012-Mar. 2016	Topic: Optical and electrical breakdown of carbon allotropes: mechanisms and applications for data storage. PhD supervisors: B. K. Tay & B. Drévillion. Main advisor: B. Lebental, 80%. Co-advisors: C. S. Cojocar & M. Chatelet. Production: 2 peer-reviewed journal paper (+1 under revision), 1 international conferences with proceedings, 1 international conference without proceedings
 Ange Maurice Aug. 2014-	Topic: A Planar Graphene Memory Based on Electro-Mechanical Switching PhD supervisor: B. K. Tay. Co-advisor: P. Coquet & B. Lebental, 40%

Post-docs

Boutheina Ghaddab Nov. 2012- July 2014 	<u>Topic:</u> A novel weigh-in motion sensor based on a thin graphene-on-clay/carbon-nanotubes piezoresistive layer embedded within asphalt <u>Funding:</u> FUI Project SIPRIS <u>Main advisor:</u> B. Lebental, 100% <u>Production:</u> 1 peer-reviewed journal paper in prep, 3 international conferences with proceedings, 1 patent
Mallesham Godumala May 2015-Jan. 2016 	<u>Topic:</u> Selective chemical functionalization of carbon nanotubes fo liquid phase sensing <u>Funding:</u> H2020 Project PROTEUS <u>Main advisor:</u> Gael Zucchi. <u>Co-advisor:</u> B. Lebental, 40%
Luka Pavic Apr. 2015-Mar. 2016 	<u>Topic:</u> Carbon Nanotube based sensors: Multiphysics modelling and experiments <u>Funding:</u> DGA Project DEFLEX <u>Main advisors:</u> A. Constantinescu, L. Bodelot. <u>Co-advisor:</u> B. Lebental, 30%
Alfredo Gutierrez Jul. 2015-Jun. 2017 	<u>Topic:</u> Printed carbon nanotube sensors for liquid phase sensing, fabrication and characterization <u>Funding:</u> H2020 Project PROTEUS <u>Main advisor:</u> B. Lebental, 90%
Loïc Loisel Apr. 2016-Jan. 2017 	<u>Topic:</u> Printed carbon nanotube sensors for liquid phase sensing, fabrication and characterization <u>Funding:</u> H2020 Project PROTEUS <u>Main advisor:</u> B. Lebental, 90%
Sasikumar Ramachandran Apr. 2016-Mar. 2017 	<u>Topic:</u> Functionalization of carbon nanotubes for liquid phase sensing, chemical synthesis <u>Funding:</u> H2020 Project PROTEUS <u>Main advisor:</u> G. Zucchi; <u>Co-advisor:</u> B. Lebental, 15%

Engineers and apprentice

Waleed Moujahid Sept. 2011-Aug. 2014 	<u>Topic:</u> Prototyping nanosensors for city monitoring (un-defended PhD) <u>Main advisor:</u> B. Lebental, 70%. <u>Co-advisor:</u> C.-S. Cojocar. <u>Production:</u> 1 peer-reviewed journal paper, 1 international conferences with proceedings, 1 national conference without proceedings
Edoardo Milana June 2015-Nov 2016  	<u>Topic:</u> Nanoasphalt, a nanoparticle-asphalt sandwich for weigh-in-motion applications; technological transfer <u>Funding:</u> FCS Paris Saclay Project Nanoasphalt <u>Main advisor:</u> B. Lebental, 90%
Yaowu Zhang Sept. 2014-Aug. 2017 	<u>Topic:</u> Detection of chemical species in liquid phase via carbon nanotube based ohmic transducers <u>Main advisor:</u> B. Lebental, 80%. <u>Co-advisors:</u> L. Bodelot & D. Marcillac

Part 2 – Body of work

1. Introduction

1.1. Solving urban challenges requires intensive urban evaluation

1.1.1. Status of the risks faced by urban ecosystems

In 2014, 54% of the world population was living in cities that were covering between 3% and 5% of Earth surface and were concentrating 70% to 90% of the world economy. About half of the urban dwellers lived in cities with less than 500,000 inhabitants, while 12% of them lived in the 28 megacities with over 10 million inhabitants (see Figure 1). The situation is quickly evolving: in 2050, the urban population should reach 2/3 of the world population [UN 14]. These global numbers hide strong geographic disparities: in France, an INSEE report from 2011 based on the 2008 census indicated that the urban population reached 77.5% and that 95% of the population actually lived “under urban influence”, meaning area (usually at city periphery) where people commute to neighbouring urban area for work [INSEE 11].

This massive urbanization threatens people quality of life, resource availability and environment preservation. Before going into details, a few global numbers can be assembled to provide range of magnitudes: in 2011 worldwide, we used 14 billion TOE (ton of oil equivalent) and emitted 30 gigatons of CO₂, respectively a 48% and a 44% growth since 1993 (to be compared to only a 27% increase in population). In 2014, we used 4 billion of m³ of water and threw away 42 million tons of electronic waste [WEC 13].

Though these global numbers hint at an overuse of limited resources and at generalized wastefulness, they may seem very much removed from our everyday lives. However, a wide range of studies are now pushing for the impact of urbanization in terms of health and quality of life to be acknowledged. Air and water quality are two particularly prominent examples.

- Numbers related to air-quality related morbidity were heavily mediatized in 2015: worldwide, the number of premature death due to air pollution was estimated at 7 million in 2012 by the WHO; at EU scale, the estimate reaches 450 000 premature death/year; in France, the number is at 42 000 premature death/year. Behind these impressive numbers, there are concrete facts: traffic-related air pollutants such as NO₂ and CO [Palmgren 07] are known to increase cardiac and pulmonary health risks [Stieb 2009], as well as the rate of preterm births [Stieb 12]. The incidence of asthma, one of the most common chronic diseases (over 300 million sufferers worldwide [GINA 15]), is estimated to have doubled over the past 10 years, especially in young children. In Europe in 2003, the total cost of asthma was estimated at €17.7 billion per year, and productivity losses due to poor asthma control were estimated at €9.8 billion per year [ERS 03]. These health issues not only result from long-term exposures: there is also a well-known effect of day-to-day air pollution changes on asthma related hospital admissions [Nastos 10]. Epidemiological data suggests that many people are exposed to levels of these air pollutants much higher than recommended levels.
- while drink water losses in the supply network are massive (up to 50% in some cities), at least 11% of the European population and 17% of EU territory to date have experienced recently water scarcity-related problems [EC 10]. Millions of people die each year world-wide as a direct consequence of waterborne infectious diseases [WHO 16]. For instance, in 1998,

municipal drinking water in Alpine, Wyoming, USA was contaminated with Escherichia Coli (E. coli O157:H17) and the outbreak caused 157 people to fall sick [Olsen 02]. In 2000, E. coli O157:H17 contaminated drinking water in Walkerton, Ontario, Canada which led to 2,300 illness and 7 deaths [Clark 03]. More recently, in 2008, an outbreak due to drinking water contamination by the bacteria Legionella pneumophila occurred in New Jersey, USA [CDC 11].

It is expected that these already acute situations will worsen with climate changes: droughts and heat waves are expected to worsen, as well as the intensity of storms. Inland and coastal flooding will get more frequent due to the rise of sea level [IPCC 14].

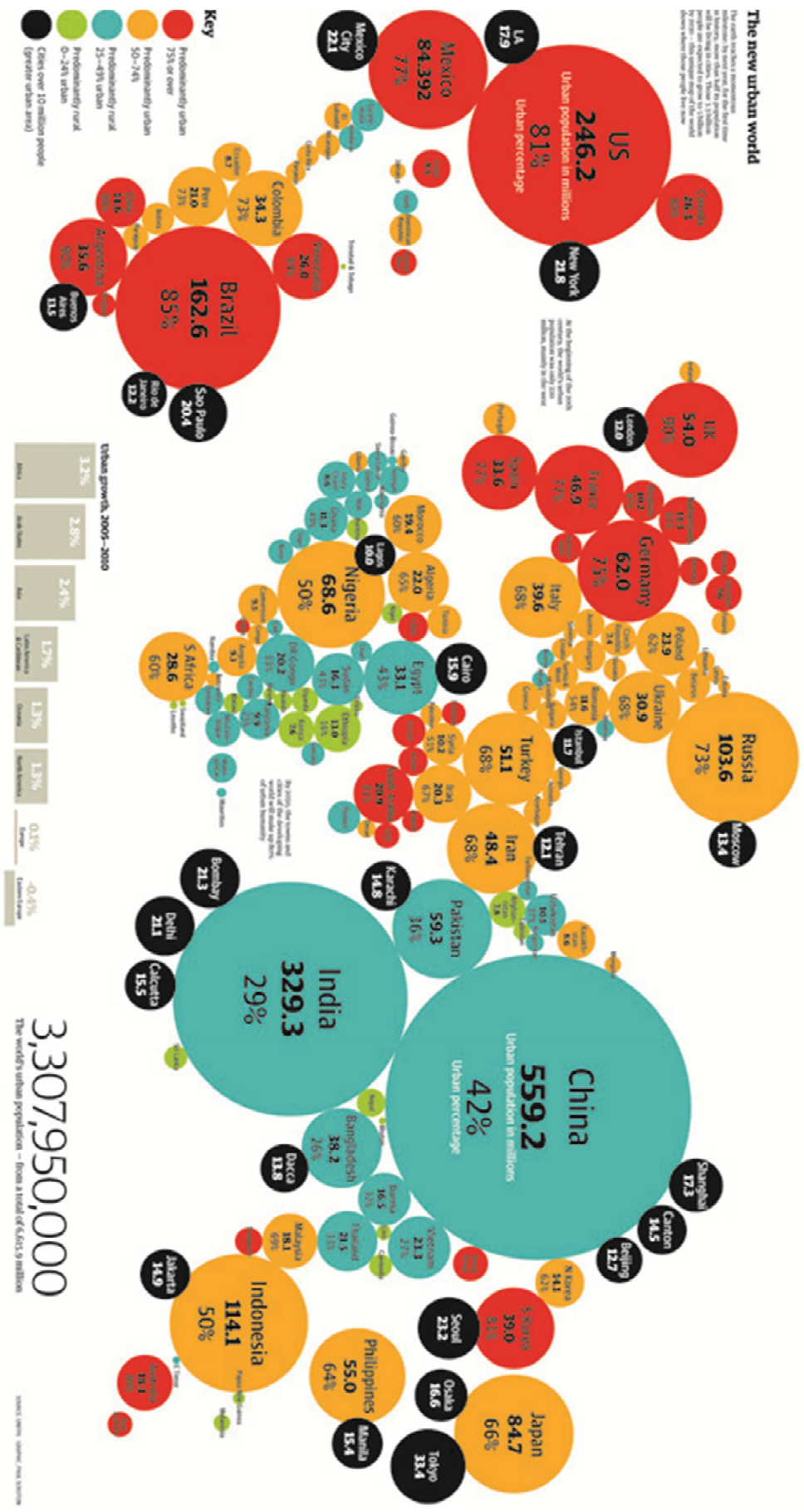


Figure 1: Urbanization Map World. <http://macnicolasset.com/the-global-urban-migration/>

1.1.2. Policy makers work on mitigating urban risks

To meet these challenges, policy makers around the world triggered a wide range of initiatives targeting various beneficial goals: to improve urban quality of life and mitigate the detrimental health impact of urbanization, to preserve of all types of resources, to protect the environment and the biodiversity, to achieve high urban resilience ... The latest born of these policies is probably the 2015 Paris Agreement regarding to the mitigation of climate changes (see Figure 2), but the last two and half decades since the 1992 Kyoto protocol were rich in actions.

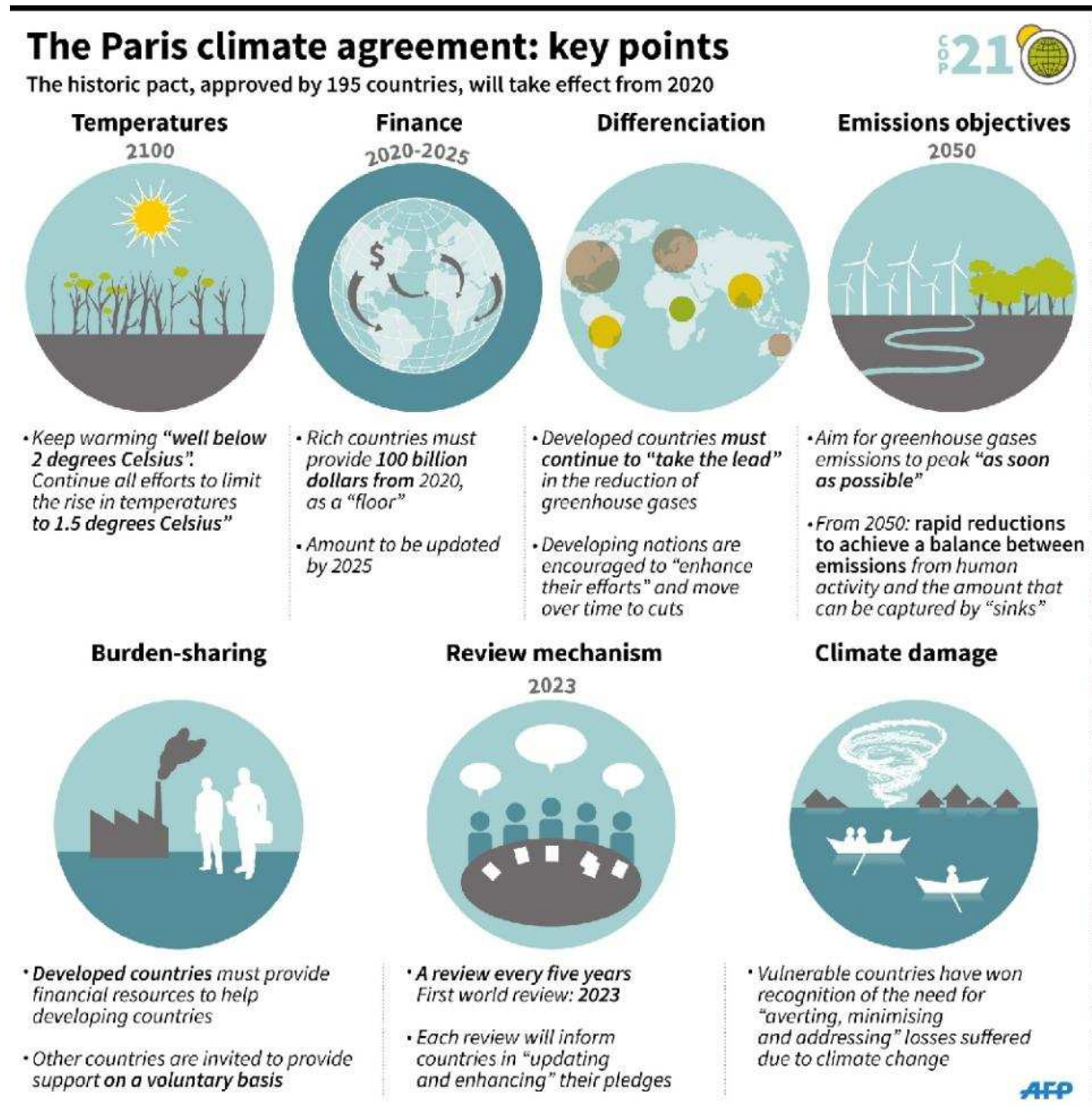


Figure 2: Key points of the 2015 Paris Agreement. Agence France Presse.

For instance, the Swiss “2000 Watts society” initiative² aims at dividing by three - and thus decreasing down to 2000 W - the average energy consumption per capita in West Europa. Among these 2000W, only one fourth should emanate from non-renewable energy sources. The Basel area

² <http://www.societe2000watts.com/>

in Switzerland is currently field testing this initiative. In France, the current law on energy transition³ requires a 50% decrease of the energy consumption and a 40% decrease of the GHG emission by 2020 (with respect to 2012 values) [PBD 15]. Concretely, the law stipulates for instance that existing buildings should be renovated at a fast pace (500 000 housing/year from 2017 onward, half of them occupied by low-income households) to turn them into low/zero-energy-buildings. By 2025, all private residential buildings with primary energy consumption above 330kWh/m²/yr will need to undergo energy-renovation.

The protection of water resources (both in quantity and quality) is also among the cornerstones of environmental protection schemes worldwide. The World Health Organization has placed drinking water quality on top of its priority list, strongly advocating for the implementation of water safety plans throughout the world [WHO 11]. So did the European Union in 2000 with the “Water Framework Directive”: strong regulatory norms are being imposed for water quality at the European level with an ever-increasing number of pollutants of different natures (chemical, biological, agricultural, industrial, pharmaceutical, cosmetic, radioactive, warfare agents) being considered a risk [EC 00].

Regarding to air quality, the 1999 “Gothenburg protocol to Abate Acidification, Eutrophication and Ground-level Ozone” (known as the Multi-effect Protocol or the Gothenburg Protocol) was a multi-pollutant protocol designed to reduce acidification, eutrophication and ground-level ozone by setting emissions ceilings for sulphur dioxide, nitrogen oxides, volatile organic compounds and ammonia to be met by 2010. As of August 2014, the Protocol (after its 2012 revision providing targets until 2020) has been ratified by 26 parties, which includes 25 states and the European Union.

Regarding to Europe specifically, the most recent wave of policies started in 2005 with the Thematic Strategy on Air Pollution. More recently, the Clean Air Policy Package was adopted by the EU in 2013, as a follow-up of the EU emission inventory report 1990-2013 (yearly updated) [EEA 15]. It proposes significant reduction of emissions of different types of pollutants throughout Europe, via wide-scale application of already available technologies as well as development of new technologies. It also aims at consistency with the Gothenburg Protocol⁴.

At the scale of individual states, international agreements are translated into directives or laws regulating emissions. For instance, in France, industrial emissions of pollutants are regulated by the Directive 2010/75/UE from November 24th, 2010. It states for instance that inventoried industrial sites must be inspected for pollutant emissions and must reduce their emission according to regulations.

At city level, communities are implementing practical changes, mostly related to automotive traffic: reduction of speed on major urban highways, reduction of heavy traffic and most-polluting vehicles in downtown area, increase in speed, noise and pollution-related fines and enforcement, creation of urban tolling systems, temporary or permanent closure to vehicles of urban axis, increasing support for public transportation systems and alternative (green) mobility.

³ LOI n° 2015-992 du 17 août 2015 relative à la transition énergétique pour la croissance verte

⁴ http://www.unece.org/env/lrtap/multi_h1.html

1.1.3. Monitoring the effectiveness of policies and urban projects?

A crucial aspect in all these policies lies in their stakeholders' capability to actually monitor effectiveness. For instance, in the WHO guidelines on drink water quality, it is recommended that the self-monitoring of the network by the operator be included in the water safety plans. Moreover external, independent organisms should verify the proper application of the water safety plans. On another topic, in the field of building energy performances, the improvement of energy performances requested by the French regulator in the first Grenelle law has triggered the rise of the so-called "Diagnostic de Performance Energétique" method (energetic performance assessment) which stipulates calculation rules such as 3CL-DPE, DEL6-DPE or Comfie-DPE⁵. In France again, the INERIS institute (National Institute for Industrial Environment and Risks) is mandated by the Ministry of Sustainable Development to verify application by industrial stakeholders of environmental regulations, for instance regarding to waste management or pollutant emission.

The case of NO₂ monitoring provides an example of good practice in terms of monitoring the efficiency of a policy. Targets for NO₂ reduction have been proposed since the 1970's, among others to prevent acid rains. Since then, a wide range of monitoring networks and methods (ground monitoring station, satellite monitoring) has been implemented to monitor progress. Long term trends on NO₂ emissions can be found for most developed countries on various websites and reports and show a clear decrease in most developed countries (since 1990, 69% decrease in the UK [DEFRA 15], 44% decrease in France [MEDDE 14], 1% only decrease in the USA[EPA2016]; see Figure 3). They are analyzed widely in the scientific community to understand finely the respective performances of country and city scale policies [Kim 06].

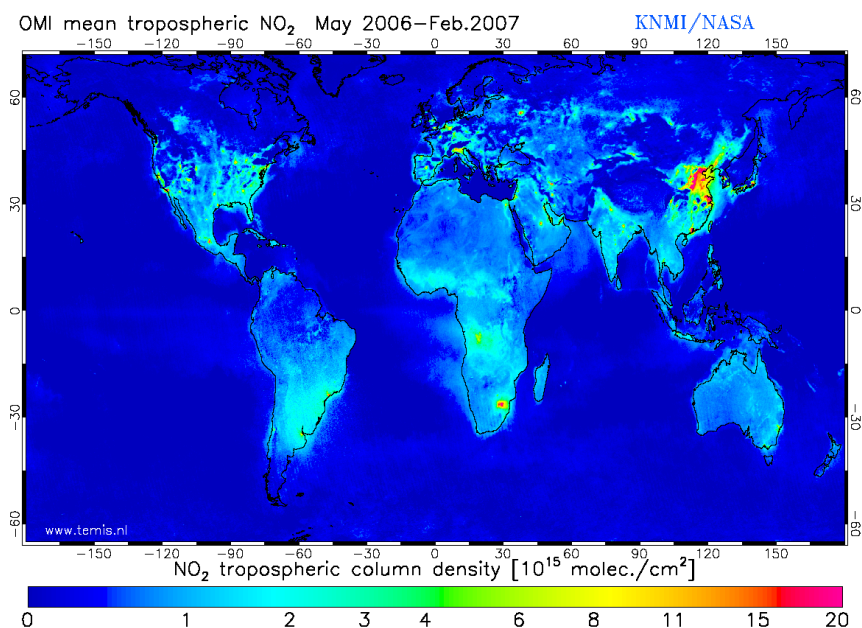


Figure 3: World map of the averaged tropospheric NO₂ column measured by OMI satellite instrument in the period May 2006 till February 2007⁶

Evaluating the effectiveness of policies started out as a roughly single-varied topic: has the specific target parameter improved due to the policy in the 1, 3 or 10 years following policy kick-off?

⁵ <http://www2.ademe.fr/servlet/list?catid=15030>

⁶ <http://www.temis.nl/products/no2.html>

However, due to the complexity of urban ecosystem, the single-varied approach quickly became inadequate: for instance, fostering green transportation in a city to reduce traffic-related CO₂ emission may have significant impacts on job creation or on social disparities.

To account for the intricacy of urban issues, it is now generally admitted that projects and policies should be evaluated according to criteria related not only to Environmental, Social and Economic impacts but also to Governance quality and Generalization capability. Accordingly, a series of urban evaluation frameworks were proposed or are being developed, such as Agenda 21; the reference framework for European sustainable cities; EURBANLAB; the Smart Cities and Communities framework; the Triple Helix framework. These frameworks can be used for early diagnostics of a territory, as well as for continuous evaluation of a policy or for post-project assessment.

In 2015, based on a bibliography study and a series of interviews, I wrote with Nicolas Hautière a review on these frameworks. This review targets a public of urban designers, city operators and policy makers. Beyond explaining the use of evaluation frameworks, the document describes how these frameworks are structured and how they can be applied to a given project. This work was integrated into the “Innovation and Sustainable Cities” booklet commissioned by the “Caisse des Dépôts” and the MEDDE and widely disseminated by Advancity [**Lebental 15b**].

1.2. The “internet of sensors”, the next stage for urban assessment

1.2.1. Urban monitoring, one of the opportunities of the “Internet of Things”

Evaluation frameworks are usually composed of hundreds of indicators, each of those needing to be accurately derived in order for the resulting evaluation of a territory to be representative. The bottleneck of evaluation frameworks thus actually lies in the capability to gather the required wealth of information. Today, it is carried out by a combination of direct inhabitant surveys, data collection in the different city offices, (often numerical-model-based) analysis of the various project documents (from both the contractor side and the contracting authority side)...

Besides the obvious complexity of dealing with such a massive amount of heterogeneous data, which requires cost-heavy manpower, there are strong and long standing doubts regarding to the reliability of some of these inputs. For instance, calculations on energy performances of buildings rely on energy invoices, well-known to be inaccurate in collective housing with individual heating (over 50% of the collective housing in France [OEMP2004]), or on data provided by building material manufacturers, also widely known to be inaccurate for imperfectly mounted materials.

The rapid rise of the “Internet of Things” opens up new possibilities for “easy” urban data gathering. To this day, the definition of the IoT remains rather flexible, but it roughly designates the network built by the whole of the connected devices, vehicles or buildings, a market estimated at about 20 billion\$ (see Figure 4). Citing Wikipedia⁷, “the IoT allows objects to be sensed and to be controlled remotely across existing network infrastructures creating opportunities for more direct integration of the physical world into computer-based systems”.

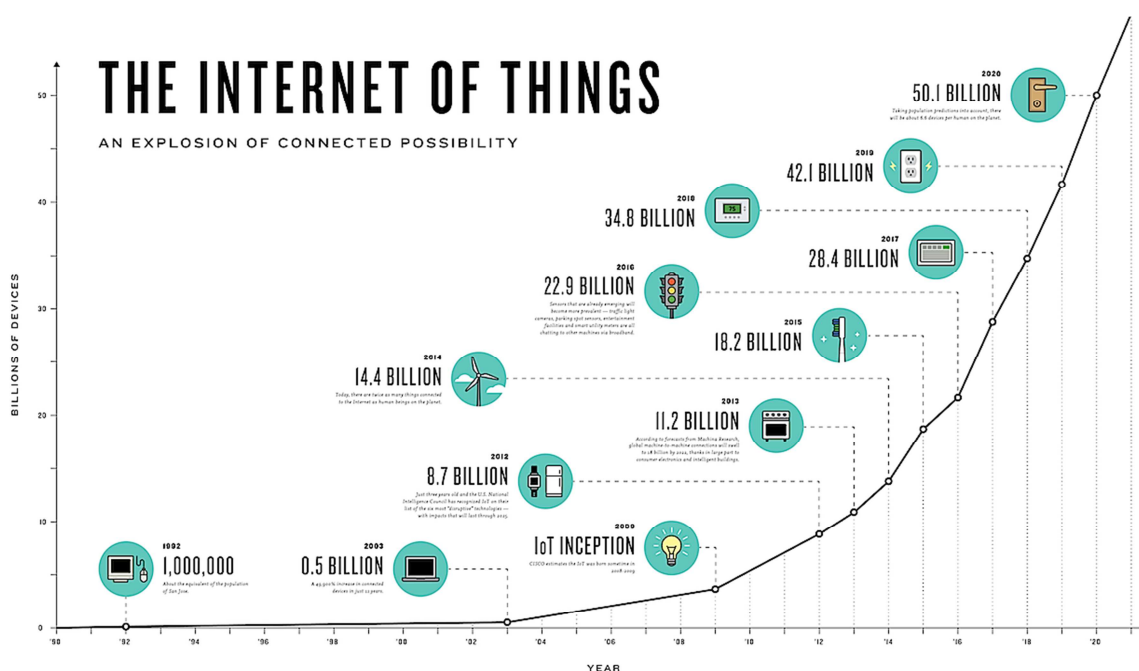


Figure 4: The Internet of Things, an explosion of connected possibilities⁸

⁷ https://en.wikipedia.org/wiki/Internet_of_things

⁸ <http://www.i-scoop.eu/internet-of-things/>

The intense development of IoT has opened up the idea to build an “Internet of Sensors” (IoS) able to monitor urban ecosystems in real-time, everywhere, across all relevant parameters **[Lebental 15a]**. For institutional purposes, the data from the IoS could for instance be fed into any of the evaluation frameworks discussed above, but first and foremost they could be provided directly to the end-users: network operators (water, transportation...), city managers or citizens.

The overall idea of the IoS, which is being promoted in the Sense-City project I coordinated from 2011 to 2016, is to use the IoS to provide to a large volume of end-users a large variety of decision support tools based on real-time-data. Due to the large scale dissemination of the solutions (which would be enabled by design), it is expected that the return on investments (not only economical, but most importantly in terms of urban sustainability and healthy living) would be significant, quick and widespread.

Potential applications abound: smart watches integrating local air-pollution data to optimize a person’s bike or pedestrian itinerary to minimize pollution exposure; water networks self-diagnosing water leakage or accidental contamination; building AC systems co-optimizing air quality, energy performances and user comfort; real-time detection of road damages or traffic jam tails for the immediate information of end-users and operators...

1.2.2. *The “internet of sensors”, achievements and technological bottlenecks*

How far along this optimist trajectory are we presently? Sensor-based continuous, real-time monitoring has now been used for years for transport infrastructures [Taillade 10], buildings [Wong 05, O'Sullivan 04, Clarke 02], gas and water distribution networks [Burgess 08], wastewater networks [Schutze 04], wind turbines [Yang 10], public lighting [Chen 09b] ... City or infrastructure operators that have invested to put these monitoring systems in place usually appreciate them immensely and acknowledge significant economic benefits from their use.

But the penetration of these systems in society remains overall low, or even almost nil in the general public (though there is a high variability from one application to the other). The actual integration of the sensor outputs into decision support tools or evaluation frameworks is also marginal, though, again, some fields have progressed further than other, for instance Building Information Modeling Systems, Outdoor Air Quality or Intermodality in Transportation Systems...

In short, at the risk of discounting a few outliers, what roughly characterizes the domain today is a vertical approach (instead of a transverse approach across topics) at the scale of reduced territories (district-wide, instead of a city- or state-wide approach), with few generalization capabilities at country-wide or world-wide level.

But this is definitely a fast-evolving situation, and large companies have now stated to evaluate the operational gain they could achieve in building and exploiting multi-disciplinary, upscalable “Smart City” solutions. As a proof of this, CITEOS (Vinci subsidiaries) got awarded in 2016 (to start September 2016) the CONNECTe-CITY project (FUI⁹ call for proposal) with ARCOM, ACTILITY, Factory-Systems, ESIEE, Université de Tours and IFSTTAR (myself as coordinator for IFSTTAR). The goal of this project is precisely to foster interoperability and across-domain management of urban equipment (city lighting, traffic light, parking metering, electric charging point).

Though such examples may inspire some optimism, our society still faces drastic challenges before the “Internet of Sensors” becomes a worldwide reality. These loosely classify into three topics: hardware; software; usages. Let us describe them roughly.

- Hardware challenge: provide connected sensors at low cost (between 1000€/unit down to 1€/unit), in medium to large volume (from thousands to millions), with high performances (better than the commercial state of the art) and high reliability (from 1 to 50 years)
- Software challenge: provide real-time (1s to 15min) tools suitable to reconstitute multiphysics phenomena based on continuous or discrete, small or large volume, data feed from massively distributed sensors (up to millions) and to process their outputs into easily exploitable information systems for widely diversified stakeholders with highly diversified goals.
- Usage challenge: ensure the compatibility (economic, social, political, and environmental) of hardware and software to the diversity of use cases, by promoting user-centered design and fostering privacy-compatible, health-risk-free approaches.

⁹ Fonds Unique Interministériel – Unitary Intra-ministry Funding. Funding program from the French Government for applied research dedicated to collaborative projects between industrial and academic partners with industrial leadership

Because my own work focuses on sensor prototyping, a topic firmly on the hardware side of things, let us provide more details here on the hardware challenges via the examples, again, of water networks and air quality. These elements are extracted from the successful Proteus¹⁰ proposal (accepted 2015 H2020 ICT project on water monitoring, which I coordinate) and from the unlucky INCAS proposal (rejected 2013 ANR proposal on outdoor air quality sensors, which I coordinated).

Because of their spatial extents and their criticality, water networks require widespread, low-cost monitoring means with highly differentiated requirements (from drink water to waste water) and adaptive capabilities (from draught to flood events, from low to high demand levels). Monitoring is needed all along the water distribution cycle, from the water collection points like lakes, rivers and groundwater aquifers, to the reservoir and water pipes that transport it to the consumer. This also applies to the sewage system that takes the used water back to the treatment plants or collecting points...

However, despite an increasing demand of the operators for adaptability, compactness and performances at ever decreasing costs, the vast majority of water network monitoring systems remains based on sensor nodes with predefined and vertical applicative goals hindering interoperability and increasing the costs (OPEX and CAPEX) of deploying new and added value services. Innovative technological products could answer the following acute needs in the field:

- Need for multifunctional probes at low cost: For a single water monitoring station, typically 10 different kinds of (monoparameter) sensors are required, each with a unit price in the order of € 300 - € 1000. It is not economically viable to multiply measurements points in the network, though it would be needed to better comply with water safety plans. Commercial multi-parameter sensing probes are starting to be available from a few manufacturers (for instance from the Aqualabo¹¹ compagny, member of Proteus consortium). In general, pH, temperature, conductivity and dissolved oxygen may be available in the same package; optional additional parameters include turbidity, chloride ions, nitrates or ammonium, depending on the manufacturer. The latest product Intellisonde V2 from Intellitect Water provides 12 different sensors, including pressure and flow-rate. The cost of these probes, ranging from € 3.000 to € 25.000, remains a bottleneck toward their widespread use. The issue is further emphasized by the decrease in water consumption, observed notably in Germany or France, which lowers the turnover for operators of water networks and thus pushes them to limit their investment in monitoring solutions.
- Need for compactness: Existing solutions for drink water monitoring do not fit in the 100mm pipes constituting most of the networks. Their large size often results from lack of integration and non-optimized design, and is in part responsible for the high cost.
- Need for enhanced energy autonomy and resilience: The probes require frequent offline calibrations and maintenance (from 1 to 12 months depending on the product; especially for battery replacement) which is incompatible with permanent monitoring and massive deployment.
- Need for adaptability:


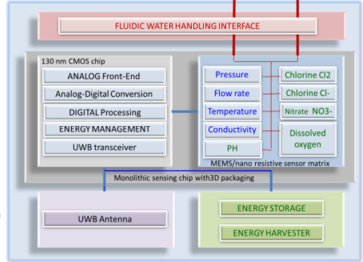
¹⁰ <http://www.proteus-sensor.eu/>

¹¹ <http://www.aqualabo-group.com/>

- While the water pressure and flow rates in the pipes may vary abruptly (several bars), individual sensing solutions are usually limited to a narrow range of pressure and flow rate (for instance pressure lower than 10 bar or flow rate larger than 1m/sec). More generally, different parts of the network (close to the factory in high pressure pipes, or close to the end user in low pressure pipes, waste and rain water network) are monitored with different sets of systems, increasing costs (both investments and maintenance) while complicating exploitation.
- Due to need to decrease the frequency of battery replacements, data acquisition and data transmission are periodic and widely spaced, so that alert events are regularly missed. An adaptive system with predictive and cognitive capabilities would be able to maintain a very low energy budget while keeping tracks of all alert events.
- Need for enhanced performances:
 - Usually based on voltammetry measurement, chemical measurements require systematic and complex post-process compensation of (even small) temperature and pH variations; the compensation step usually provides only lukewarm results.
 - Avoiding pathogenic bacterial growth in drinking water requires chlorine-based additives. Due to the complexity of chlore cycle in water, the real-time assessment of chlorine concentration in its different forms (free, total, active) remains insufficiently accurate.

An adaptive multifunctional smart system for water network monitoring with minimal CAPEX and OPEX is highly required. The following Table 1 summarizes the achievements that Proteus proposes on this topic, proposals that are presently under development by the consortium (2015-2018 project). They provide a satisfying summary of current expectations in the field of water quality sensing.

Table 1: Proteus improvements with respect to the state of the art of water quality sensor technologies: an example of expectations within the Internet of Sensors

	Market state of the art¹²	PROTEUS product
Product	 <p>TRIPOD from AQUALABO/PONSEL MESURE¹³</p>	 <p>PROTEUS Smart sensor system</p>
Volume	1739 cm ³	Approx. 125 cm ³ : 10x decrease in volume
Measured parameters	<p>7 parameters in predefined ranges</p> <p>Temperature, pH, Redox potential, Conductivity, Salinity, dissolved Oxygen, Turbidity</p>	<p>9 parameters with enhanced range of operation based on reconfigurability</p> <p><u>Identical</u>: Temperature, pH, Conductivity, Dissolved Oxygen. <u>Additional</u>: Pressure, Flow rate, Chlorine, Chloride, Nitrate <u>To be added in industrialization step</u>: Salinity, turbidity</p>
	<p>Not applicable waste/rain water networks</p>	<p>Adaptation to waste/rain water networks</p> <p>based on reconfigurability and reliability</p>
Lifetime	>3 months	> 2 year, x8 increase in lifetime
Communicating	Wired; handheld recorder	Fully wireless with UWB communication including cognitive networking
Data processing	No in-built data treatment	On-chip data processing for reaction, prediction and cognition
Autonomy	Wired power supply	Autonomous via vibration harvesting
Selling price	2500€	<p>Pre-series: < 1000€; x2.5 decrease</p> <p>Industrial level: <100€; X30 decrease</p> <p>No cost reference for use with waste water</p>

¹² IntellitectWater (<http://www.intellitect-water.co.uk>) proposes a smaller (10 cm) and more multifunctional probe (12 parameters) with GPRS connectivity, but price appeared to be over 10 k€; regarding to other aspects, it suffers the same issues as Ponsel's tripod (power supplied, short-lived, not cognitive)

¹³ <http://www.ponsel-web.com/cbx/datasheettripod.pdf>

If we now consider outdoor air quality, we face roughly the same issues:

- High performances systems used presently are very expensive: current urban air monitoring systems rely on automatic and manual samplings followed by precise analysis via high resolution, large, power-hungry and expensive equipment such as optical spectroscopy or gas chromatography/mass spectrometry (CG/MS). Although research is in progress to decrease the size and cost of these instruments in a lab-on-chip approach [Nachef 12, Reddy 12, Liu 13], one does not expect less than 100€, massively deployable instruments to reach the market on the middle term.
- Low cost sensing devices (15€ to 100€) exist¹⁴ but have drastically inadequate performances. They are usually destined to be integrated into battery-operated portable instruments or large, wired modules for detection and alarm in case of individual overexposure in industrial settings¹⁵. They also occur in smoke detectors and CO detectors for home settings¹⁶. Most of these sensing devices are based on heated semiconducting materials (150°C-600°C), initially Si and GaAs, now also single- (e.g., ZnO, SnO₂, WO₃, TiO₂, and Fe₂O₃) and multi-component oxides (BiFeO₃, MgAl₂O₄, SrTiO₃, and Sr_{1-y}Ca_yFeO_{3-x}) [Lundström 75, Kang 94, Hoffheins 96]. Electrochemical¹⁷, chemical¹⁸ (irreversible), optical or infrared¹⁹ sensors are also encountered. Most of these devices operate at high temperature with very high energy consumption; they demonstrate short time stability and low accuracy, often due to low selectivity. Accuracy is often much worse than can be expected from the technical specifications (due to questionable benchmarking process).

Despite these reservations, the large development of autonomous wireless sensor networks for monitoring in urban setting (for instance pavement [Broquereau 13] or parking [Karbashi 12] monitoring) has triggered the boom of wireless sensor networks dedicated to urban air monitoring [Liu 15, Wen 13, David 15, Sivaraman13], including mobile networks and participatory sensing.

However, lukewarm feedbacks on these networks, notably regarding to lifetime, reliability or accuracy, have incited the scientific community to proceed with extreme caution for generalization of the deployments and for data exploitation. Reliable sensor systems are found only in high risk situations, such as in industrial sites with risks of dangerous gas leaks (oil platforms), around volcanos or for military applications [Jain 12, Chen 10, Becher 10, Mitra 12, Manes 12, Werner-Allen 05], where high-end sensing devices are acceptable.

In addition to these mostly technical concerns, exemplified here for air or water quality, higher level industrial concerns should be mentioned, such as those reported in the 2013 EPoSS Strategic Research Agenda [EPoSS 13], the 2010 European Competitiveness Report [ECR 10] or the 2011 report of the High-Level Group on Key-Enabling Technologies [KET 11]:

¹⁴ For instance TGS 826, 2610, 2611 Figaro gas sensors at <http://radiospares-fr.rs-online.com>

¹⁵ For instance CD100A/RS or CO71A Kane gas detectors or Crowcon GS series at <http://radiospares-fr.rs-online.com>

¹⁶ For instance H450EN Honeywell CO sensor at <http://radiospares-fr.rs-online.com>

¹⁷ For instance IQ series of portable electrochemical sensors at <http://www.intlsensor.com>

¹⁸ For instance Profil'air® Series at <http://www.etheralabs.fr>

¹⁹ For instance SmartScan series at <http://www.comag-ir.com>

- Lack of exploitation potential: small series are too small for worthwhile exploitation and industrial series cannot be risked because the market is not mature enough
- Lack of alignment with strategies, legislation and standardization: end-users do not see the need for the system, or the system is incompatible with standard or legislation.
- Fragmented supply chain and poor manufacturability

As a summary, the field has a strong need for sensor technologies with advanced:

- Sensing capabilities (enhanced sensitivity and selectivity, new observables)
- Multifunctionality and miniaturization
- Energy autonomy
- Resilience and reliability proved in the environment of use
- Low cost and good manufacturability

Finally, whatever the application of interest, there is a generic challenge that also slows down the progress of Smart Systems, namely achieving the transfer of the solutions from mostly controlled lab/factory setups to mostly non-controlled urban environments: how to insure that the sensors measure only the quantities they have been designed to measure? Where and how to position the sensors to properly gather local information and measure gradients? How to evaluate measurement drift related to sensors aging? How to anticipate the potential hazard to environment and people occasioned by the sensors themselves?

1.2.3. *Sense-City, smart technologies for sustainable cities*

The Sense-City²⁰ project was precisely built in 2010 to help researchers tackle these issues and to bring their innovations closer to industrial stakeholders. Sense-City is a project of Université Paris-Est, gathering in its consortium seven institutes, IFSTTAR, ESIEE, Ecole Polytechnique, CNRS, CSTB, UPEM and INRIA. Funded within the framework of the “Investment for the Future Program” since 2012, Sense-City focuses on the prototyping and validation of micro and nanosensors for sustainable cities applications. It enables researchers to explore the concept of “sensitive” city in a realistic manner, with the end goal to empower the city to constantly self-diagnose in order to save resources, preserve its environment and protect its inhabitants.

Sense-City concept consists on the massive deployment of micro and nanosensors in realist urban scenarios. These sensors, may they be physical, chemical, optical, mechanical or biological, aim at deepening our understanding of the workings of urban ecosystems. Thus, they open the path toward closed-loop optimization of city processes at the citizen scale.

Sense-City scientific program revolves around applicative and transverse programs:

- Applicative programs:
 - Environment: invisible pollutions and their impact on health
 - Building and neighborhood energy performances
 - Infrastructures and networks: resilience and attractiveness
- Transverse programs:
 - From micro and nanosensor to the internet of things
 - From the modelling of urban phenomena to their visualization
 - Decision-making tools: usages, co-design and business models

Sense-City is also a large experimental project. Its main feature consists on a large environmental chamber designed to host urban scenarios. These are full-scale realistic models of a city’s main components: buildings, infrastructures, underground distribution networks. From 2017 onwards, this unique equipment will provide 4200m³ of experimental volume over a 400m² surface area, with controlled environmental conditions (temperature and hygrometry, rain simulation, solar radiation, liquid or gas pollution, water saturation of the soil, etc.) [Derx 12] (Figure 5).



Figure 5: Architect view of the upcoming Sense-City equipment, at the heart of Cité Descartes in Marne-La-Vallée.

²⁰ <http://sense-city.ifsttar.fr/>

In anticipation of the coming equipment, Sense-City first urban scenario, the so-called “connected district”, was inaugurated in March 2015 (Figure 6). Since then, it has welcomed a wide range of smart city-related experiments:

- Internet of things in urban area
 - Collection architecture for urban data
 - Dense and low energy wireless sensor networks
 - RFID for urban monitoring
 - Electromagnetic communication at ground level
- Air quality monitoring
 - Implementation of a dense air quality monitoring infrastructure
 - Pollution mapping and sensor optimal positioning
 - EcoGranic®, depolluting pavement
 - Air Serenity, multiprocessing of indoors pollutants
- Building and neighborhood energetic
 - Temperature mapping in urban context
 - Real time instrumentation of a building energy behaviour
 - Outdoor thermal monitoring by connected infrared thermography
- Smart Road
 - Self-configuring sensor network for vehicle detection
 - Cyclists-pedestrians interaction study
 - Photovoltaic road demonstrator
 - Nanosensors for weigh-in-motion **[Ghaddab 14]**
- Smart infrastructures and networks
 - Ground penetrating radar detection of buried objects **[Sagnard 16]**
 - Concrete instrumentation with embedded nanosensors **[Michelis 15a]**
 - Drinking water network instrumented with micro and nanosensors

As scientific coordinator of the project between 2011 and 2016, I have been one of the main players in the technical design of Sense-City, with François Derkx, Erick Merliot and now Philippe Bruley (LISIS), and in the continuous building of its scientific program, with the colleagues from COSYS (Frédéric Bourquin) and LISIS (notably Anne Ruas, Patrice Chatellier, Julien Waeytens, Rachida Chakir, Fatima Bouanis) and of course the project partners.

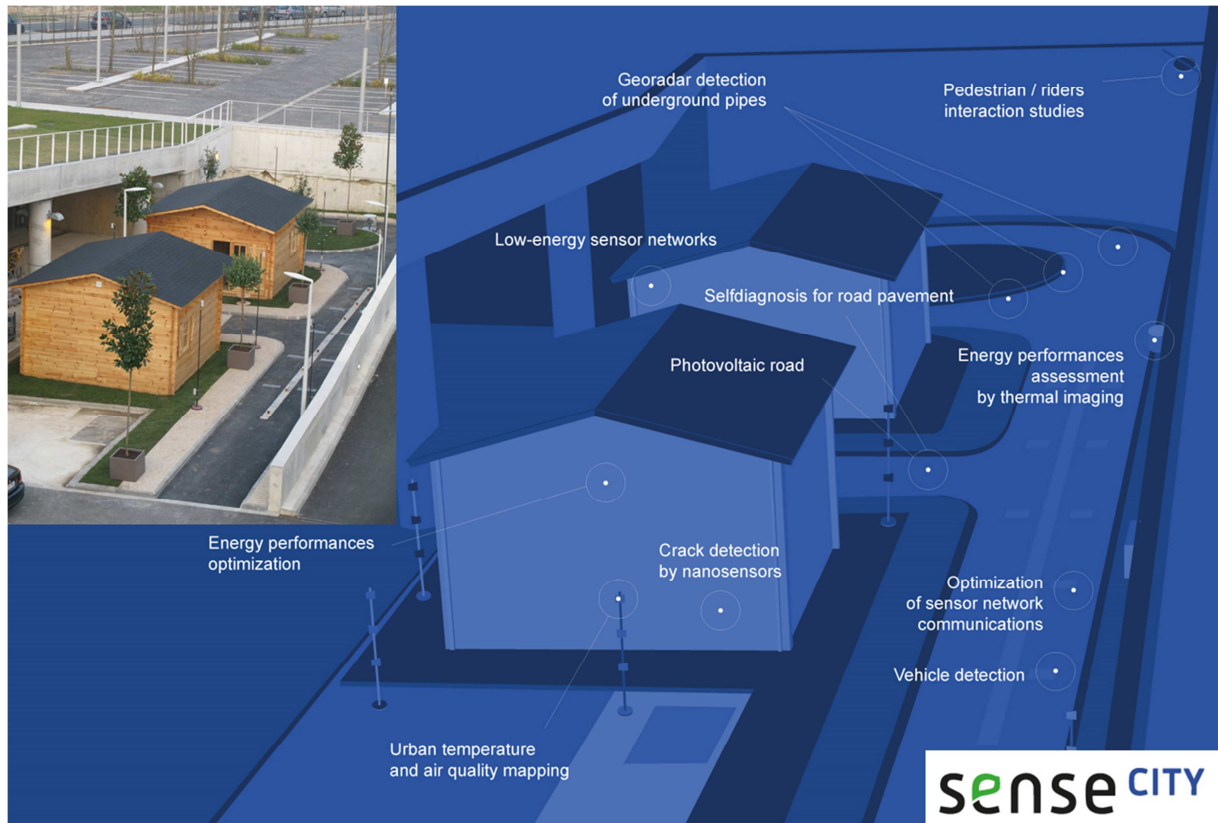


Figure 6: Ongoing experimentations in Sense-City connected district (inset). This urban scenario, located in IFSTTAR's Bienvenue building, was inaugurated in March 2015.

1.3. Nanosensors: a key-enabling technology for urban monitoring

Considering the quick rise of Nanotechnologies in the last 20 years (see Figure 7), it appears natural that nano-enabled Smart Systems have been repeatedly proposed as a solution to these long standing bottlenecks of urban sensing.

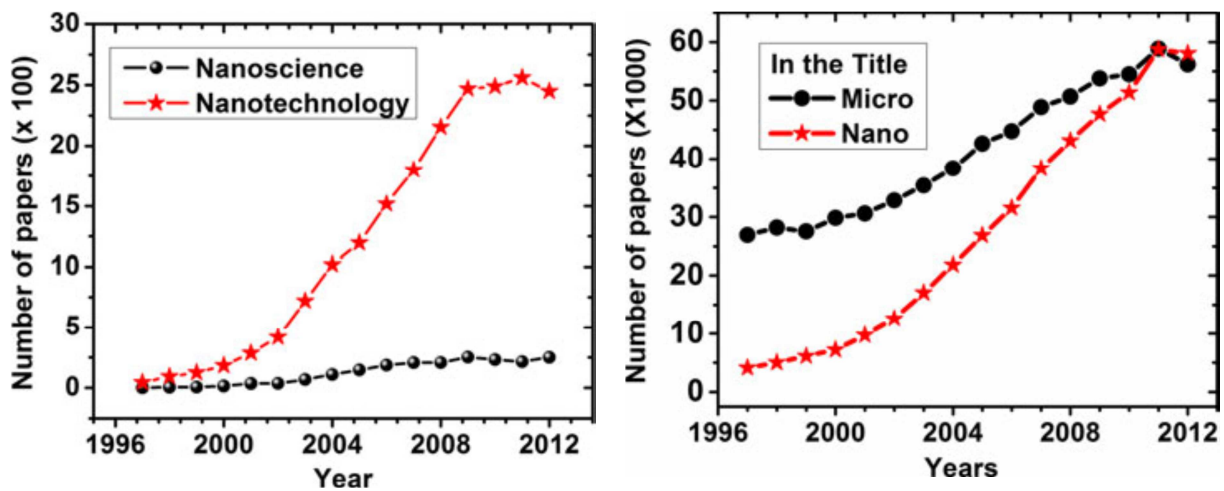


Figure 7: Number of published research articles from 1996 to 2012 containing the following keywords: left) "nanotechnology" and "nanoscience"; right) "micro" and "nano" [Munoz-Sandoval 14]

Strictly speaking, the whole of the Internet of Things is actually a product of nanotechnologies, because its connected devices incorporate microprocessors. And each of those contains billions of CMOS transistors who *are* nano-enabled: they contain thin films that are less than 100nm thick and their channel length is now considerably smaller than 100nm. However, this is not a common acceptance: usually the microprocessors and below 100nm-node transistors are considered products of the microelectronics industry, and not directly nanotechnology products. In what follows, we will thus focus on "pure" nanotechnology issues.

Setting thus aside in the rest of this discussion the trillion-dollar worth issue of the CMOS electronics, nanotechnologies are still expected to provide the next generations of building blocks for Smart Systems. R&D work is going on strong in topics such as:

- Miniaturized antenna for high frequency communication [Llatser 12]
- High-power density batteries [Gohier 12]
- High performance interconnects [Maffucci 08]
- Beyond CMOS electronic building blocks (memories, switches, transistors) [Vlasov 12]
- Enhanced sensing devices [Cui 01].

This last topic, nano-enabled sensing devices, in short nanosensors, has been the focus of my own work since 2007. Roughly, the field has generated 25 000 scientific papers over the last 15 years (see for instance detailed SOTA of carbon nanotubes sensors in Appendix 2). The relevance of the "nanosensor" topic for urban monitoring stems from the following findings:

- Their small size enables highly localized [Lebental 10] and highly sensitive [Qi 03; Bondavalli 09] measurements.
- Small size also leads to low energy consumption [Cho 07] and could thus foster sensors deployment in autonomous systems [Basset 09, Michelis 15b].

- Moreover, small size enables sensors multiplexing [Chen 09, Angelescu 08], thus yielding more precise, more flexible and richer measurements (**see for instance our Proteus project**).
- They can be fabricated in large number and at low cost [Cao 08], so could be used in massively distributed sensors networks and for general public applications.

However, the field drastically lacks contributions on two of the critical topics listed above in Section 1.2.2 as bottlenecks for urban monitoring via nanosensors:

- Enhanced resilience and reliability, proven in the environment of use
- Lower cost and improved manufacturability

1.4. Outline of the manuscript

Because of the applicative criticality of these two topics and because of their scientific originality in the field of nanosensors, these two topics have served as guidelines for my work. This is what this manuscript reports on.

As I elected to develop my research using nanocarbon (graphene, carbon nanotubes and associated materials), the chapter 2 includes a quick overview on nanocarbon-based technologies, especially sensors. After discussing the different type of sensors we developed, the document focuses on the reproducibility of carbon nanotube-based strain gauges and on their actual deployment in the field for embedded monitoring of concrete (chapter 2).

Along the way, it appeared that evaluating the reliability of nanodevices is critical for their future applicability. Chapter 3 presents my research on this topic, which aims at creating an experimental and numerical framework for the field of “nanoreliability”. Along this path, we contributed notably a noise-resilient methodology for interpretation of Raman spectroscopy in carbon, or a new model for dense, multilayer networks of wavy carbon nanotubes.

This work has opened a very wide range of research (and development) directions, among which I sorted out to identify the most likely trends for my future work (chapter 4).

2. Nanocarbon-based sensors: from design to deployment

2.1. Nanocarbon-based sensors: state of the art

Nanosensors are electronic devices whose sensing performances are enabled or enhanced by the incorporation of nanomaterials. As such, fabricating nanosensors first requires to

- To produce (or buy) nanoparticles,
- To manipulate these nanoparticles to incorporate them into an electronic device,
- To characterize electrically the resulting devices,
- To study how the electronic properties correlate with the property (or properties) to be sensed.

My work covers these four stages, either directly or via collaborations, applied to nanomaterials based on carbon allotropes, in short nano-carbon.

Though it is now a commonplace in the literature (1 400 000 search returns for the keywords “nano” AND “carbon” on Google Scholar since 2000), let us briefly summarize what is nanocarbon, why it has attracted so much attention in the literature, and what kind of sensors it has helped provide.

The term nanocarbon is actually a neologism that designates a nanomaterial based mostly on carbon atoms. Nanocarbon notably includes all of the nanomaterials derived from carbon allotropes, notably sp^2 or sp^3 hybridized carbon, amorphous or hydrogenated carbon (Figure 8). Combinations of different allotropes are also possible, such as textured carbon (amorphous carbon matrix with oriented, graphite-like inclusions) [Xu 12].

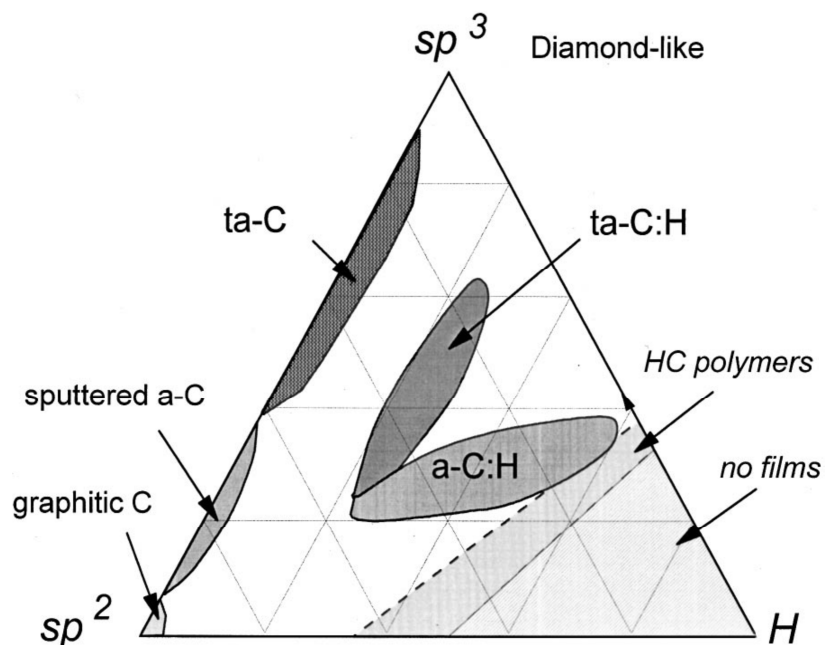


Figure 8: Ternary phase diagram of amorphous carbons. The three corners correspond to diamond, graphite, and hydrocarbons, respectively. [Ferrari 00]

Sp^2 carbon based nanomaterials include graphene, carbon nanotubes and fullerenes, and their derivatives (multi-layer graphene, single- or multi-walled carbon nanotubes, metallofullerenes, doped or functionalized graphene or CNT, graphene sandwiches with other 2D materials...). Sp^3

nanocarbon includes the nanomaterial forms of diamond, such as diamond nanoparticles and diamond thin films (see Figure 9).

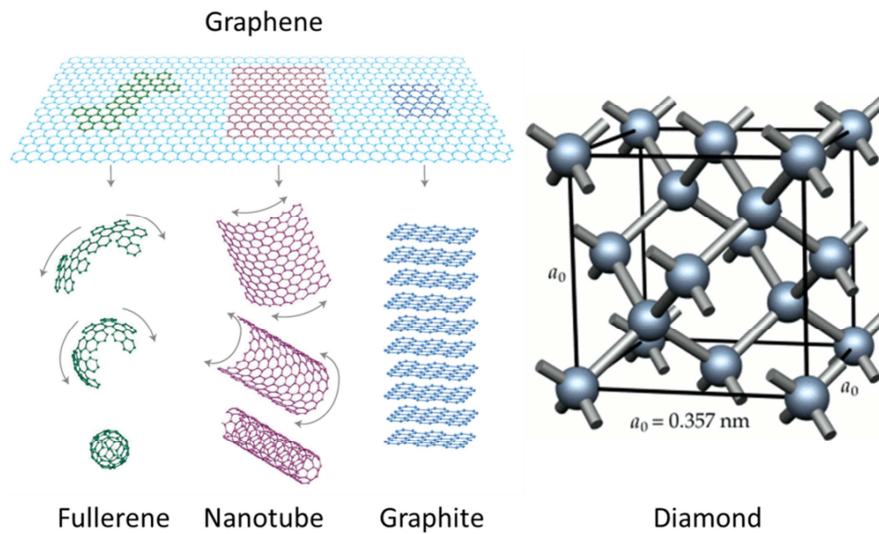


Figure 9: sp^2 and sp^3 forms of carbon

The exceptionally intense enthusiasm for these materials partially stems from historical reasons: being natural materials with highly uncommon properties (mechanical, optical, electrical, thermal...), graphite and diamond have been studied for centuries by material scientists. Their band structures were calculated analytically over 50 years ago, including that of graphene (at the time only a theoretical material) [Heine 69, Slonczewski 58]. So when fullerene [Kroto 85], carbon nanotubes [Iijima 91] and graphene [Novoselov 04] were finally isolated, researchers finally got the chance to observe experimentally the properties that had been predicted decades ago, and to update long standing dreams (such as that of the space elevator²¹).

Let us provide examples of the exceptional properties of nanocarbon [Smalley 03, Allen 09, Mochalin 12]: graphene and carbon nanotubes feature electron mobility reaching respectively 200,000 and 100,000 cm²/V.s, respectively 140 times and 70 times in excess to that of silicon (1,400 cm²/V.s), which is interesting for electronic applications. For flexible electronics and for electromechanical applications, they feature a Young's modulus (1TPa) 5 times in excess of that of steel (200GPa), with an extremely low thickness in their sp^2 form (0,34nm for graphene, 1nm to 10nm for carbon nanotubes with high crystalline quality) enabling good flexibility. Carbon nanotubes and graphene can also be deformed reversibly up to one third of their initial size. For thermal dissipation issues, nanocarbon materials have a thermal conductivity (around 2000W/m/K for graphene, and 3500W/m/K for carbon nanotubes, 2300W/m/K for diamond) roughly 5 to 10 times higher than copper (390W/m/K), the material presently used in interconnects. In addition, nanocarbon features very good chemical stability (oxidation in air at 700°C, fusion temperature in vacuum at 4000°C) with highly diversified functionalization options.

To exploit these properties, nanocarbon materials are used in a wide range of applications (see for instance [DeVolder 13]):

²¹ <http://www.niac.usra.edu/studies/521Edwards.html>

- in all types of electronic devices: field effect transistors in various geometries (bottom or top gates, double-gated, suspended gate...), small logic gates, interconnects, (transparent) electrodes, capacitors, memory devices, electromechanical switches, antenna, batteries, energy harvester (thermoelectric, photovoltaic)...
- as filler materials in nanocomposite materials (any bulk material incorporating nanoparticles, notably polymers, concrete, bitumen), for mechanical reinforcements or to create self-sensing materials.
- in water filtration systems
- for drug delivery and drug therapy.

Regarding to the specific topic of Sensors (see for instance detailed SOTA on carbon nanotube gas and chemical sensors in Appendix 2), the most popular application (in terms of publication number) is liquid- and gas-phase chemical and biological sensing (for instance [Liu 12, Llobet 13, Yang 15]):

- various gas such as vapor water (relative humidity), O₂, O₃, NO₂, NO, NH₃, H₂, H₂S, H₂O, DMMP, TNT, acetone, ethanol, nitrotoluene, various volatil organic compounds such as formaldehyde and hydrocarbons or biomarkers in human breath
- various chemicals such hydroxide ions (pH), chlorine, heavy metals,
- various biological species such as peptides, proteins, enzymes, glucose, or other biomarkers in saliva or blood

What makes nanocarbon such popular material for chemical and biological sensing is

- on the one hand the high adsorption capability of analytes on sp² carbon and the high surface over volume ratio of carbon nanotube and graphene, enabling high sensitivity,
- on the other hand the wide range of available chemical and biological functionalization, enabling selectivity.

Other very popular sensing applications for nanocarbon are strain sensing, (water) flow sensing, thermal sensing (including via infrared detection).

In most of these sensing applications, sensing is demonstrated either via purely electronic, or electrochemical, or electromechanical, or optical phenomena, namely:

- Electronics: resistor with resistance or capacitor with capacitance depending on the environmental parameter under study, field-effect transistor devices with transfer characteristics depending on the environment, small logic gates with operating parameters depending on the parameter under study...
- Electrochemistry: nanocarbon as electrode materials or as coating for traditional electrode materials, with the features of the voltammetric (I-V) curves obtained with these electrodes depending on the environment.
- Electromechanics: nanocarbon as coating or directly as moving material in electromechanical devices (usually microscale devices, or ultrasonic transducers), with usually the resonance frequency (sometime also the amplitude of vibrations) of the device being monitored.
- Optics: properties of light reflection, absorption, transmission or emission (fluorescence) of nanocarbon materials being modified by parameters in the environment.

2.2. A repertoire of carbon nanotubes and graphene sensors

Among this state of the art, I have contributed a wide range of results via PhDs and MScs internships. Only a small fraction of this work is published in peer-reviewed journals, due to either lack of time or lack of opportunity for (relatively) high impact factor publications. The rest has been capitalized either in conference proceedings, in PhD thesis or in internship reports.

2.2.1. Humidity sensors

In [Lee 12] (Chang Soek Lee and Waleed Moujahid PhDs), we demonstrated that a ohmic device based on interfacial few-layer graphene on glass (low temperature - 450°C - PECVD graphene grown at the interface between a Nickel thin film and glass, featuring nanocrystallinity) with inkjet-printed silver electrodes could operate as a relative humidity sensor (Figure 10).

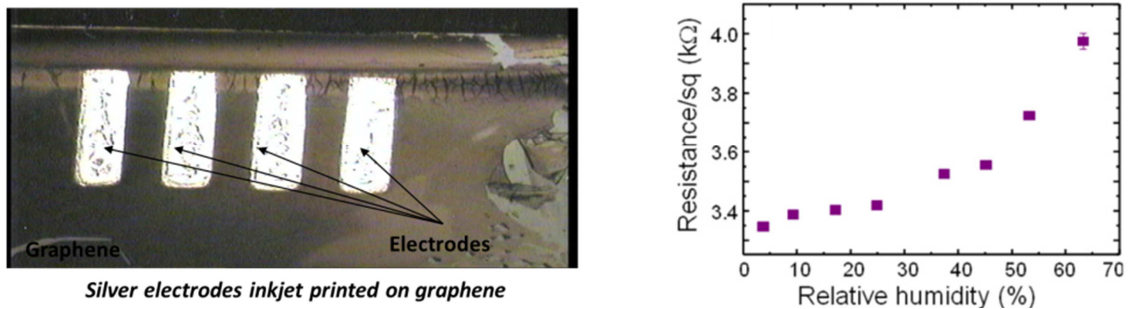


Figure 10: Humidity sensing with interfacial graphene on glass

In Evgeny Norman's PhD thesis [Norman 11], we studied the humidity sensitivity of CNTFETs on Silicon. In the considered devices, CNT were single-walled, grown directly in place (without transfer) by CVD. We demonstrated strong humidity sensitivity, particularly above 60%RH. All of the transfer characteristics of the transistors appeared to be sensitive to humidity, notably the threshold voltage of the CNTFET. This property was exploited in [Cojocar 11] to demonstrate a CNTFET-based inverter used as humidity sensor. A major drawback of these devices used for humidity sensing is their major device-to-device variability (in terms of electronic and sensing performances) (Figures 11 and 12).

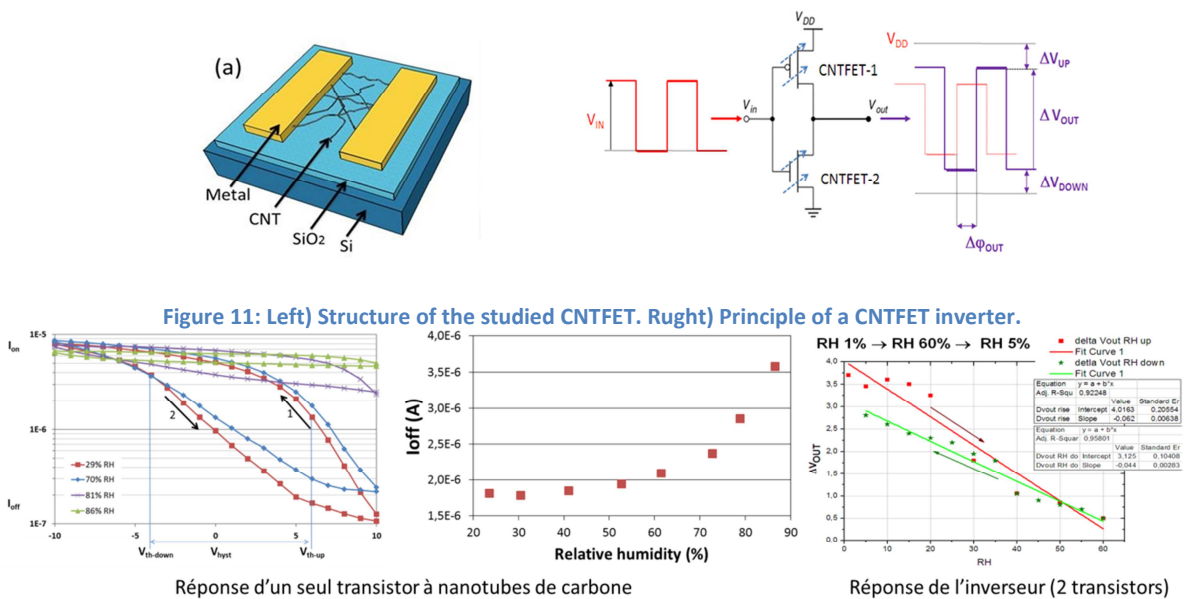


Figure 11: Left) Structure of the studied CNTFET. Right) Principle of a CNTFET inverter.

Réponse d'un seul transistor à nanotubes de carbone

Réponse de l'inverseur (2 transistors)

Figure 12: Left) Transfer characteristics of a CNTFET at different humidity levels. Middle) Sensitivity of the OFF current to humidity. Right) Sensitivity of the CNTFET inverter to humidity

Finally, in Fulvio Michelis PhD thesis [Michelis 15a], we demonstrated the humidity sensitivity of ohmic devices based on random networks of multi-walled carbon nanotubes inkjet-printed on polymer (ETFE) on top of evaporated gold electrodes. (Figure 13 and Figure 14)

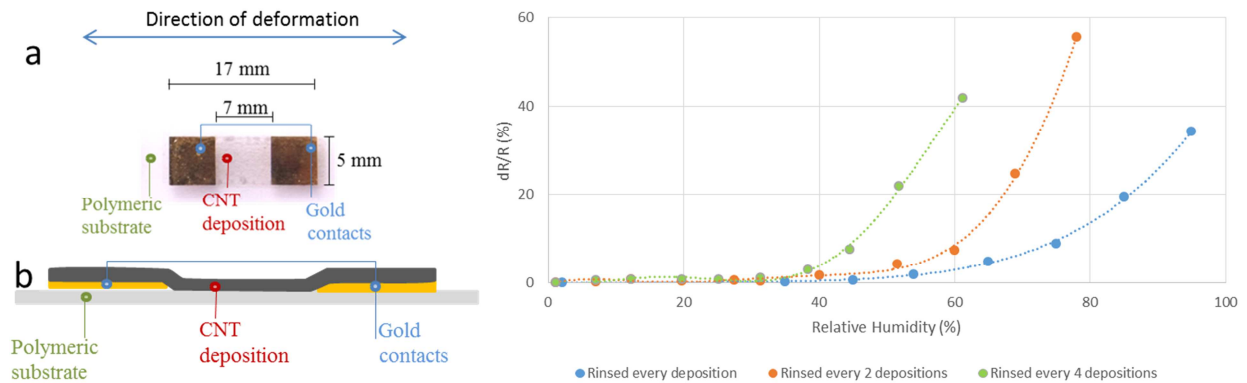


Figure 13: Left-a) Image of a ohmic device based on random networks of multi-walled carbon nanotubes inkjet-printed on ETFE. Left-b) Schematics of a device. Right) Relative humidity sensitivity of the device (sensors resulting from three slightly different fabrication processes are considered).

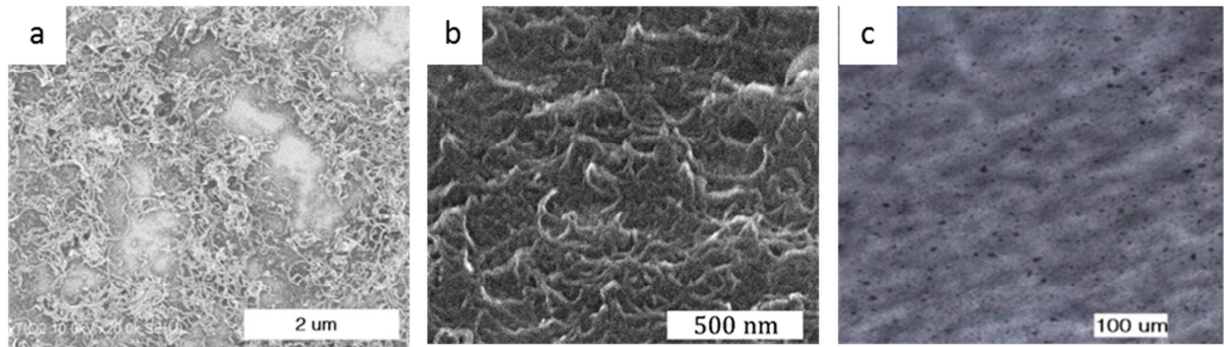


Figure 14: a) SEM image of 1-layer deposition of MWNT by inkjet printing. Micrometric holes are observed in the layer; they are attributed to loss of matter during rinsing. b) SEM image of a 20-layer deposition (number of layers commonly used in the results presented here). A uniform coverage can be observed. c) Optical microscopy image of a 20-layer deposition, showing homogeneity and uniformity at a micro scale.

A common denominator of all these results is that the sensitivity only starts from roughly 30% RH upward and increases strongly above 60% RH. Roughly summarized, an increase of resistance and a decrease of mobility are observed with increasing relative humidity. Though we did not carry out an exhaustive study of the phenomenon, there is a strong suspicion (based on the literature) that this sensitivity is mediated by the substrate, especially in devices on silicon and glass where water molecules are known to adsorb on Silicon surface defects [Lebental 14b].

2.2.2. Strain sensors

One of our focuses has also been strain sensing using ohmic sensors based on percolating networks of nanoparticles. The principle of operation is based on a very classical effect, the piezoresistivity of percolating networks (for instance [Gong 14]). Indeed, in a percolating network, the resistivity is determined mostly by the number of percolating paths over the network. If tensile (resp. compressive) strains are applied, the number of contact points between particles decreases (resp. increases) because the average inter-particle distance increases (resp. decreases), so the number of percolating paths consequently decreases (resp. increases). There may be a contribution from the change in resistivity of the particles themselves, but it is usually very small and quasi-systematically

neglected. In networks close to the percolation threshold, there is also a significant contribution of the tunnel resistance between particles in the total resistance. This resistance is exponentially dependent on the interparticle distance and thus is very sensitive to strain.

In our work, we observed piezoresistivity in two types of percolating networks high above the percolation limit:

1) Devices based on multi-walled carbon nanotubes ink-jet printed on top of gold electrodes, the gold electrodes themselves evaporated on thin ETFE layers (same device architecture as in Figure 13, left). The devices were studied for strain sensitivity **[Lebental 15c]**. The strain gauge factor was found to be $0.9 \pm 15\%$ over 8 devices, while the temperature sensitivity on the resistance was found to be $0.1\%/^{\circ}\text{C} \pm 8\%$ over 7 devices. This device architecture is not original *per se* [Dharap 04], but was developed to serve as a starting block to study other concepts, namely nanosensor reproducibility and deployment (see Sections 2.3 and 2.4) (Figure 15).

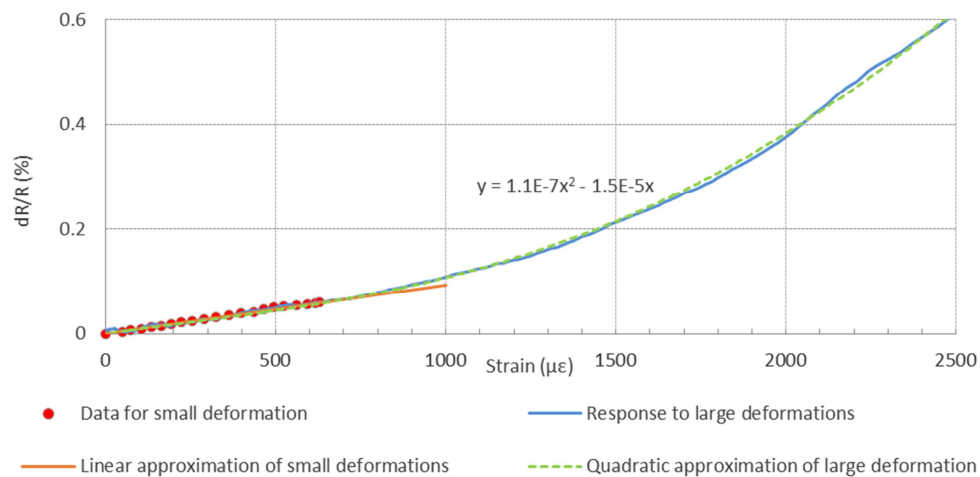


Figure 15: Piezoresistive behavior of a CNT network-based strain sensor. The linear regime reaches up to about 700 μ ϵ here. The average gauge factor is $0.9 \pm 15\%$ over 8 devices.

2) Devices made out of composite nanoparticles, drop-casted on polymer (ETFE), fiberglass, or even asphalt, and contacted top-side by silver paste and/or copper/aluminum thin sheets, were also studied. Device footprint varied between 1cm^2 and 100cm^2 . The particles themselves are specially made for our purpose by Eduardo Ruiz team at CSIC Madrid using a patented CSIC process with particularly low cost raw materials (clay, sugar) [Ruiz 11]. The particles (Figure 16) consist of partially graphitized carbon wrapped around clay (sepiolite) particles, mixed with (commercial) multi-walled carbon nanotubes at very low concentration ($<0.5\text{wt}\%$). This work was started out with the BSc intern Birger Hennings from Columbia and then continued by Boutheina Ghaddab in her post-doc **[Ghaddab 14]** and by Océane Antoine (MSc intern). It is now pursued by Edoardo Milana (research engineer). It gave rise in 2014 to the asphalt sandwich concept (Figure 17) for vehicle weigh-in-motion (Figure 18) patented in 2014 **[Lebental 14a]**. The technology transfer of the associated prototypes is now in progress within the framework of SmartR maturation project with SATT Paris Saclay.

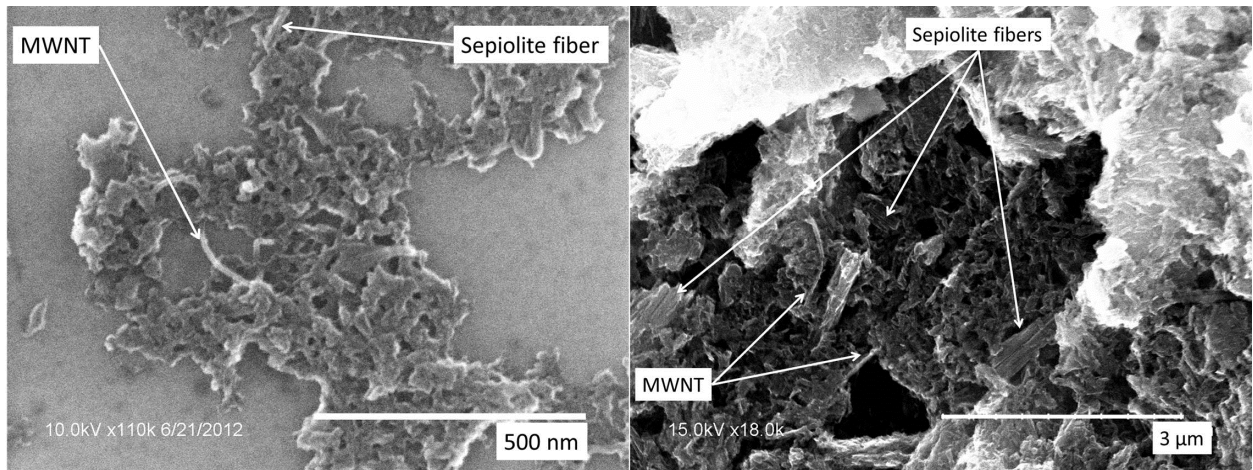


Figure 16 : SEM images of the carbon-sepiolite-MWNT (C/Sep-MWNT) nanoparticles (0.5% wt MWCNTs) at different scales. Well separated MWNTs and sepiolite fibers are encased in a disordered, porous carbon matrix.

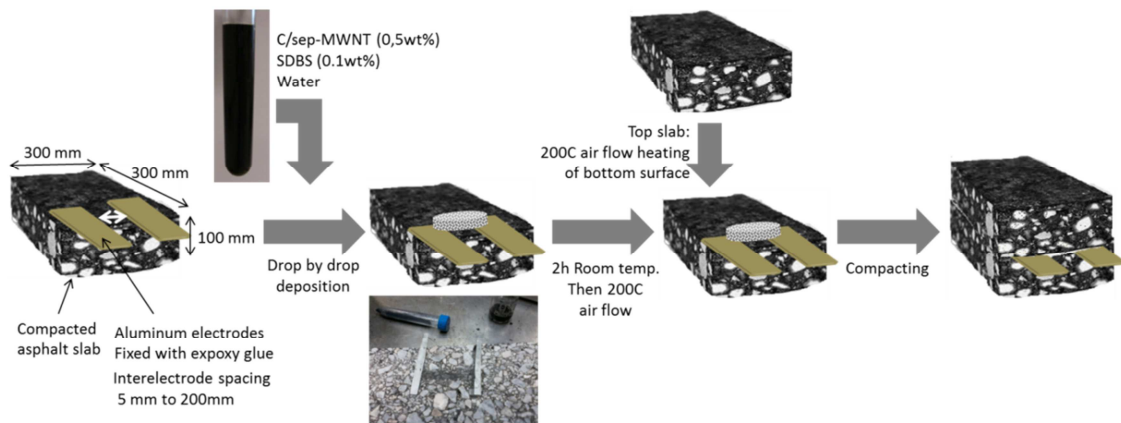


Figure 17: The asphalt sandwich: fabrication process. A layer of C/Sep-MWCNTs particles is deposited directly on a precompact asphalt slab and a pair of electrodes.

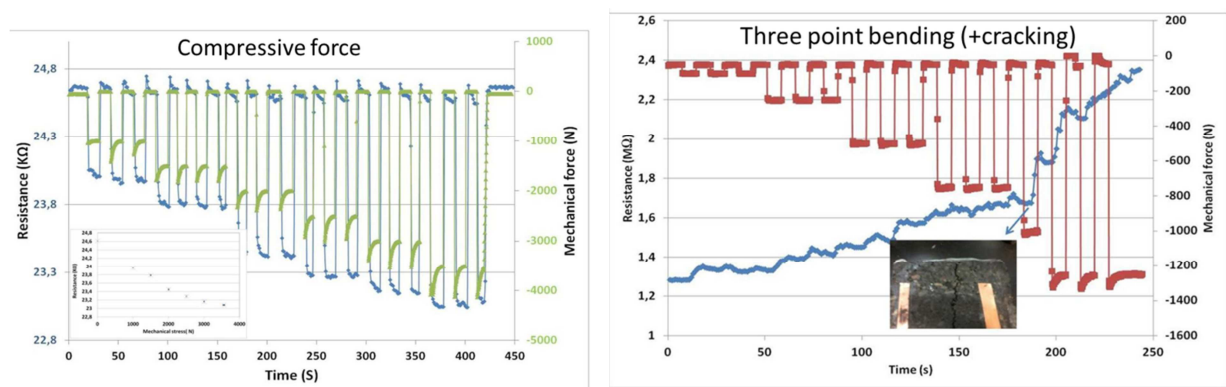


Figure 18: Response of the asphalt sandwich to compressive force and three-point bending.

2.2.3. Chemical sensors

In the last three years, we have started investigating the chemical sensing potential of carbon nanotubes devices, motivated by three main reasons:

- First, the larger panel of available observables to study (each different analyte concentration can be seen as a different observable), providing the opportunity for long-term developments
- Second, the extremely wide panel of applications, especially in environmental and health issues, that are of strong interest to me
- Third, the middle-term opportunity to actually verify some long promised concepts in nanosensor research, namely the capability to get selective sensing via functionalization strategies.

We started out by studying pH sensing (Fulvio Michelis, Benjamin Caduc internship, Yaowu Zhang apprenticeship), pH being the most elemental observable: we proved that, provided a proper device conditioning, the CNT ohmic devices on ETFE used for strain and humidity sensing (see Figures 13 to 15), could also serve as pH sensors (see Figure 19).

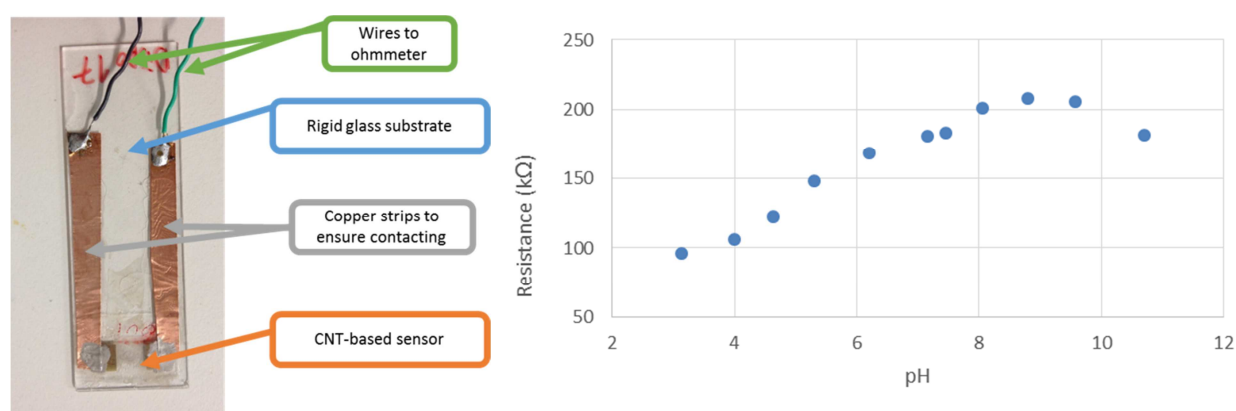


Figure 19: Left) Conditioning of a CNT sensor for pH sensing. Right) Sensitivity of the resistance to pH.

Now, within Proteus project, in strong collaboration with Gael Zucchi (LPICM) and Laurence Bodelot (LMS), along the course of the postdocs of Alfredo Gutierrez, Loic Loisel, Mallesham Godumala, Sasikumar Ramachandran and of the PhD of Yang Wang Xin, we have been able to move on to more sophisticated observables beyond pH.

We have adapted the fabrication process of the CNT ohmic sensors for printing on Silicon chips (provided by ESIEE for the purpose of Proteus project). Device footprint is now in the range of 1mm². The process is carried out not only with pristine MWNTs, but also with MWNTs non-covalently functionalized by conjugated polymers specially designed and fabricated to be sensitive to specific analytes (at this time, chlorine, chloride, lead, hardness). Our current results, to be enhanced and published in the next few months, strongly suggest that our approach enables selective sensing between pH, Chlorine and Chloride. A patent submission being in progress, no more details can be provided here.

2.3. The state of the art in reproducibility for sensors based on CNT networks

From this, it should be clear that we have developed a relatively wide repertoire of nanosensors, mostly based on carbon nanotubes and derivatives. Throughout this work, the most common issue that we encountered was reproducibility:

- If devices cannot be produced reproducibly in at least small batches, the sensitivity cannot be assessed (and understood) reliably.
- If the sensitivity is not reproducible from one device to another, the devices cannot be used in further applications.

Actually, we realized that this was a fairly general and mostly unsolved problem in the literature, especially for carbon nanotube sensors on flexible substrates. For instance, Table 1 in Appendix 3 presents the July 2015 state of the art on reproducibility of sensors based on carbon nanotube networks on flexible or rigid substrates. As we published in **[Lebental 15c]** (see Appendix 4), we observed in the literature that while the variability on the fabrication process is frequently studied (11 papers over 35), very few references (only 7 over the 35 reported here) address the issue of variability on device sensitivity. The studies that address it compare only the sensitivity of very few devices (up to 4) and provide no satisfying analysis of standard deviation on the sensitivity. This appears to be true for all types of carbon nanotube sensors reported to this day, both on rigid and flexible substrates, either for mechanical, chemical (gas and liquid phase) or light sensing.

Based on this literature review, we then concluded that our CNT strain sensors on ETFE actually made the state of the art in 2015 regarding to sensitivity reproducibility. Regarding to the fabrication process, the variability on our device initial resistance was studied for 5 different batches of sensors from 3 to 72 devices each. The variability ranged between 8.4% and 43% depending on the size of the batches, with a 20% average. Regarding to sensitivity reproducibility, an 8-device batch with 15% variability on initial resistance was further studied for variability on the strain and thermal sensitivity. Standard deviation values were found to be as low as 16% on the strain sensitivity and 8% on the temperature sensitivity. Moreover, the devices were found to be hysteresis free, a rare achievement for CNT strain sensors on plastics.

As we will see in the next chapter, this success in terms of reproducibility was essential to subsequently achieve field deployment of nanosensors, as it enabled us to design the acquisition circuit that is required to transform any transducer signal into a signal compatible with a connected device.

2.4. Deployment of nanosensors for embedded monitoring of construction materials

This result on CNT sensor reproducibility enabled us to consider the actual deployment of these sensors in the field. This work was done within Fulvio Michelis PhD thesis, in strong collaboration with Jean Marc Laheurte (ESYCOM). It is reported notably in [Michelis 15b] and [Laheurte 16], as well as in Fulvio Michelis PhD Thesis [Michelis 2015a]. A peer-reviewed paper is also being prepared.

First thing first, why is reproducibility critical for field deployment? To use a nanosensor in the field, it needs to be plugged into an acquisition system, preferably a connected device (to use an Internet of Things denomination) that will convey the sensor information to the end user. Compared to “traditional” acquisition cards such as the well-known products from National Instruments, the use of connected devices is expected to constitute a more versatile, more easily upscalable and (hopefully) more resilient (to field conditions) solution.

In any case, the critical part consists in converting the nanosensor output (a varying resistance for ohmic sensor, a varying transfer characteristic for transistor, a varying resonance frequency for electromechanical sensor) into a tension (-5V to +5V; 0 to 3.3V...) that can be fed into the Analog-to-Digital Converter of the acquisition system. This is the role of the “conditioning circuit”. It is precisely the design of this conditioning circuit that requires for the electronic response of the nanosensor to be reproducible from one device to the other.

The reproducibility we achieved on the CNT strain sensors, 15% standard deviation in resistance and strain sensitivity, 8% in temperature sensitivity, enabled us to propose an interesting conditioning electronics, whose schematic is depicted in Figure 20. Its forces are its capability to compensate for the temperature sensitivity of the strain CNT sensors (temperature-related error: 0.12%/°C only) and its low power consumption (<400μW). Other advantages are its relatively low number of components (15), enabling subsequent low cost fabrication, its low noise (SNR>30dB) and its small size (3cm²). These performances are important in view of the desired application for urban monitoring, which requires the sensor use in wireless, autonomous, low-cost sensor nodes.

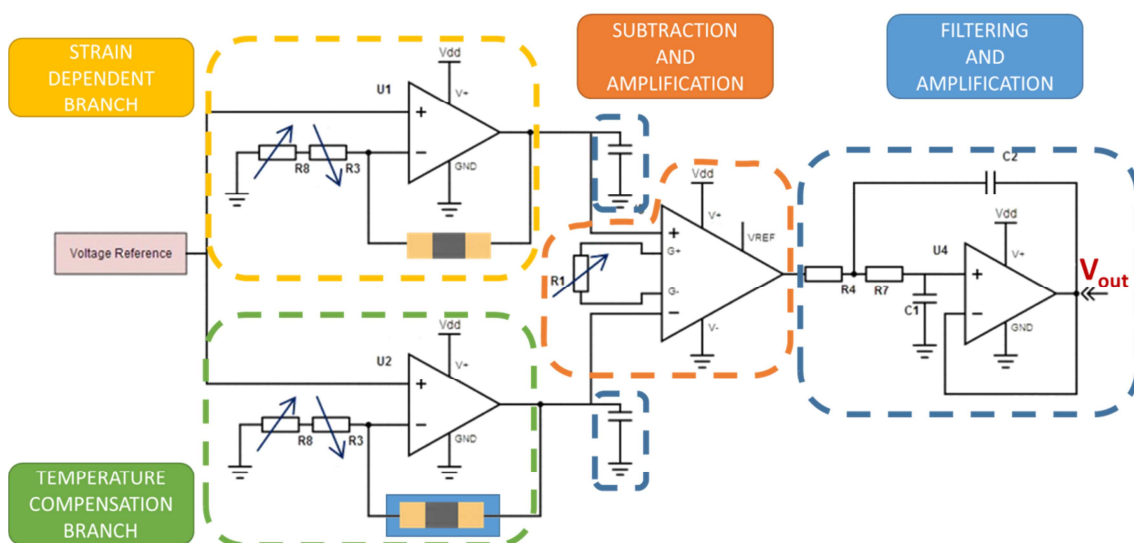


Figure 20 : Temperature-compensated electronics for CNT strain sensors. The normalization of the resistance is achieved with a non-inverting amplifier. Temperature compensation and signal amplification are achieved by means of a differential instrumentation amplifier.

The design of the conditioning electronics itself may be relatively independent from the application. But the choice or the design of the connected system is fully determined by the use case. The use case on which we focused is the structural health monitoring (SHM) of concrete materials from the inside, via sensors directly embedded in the volume of the material. The advantage of this approach is to enable early detection of detrimental processes (cracking, swelling, shrinkage, reinforcement corrosion) occurring in the structure. It is generally accepted that in case of degradations in concrete structures, the earlier the repairs the lower the economic and environmental costs.

In his thesis, Fulvio Michelis designed a RFID, battery-powered connected device suitable for embedded monitoring of concrete materials via CNT-based strain sensors. The device integrates a commercial RFID chip, the conditioning circuit for the nanosensor and an antenna specially designed for communication within concrete [Laheurte 16] in a dedicated package. As a result, the resulting system in only 43cm³ in volume and 1.5cm thick, 3 times smaller than the current SOTA for embedded nodes for concrete monitoring (Figure 21). Wireless communication through mortar is demonstrated up to 5cm.

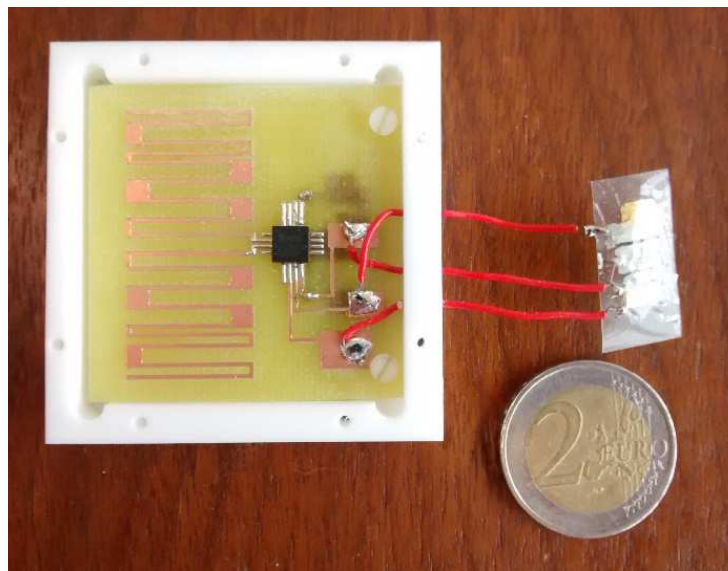


Figure 21: CNT strain sensor assembled with its conditioning electronics and its RFID tag for concrete monitoring. All the electronics beside the sensor itself is enclosed into a protective Teflon box with silicon sealing.

The CNT sensors and their conditioning electronics have actually been embedded in Sense-City first scenario, “the connected district” since early 2015 (for more details on Sense-City, see section 1.2.3), within the foundation of one of Sense-City house (Figure 22). The sensors outputs were analyzed for 6 month after embedding, and some nanosensors remain alive after almost two years. This experiment constituted the first deployment of nanosensors within a scale one structure.

We observed that 57% of the CNT sensors had survived after 6 months of embedding, to be compared to a survival rate of only 11% for commercial strain sensors embedded at the same time as the CNT sensors. Results also suggested that the sensors were able to track the microscale deformations of the concrete slab due to day-to-day temperature variations.

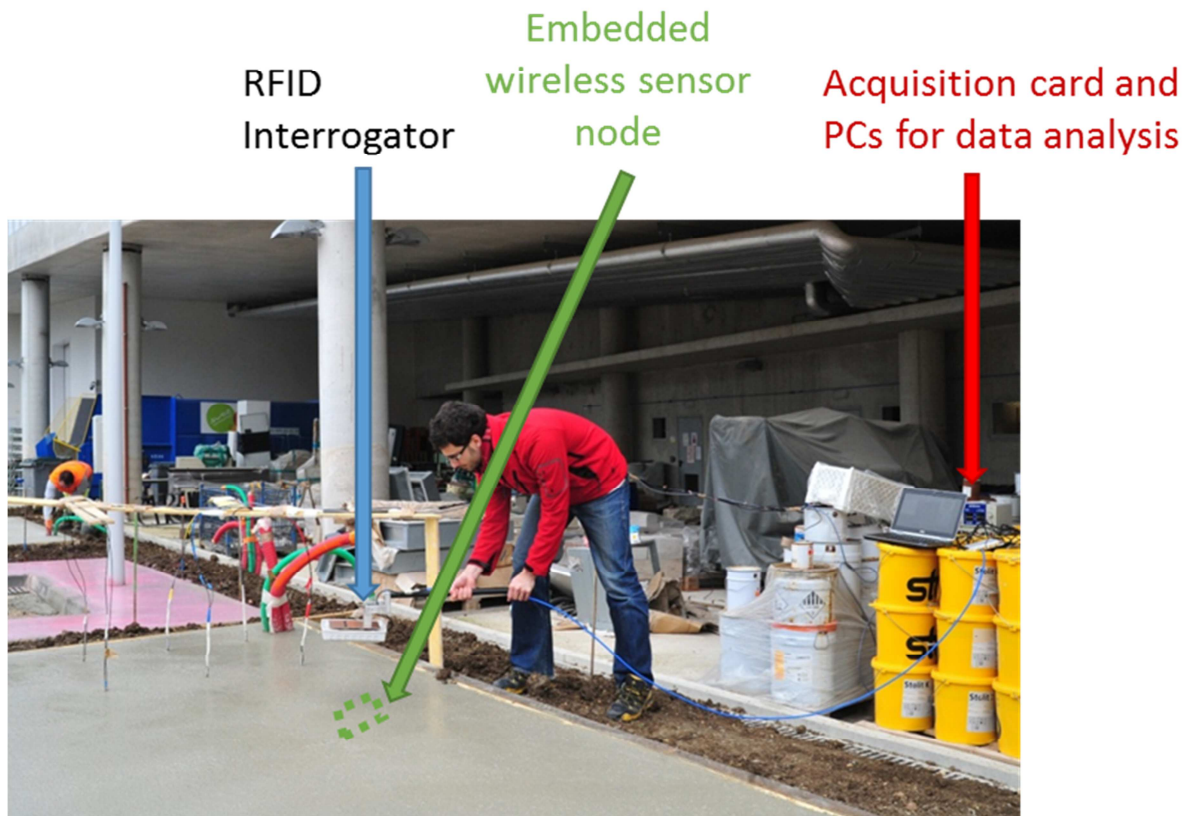


Figure 22 : Fulvio Michelis interrogating an embedded RFID tag right after casting of the concrete slab.

Though a lot remains to be figured out to enable the actual industrial use of CNT sensors within concrete for SHM applications, the work that was carried out constitutes a solid proof of concept for embedded monitoring of concrete via nanosensors.

2.5. Conclusions

To summarize, we contributed to the field a relatively wide repertoire of nanocarbon-enabled sensing devices for humidity, strain and chemical monitoring. Our research has focused on the reproducibility of the devices, namely reaching the state of the art for CNT flexible sensors. Armed with this success, we have been able to achieve the full electronic integration of our CNT strain sensors into a specially-designed RFID node for embedded monitoring of concrete. The resulting node is 3 times smaller than the state of the art of embedded nodes for concrete. It enabled us to provide the first scale-one proof of concept of embedded use of nanosensors inside concrete. We showed the enhanced resilience of our sensors compared to commercial sensors for this application.

However, though these results are definitely promising, “enhanced resilience” cannot be considered enough for most urban applications, especially applications where the sensors are not easily retrievable or replaceable. To be able to consider real life applications of nanosensors, namely to arise industrial interest for these technologies, one needs to *guarantee* their lifetime in given conditions of use. This is why, since the acceptance in 2014 of the SESAME Paris-Region project PLATINE (multi-loading PLATform for In-situ reliability assessment of Nanodevices; partners: Ecole Polytechnique and IFSTTAR), my research has strongly focused on the topic of nanoreliability. The following chapter describes the challenges and some of our achievement in this field.

3. Reliability assessment of nanodevices by multiscale characterizations

3.1. The challenge: to improve the reliability of nanodevices.

Failure mechanisms and lifetime prediction in microelectronics have been crucial topics since the early 60s, namely the early days of the transistor in Bell Labs. Industrial needs have given rise to a sophisticated conceptual framework, whose keystone is the notion of reliability, broadly defined as the probability that a micro component performs its intended functionality without failure under given conditions for a specified period of time.

Reliability studies in electronics and mechanics have had a huge impact in industrial production processes. Standardized procedures are now carried out daily in the industrial world to assess properly the lifetime of marketable products, through the so-called HALT (Highly Accelerated Life Test—to identify the mechanisms of ageing) and HASS (Highly Accelerated Stress Screen—to determine probability of device service expectancy) procedures. The market of entire companies is based on offering chains of equipment to carry out these tests (see for instance the Qualmark Corporation).

HASS or HALT procedures tend to address millimeter-scale issues, generally on integrated components that already have a large market. In those components, failure modes [Wunderle 09] include solders fatigue, strain-inducing moisture-ingress in polymers, moisture-, vibration- or temperature-induced delamination, as well as load-induced cracking.

Nanocomponents challenge this framework because their low-scale properties stem from more-recent, not-fully-understood fields of science, often involving multiphysics phenomena. When size reaches the nanoscale, dramatic changes in electrical conductivity, reaction kinetics, corrosion processes, mechanical strength... have been observed [Greer 05]. Important concepts in reliability engineering, such as fatigue, friction, damping, wear-out and repair mechanisms, have different physical meanings at atomic or molecular scales [Jeng 07].

It is a great obstacle to the market prospects of nanotechnologies; indeed, though the market of nanotechnologies is quickly increasing (\$3trillions in revenues in 2015 worldwide [Sargent 13]) and involving evermore workers (2 million worldwide in 2015 [KET 11]), industrial investments in favor of nanoelectronic devices are drastically slowed by a strong lack of confidence in their reliability. In laboratories also, fundamental and applicative researches toward improved nanoelectronic devices are slowed by the short lifetime of devices.

To reach its heralded potential in terms of marketable products, global revenues and job openings, the field of nanoelectronics requires that the issues of reliability be addressed in depth: acknowledging that existing HALT and HASS procedures work well for microelectronic devices but have not proved their validity for nanoscale devices, academic and industrial stakeholders need to propose reliability assessment procedures that are fully suited to nanoelectronic devices.

Within the PLATINE project, started since 2014, we precisely promote the emergence of “nanoreliability”, a field aiming at identifying failure mechanisms and deriving comprehensive models and figure of merits for nanodevice reliability. PLATINE is actually built as a shared platform between several labs of Ecole Polytechnique (LPICM, LMS, LSI, PMC) and my lab LISIS at IFSTTAR. It is

designed to enable systematical characterization of a wide pool of devices and materials with the goal of determining and optimizing device life time (see Figure 23). It revolves around three axes:

- An in-situ characterization bench for fatigue behavior analysis under complex loadings;
- An ex-situ high-resolution characterization bench for multi-scale analysis of failure mechanisms.
- A chain of modelling tools to provide fatigue-compliant multiscale device models enabling lifetime prediction.

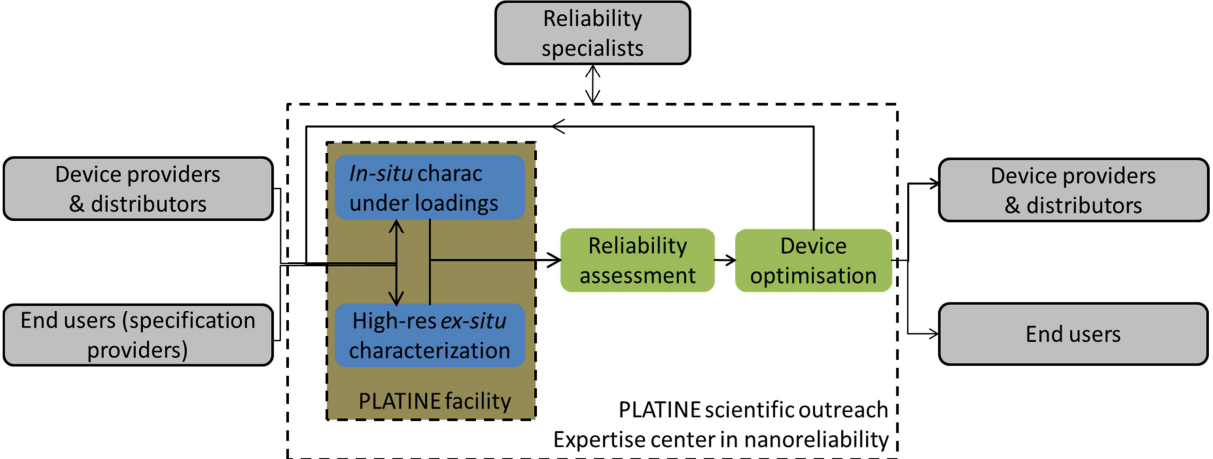


Figure 23: Schematic of the PLATINE project, highlighting the central role of the experimental platform

3.2. PLATINE in-situ characterization bench for fatigue behavior under complex loadings

The first component of PLATINE is its characterization bench enabling the in-situ measurements of nanodevice physical parameters (electrical, thermal, mechanical) during single or coupled loadings (electrical, thermal, mechanical, environmental). Its goal is to identify experimentally the electrical limit states of nanodevices (asymptotic behaviors resulting from cyclic loadings, for instance the concepts of ratcheting—reduced life time—or elastic shakedown—infinite lifetime—in mechanics) and then to determine experimentally the expected lifetime (number of cycles before failure) for these limit states.

The core experimental setup for the platform includes the following subparts:

1. **systems to generate single or coupled loadings,**
2. **systems to image the strain state of the devices during loadings,**
3. **systems to measure the thermal state of the devices during loadings.**

PLATINE equipment #1 is designed to achieve coupled loadings. It consists in:

- a specially-designed integrated 10L environmental chamber (temperature and hygrometry controlled) with optical access (for imaging and for solar exposure) and electrical access,
- a dedicated programmable source measurement unit for simultaneous electrical loading and electrical response measurement,
- a dedicated metrological-level, motor-driven, sensor-controlled, biaxial setup on its antivibration table and compatible with magnetic and environmental loadings,
- a semi-automatic wire-bonder to provide stable contacts for the devices, bonding quality being an essential part of nanodevice reliability,

Regarding to in-situ strain imaging, equipment #2 consists in a high-resolution CCD camera, a high-magnification lens and proper cold lighting units. Processing of the images by Digital Image Correlation (DIC)²² is available to give access to the strain fields at the surface of the nanodevices. Most nanodevices lend themselves well to performing DIC with natural speckle patterns. In a later stage, we are also considering coupling the strain imaging system with a polarimetric imaging set-up suitable for Müller matrix analysis (one of the expertises of LPICM). Preliminary experiments from LPICM suggest strong correlations between Müller matrices and stress-strain states in thin films.

Equipment #3 is dedicated to achieving in-situ thermal imaging. The expected spatial resolution is in the 5 μm range using a high-resolution matrix of detectors and a high-magnification lens. The interest of this building block is to determine where the “hot” spots of the devices are and how their apparition correlates with the degradation of electrical performances. The rationale behind this is that in macro- and micro-mechanics as well as in microelectronics, thermal loading is a major cause of failure, either because it causes intrinsic degradations of the material properties or because it causes mechanical stresses (which themselves cause secondary degradations such as delamination or

²² DIC is based on pattern tracking and requires that the images of the deforming sample exhibit a speckle aspect covering a wide range of gray shades. The reference image is divided into square subsets that, thanks to the speckle aspect, have a unique signature of gray levels. Such subsets can subsequently be tracked in the following images, leading to displacement fields and, by differentiation, strain fields. In most engineering applications, an artificial speckle pattern is created on the object thanks to white and black spray paint but, for high-resolution applications, the texture of the object itself often exhibits a natural speckle aspect.

cracking). Although it is not fully demonstrated for nanodevices, a variety of results suggests that thermally-induced stresses and strains may be the primary cause of failure at the nanoscale too [Jeng 07].

Pieces of equipment #1 and #2 were assembled in 2015 and early 2016, with major involvement from Laurence Bodelot, her colleagues at LMS, and Jérôme Charliac at LPICM, and are only now close to completion (Figure 24). For equipment #3, the infrared camera and associated tools, we (Laurence Bodelot and myself, now assisted by Boris Gusarov, recently recruited as tenured engineer dedicated to Platine platform) are currently in the process of acquiring the desired equipment, to be installed by the end of 2016.

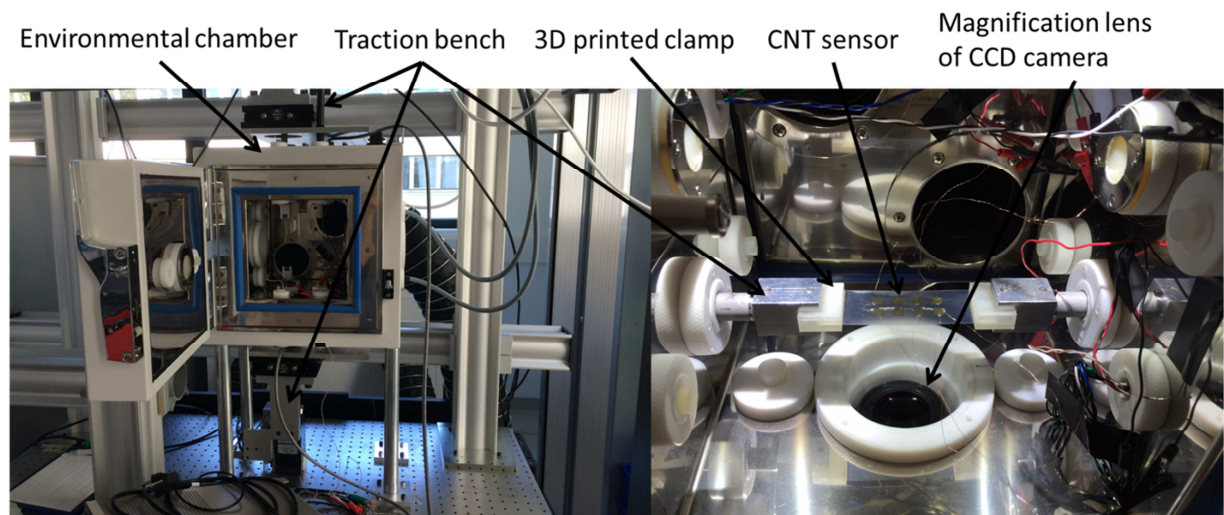


Figure 24: Platine dedicated environmental chamber with integrated traction bench and high-resolution optical imaging.

We have not yet been able to test the full potential of the platform for nanodevices characterization, but preliminary results (obtained with subparts of the equipment) have been for instance published in [Lebental 15c]: we observed the small strain (0.1%) cyclability of our CNT strain sensors, while large strain (0.4%) cyclability showed clear irreversibility (onset of creep) (Figures 25 and 26).

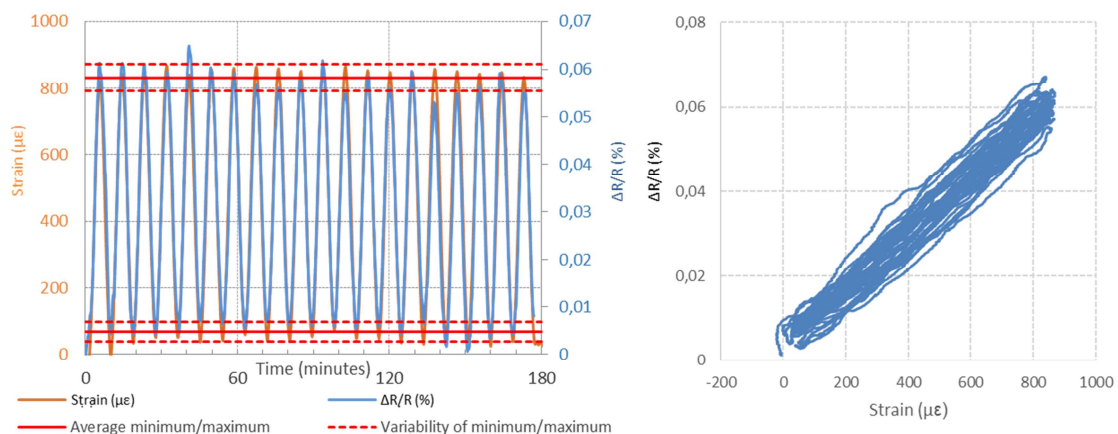


Figure 25 a) Response of a CNT strain sensor to 20 cycles of strains between 0 and 800 $\mu\epsilon$. No evident hysteresis or baseline drift is observed. b) Corresponding resistance-strain plot. The extent of the bundle of resistance-strain curve is due to a slight variability (4.7%) in min and max resistance value. It is attributed to temperature variations in the range of approx. ± 0.3 $^{\circ}\text{C}$.

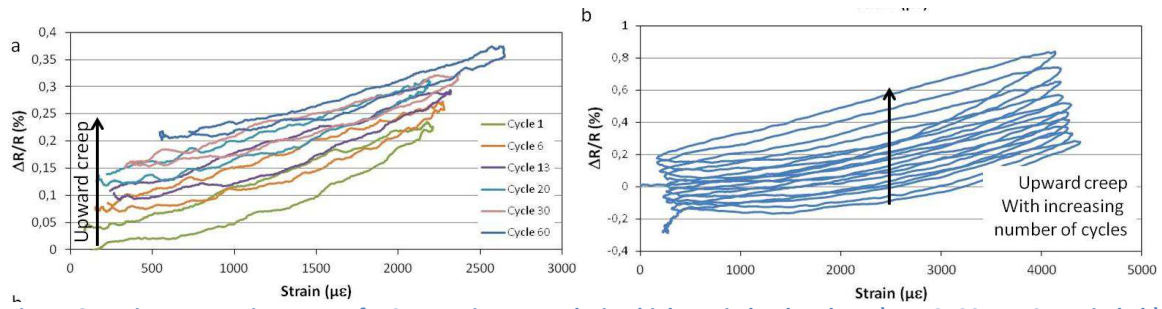


Figure 6: Resistance-strain curves of a CNT strain sensor during high strain load cycles: a) 4N, 2500 $\mu\epsilon$, 10s period ; b) 8N, 4000 $\mu\epsilon$, 5min period

Though such cycling results are critical to understand the ageing behavior of nanodevices, future results are expected to be much more advanced: we aim at providing, with micrometer to millimeter resolution, the location of ageing “hot-spots”, i.e. locations where strain or temperature fields peak and where degradations are initiated.

3.3. Ex-situ characterization to identify the nanoscale causes for failure

To analyze these ageing hot spots, a wide range of high resolution ex-situ characterization tools are available at Ecole Polytechnique: MEB (typically 10 nm resolution), TEM (down to atomic resolution), AFM (0,1 to 10 mn resolution) for high-resolution images of defect areas, Raman mapping (1 μ m resolution) for assessment of crystalline changes. By coupling all of these high-resolution characterization tools with the in-situ characterization bench described above, we plan to analyze ageing hot spots, in order to identify the nanoscale mechanisms responsible for degradations and failure.

Awaiting the full availability of the in-situ characterization bench, we have worked on the coupling of multiple high-resolution characterization tools in view of understanding finely mechanisms of ageing in nanocarbon materials. This was carried out notably in Loic Loisel thesis [Loisel2016a], a partnership between Nanyang Techchnological University (NTU, Singapour) and Ecole Polytechnique. Results were published in [Loisel2015] and [Loisel2016b]. These papers discuss the degradation and phase change of textured carbon thin films (see TEM images of textured carbon in Figure 24) upon annealing by respectively a single nanosecond laser pulse and a continuous laser beam. Both papers combine SEM and TEM with Raman imaging to determine the crystalline nature of the annealed matter and to identify the degradation mechanisms. In both of these papers (as in most of nanocarbon research), SEM yields information on surface features, while Raman spectroscopy is the key to understand at the microscopic scale the crystalline nature of the materials. TEM is then used to confirme at the atomic scale the Raman spectra. The paper [Loisel2016b] is provided in Appendix 5 as an example of this approach.

Along the course of both these papers, Loic developed an original method to exploit Raman data. Briefly, Raman spectroscopy relies on the inelastic scattering of monochromatic light emitted by a laser beam in the visible, near infrared, or near ultraviolet range. The laser light interacts with the molecular vibrations (phonons) of the system, resulting in the energy of the laser photons being shifted up or down. The shift in energy gives information about the vibrational modes in the system.

Raman is a preferred tool in nanocarbon research because sp^2 - and sp^3 -hybridized carbon materials have very distinct signatures under Raman spectroscopy. The interpretation framework (namely the correlation between the actual crystalline features and the significant features of the spectra) is slightly different between highly graphitic carbon (graphene) [Ferrari 06], and partially graphitic carbon (textured carbon) [Ferrari 00; Ferrari 04], but the principles are the same.

G (1580 cm^{-1}), D (1350 cm^{-1}) and (sometimes) T (1060 cm^{-1}) peaks are observed: the G peak is associated to bond stretching of sp^2 pairs, while the D band is associated with defective rings of sp^2 atoms. The T band, more commonly monitored with UV Raman spectroscopy indicates the presence of atoms in sp^3 configuration (and is thus not observed in graphene and carbon nanotubes). Classically, the width of the peaks and the ratio of intensity between the peaks yield information on the quantity of defects (in highly graphitized materials) or on the degree of graphitization (in poorly graphitized materials). These parameters are usually extracted by Lorentzian least square fitting of the curves after normalization.

What is never mentioned is that, when peaks are very broad (in poorly graphitic materials) or very noisy (the D peak in highly graphitic materials, the T peak in poorly graphitic material, or all peaks in highly abraded films, such as after annealing) (see Figure 26), the parameter estimation by Lorentzian

fitting gets significantly inaccurate because the maxima of the peaks are positioned inaccurately by the fitting algorithms.

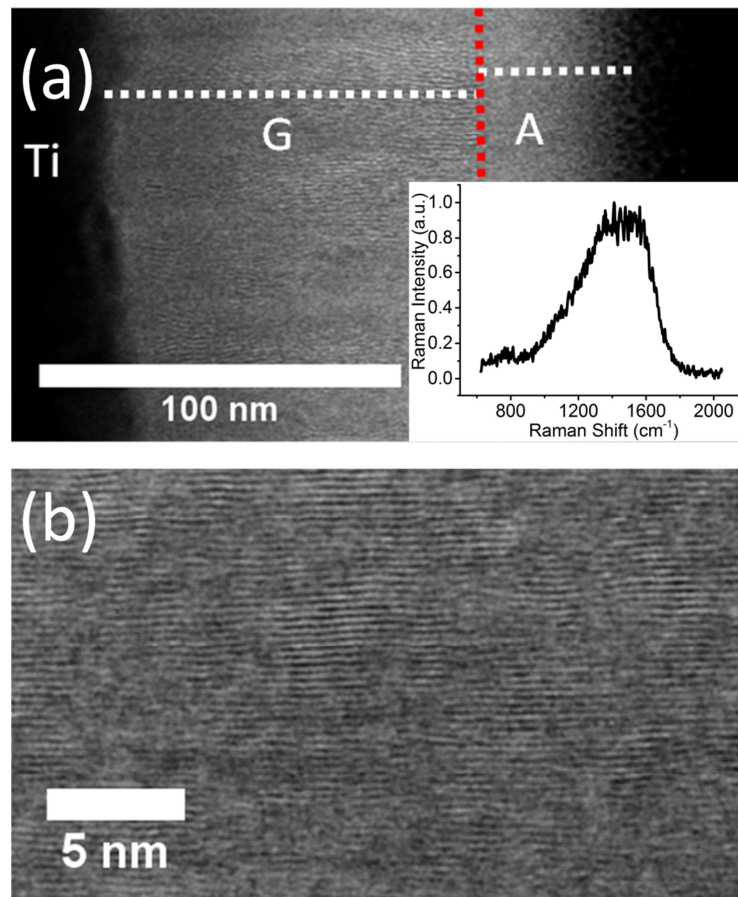


Figure 26: TEM characterization of a pristine thin film of textured carbon (amorphous matrix with graphitic inclusion oriented normally to the substrate). (a) Dark-field STEM micrograph showing two sublayers within the un-annealed textured carbon film: a 40 nm-thick amorphous layer ("A") on top of a 100 nm-thick graphitic layer ("G"). Inset: Corresponding Raman spectrum: due to their broadness, the G, D and T peaks form a single noisy peak (the smaller T peak actually forms the left shoulder of the peak). (b) HR-STEM-Dark Field micrograph on a zoomed area from the graphitic "G" layer illustrating the oriented graphitic planes

In this case, can the trends observed on the Raman parameters really be trusted to provide information on the evolution of the crystalline structure? What is the actual noise on the parameter estimation by Lorentzian fitting? In other words, what are the error bars due to parameter estimation when plotting trends in Raman parameters? I have personally never found any analysis on the topic in the nanocarbon literature (though I admit that Raman is so commonly used that I may have overlooked the right paper).

Anyway, this was precisely the case in which Loïc's work fell: definite trends were observed in the Raman parameters of annealed carbon films, but the relative variations were quite small, and the spectra were significantly noisy. Could the trends be trusted or were they just noise? To decide this issue, we devised a method to calculate the standard deviations on the parameters extracted by Lorentzian fitting. We actually exploit an "old" method called "bootstrapping" [Efron 86], which is nowadays widely used in other fields of data processing.

The principle of the method is to generate K subsets of data out of the initial Raman spectrum data. Each subset of data is composed of as many data points as the initial spectrum; the subset data are selected randomly among the initial data set; because selecting several times the same data point is possible, each subset samples differently the initial spectrum. The traditional Raman parameter extraction procedure is applied on each subset of data. The mean and standard deviation are calculated from the K subsets and are considered the true value and error for the Raman parameters.

Based on this method, in [Loisel2016b] (see Appendix 5), standard deviation on the $I(D)/I(G)$ ratio were found to be in the order of 0.04, for a parameter varying between 0.7 and 1.1 (3 to 6% relative error). So the error was found to be significant, but not enough to invalidate the observed trend (a decrease of $I(D)/I(G)$ of 25% over the duration of laser annealing).

Based on the Raman data, what the paper shows is that continuous laser exposure (namely a type of exposure that *always* occurs when characterizing nanocarbon samples with Raman) occasions phase changes in the material after only a few second: graphitization happens at the periphery of the beam by slow thermal annealing while amorphization and phase loss by oxidation happens at the center of the beam (Figure 27).

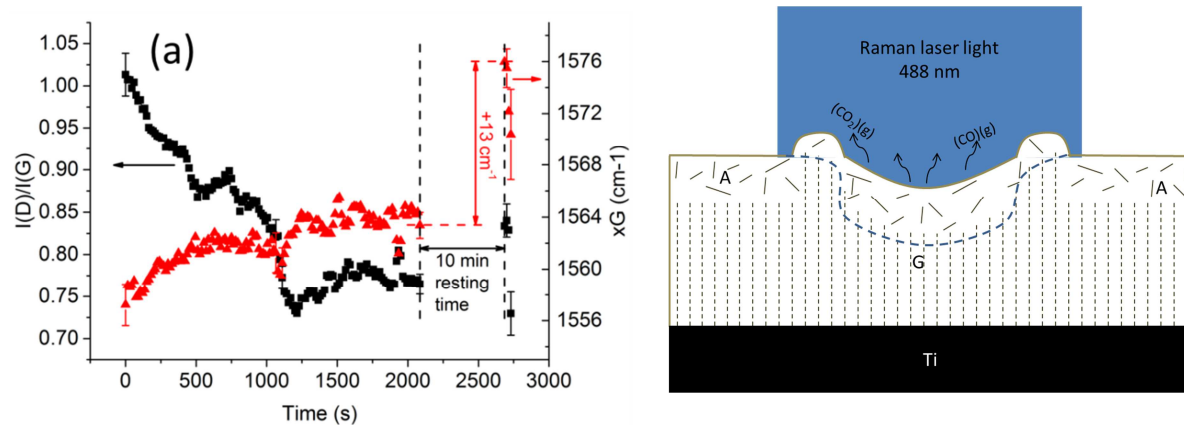


Figure 27: Left) Evolution of the $I(D)/I(G)$ ratio (black squares) and G peak position values (red triangles) as a function of time for a film annealed at $16 \text{ kW}\cdot\text{mm}^{-2}$. The last four spectra (after 10 min resting time) were taken with much lower Raman power densities. Right) Schematic cross-section of the carbon thin film, composed of the two layers "A" and "G", during Raman laser annealing. It shows the matter loss process by oxidation in the center (formation of gas (CO) and (CO₂)), the amorphization process by adsorption, the sp^2 clustering leading to a change in density. An arbitrary estimate of the region where most of the Raman information is collected is drawn in dashed blue. It highlights the importance of estimating the penetration depths of the photons when the characterized material is in-homogeneous along its depth

This paper exemplifies the approach we plan on pursuing further in Platine: quantitative analysis of imaging and spectroscopy data based on statistical and imaging processing tools, in view of understanding finely the ongoing mechanisms.

This is a strategy that I started out during my PhD thesis (see for instance [Lebental 11]): Pierre Chainais and I developed image processing tools enabling to recognize and count individual CNTs in random or oriented dense CNT depositions. I also proposed a method for AFM thickness assessment of ultrathin single-walled carbon nanotubes deposition, or a framework for interpretation of AFM-acquired force-distance curves on suspended SWNT bundles, used to establish the average thickness of a heterogeneous suspended SWNT membrane [Lebental 10].

3.4. From in-situ and ex-situ characterization to nanodevice modelling: a key to understand operation and failure mechanisms

Beyond in-situ and ex-situ characterizations of ageing such as those presented in the previous sections, actually evaluating reliability in a quantified manner require parametric, multiscale, fatigue-compliant device models. For instance, the relationship between resonance frequency, device geometry and material properties (Young's modulus) in a MEMS device constitutes such a model. In this model, fatigue may for instance be taken into account by deriving (experimentally) the evolution of the geometry (apparition of cracks) depending on the intensity and type of loadings [Muhlstein 04].

When available, such models can be exploited, for instance using theoretical work borrowed from fatigue of solids (a typical multiscale scale fatigue criterion is the Dang Van criterion, illustrated in Figure 28) [Dang 93; Bertolino 07], to predict the limit cyclic response of devices. This is clearly the end goal of Platine.

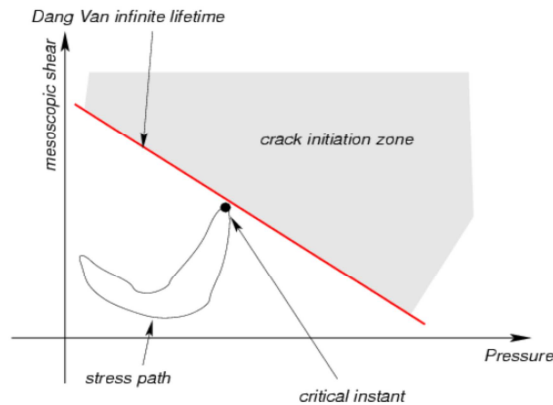


Figure 28: Illustration of Dang Van criterion

However, accurate models are rarely available for nanodevices, neither for relatively homogeneous materials, such as graphene or textured carbon films, nor for heterogeneous, random layers of nanoparticles. Even when available (see for instance [Fregonese 08] on compact modelling of CNTFET or [Fregonese 13] on compact modelling of graphene FET), the applicability of these models to specific devices is not straightforward, because relatively minor changes in physical or geometrical parameters may change the ongoing physics (operation of a CNTFET in diffusive or ballistic regime depending on CNT length [Fregonese 08], switching of a graphene memory via the substrate or by electromechanics depending on graphene thickness [Loisel 16c]).

So, presently, we are at the stage where we establish the models that will be later used for predicting lifetime. The work carried out by Fulvio Michelis on the modelling of CNT strain sensors using dense random network of carbon nanotubes [Michelis 15a] is a good example of the approach.

In CNT networks, the principle of operation (Figure 29) is that the change in the number of contacts changes the number of percolation paths and hence the resistance of the layer. Moreover, close to the percolation, there is an additional conduction by tunneling between neighboring CNTs, but this effect is known to be negligible as soon as one reaches actual percolation [Hu 08].

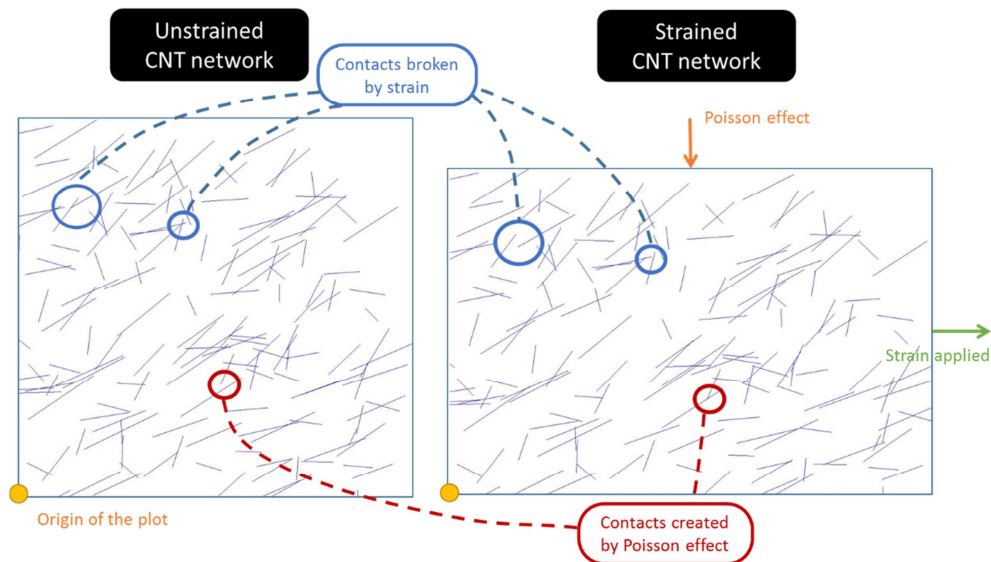


Figure 29: Schematic of the CNT network under elongation. On the left, the simulated network unstretched. On the right, the simulated network elongated along the horizontal direction and consequently shrunk in the vertical direction due to the Poisson's effect.

There is a relatively large literature on electrical and mechanical modelling of these CNT networks [Kumar 05; Li 08; Lin 10; Hu 10; Yu 13], but it addresses only low density networks close to the percolation threshold, because that is the most current applicative configuration (CNT filler in composite materials or CNTFET based on CNT networks close to the percolation threshold). As a consequence, there was no readily available result for the configuration of our sensors (Figure 30), that is, for a dense network with a multilayer structure (with the inkjet printing process, the CNTs are deposited layer by layer). Moreover, most of the literature considers rigid nanotubes, which our CNTs are obviously not. It stems from two reasons: first, it is technically easier to model rigid CNTs; second, the original papers stem from the CNTFET literature (for instance [Kumar 05]), where SWNTs, usually much more rigid (and hence straighter) than MWNTs, are used (for semi-conduction).

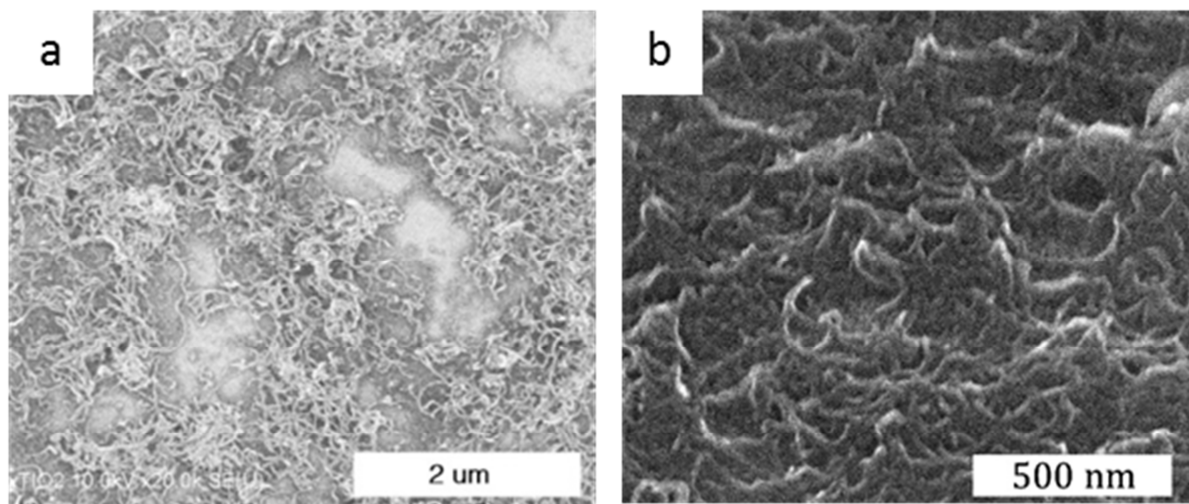


Figure 30: a) SEM image of 1-layer deposition. Micrometric holes are observed in the layer; they are attributed to loss of matter during rinsing. b) SEM image of 20-layer deposition. A uniform coverage can be observed.

So we started out devising our own model, with the goal to develop a predictive model for flexible CNTs network piezoresistivity. We started out with rigid CNTs, and then moved on to wavy CNTs to better account for experimental results.

For the rigid CNT network configuration, the classical approach (throwing random lines on a 2D plane and calculating analytically the position of crossings) was used and simply adapted to a multilayer configuration (Figure 31 left). This approach yields the percolation threshold, the relationship between number of contacts and strain (found to be linear), the gauge factor, the standard deviation on the number of contacts and on the gauge factor. These parameters can be calculated for different morphologies of the deposition (number of layers, density of CNTs by layer).

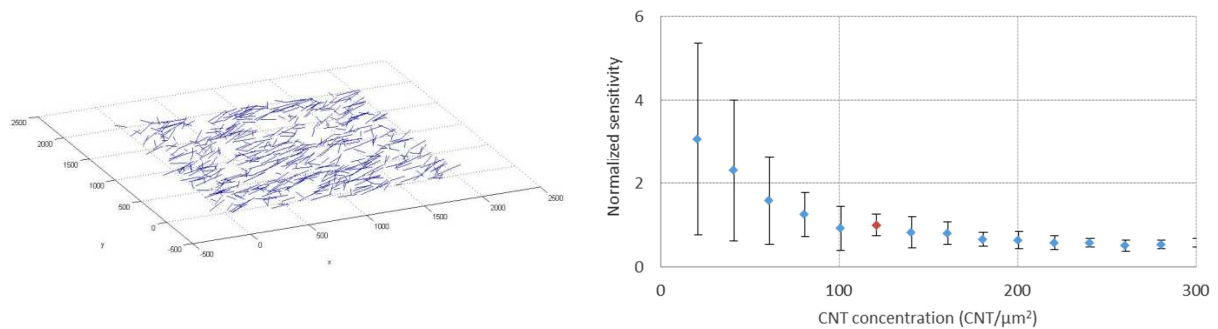


Figure 31 : Left) Model of a single layer. The unit of the axes is the nanometer. CNTs are treated as rigid sticks whose length is normally distributed around an average length of 300 nm (with standard deviation 50 nm). Right) The dependence of sensitivity and its variability on the concentration of CNTs. The error bars represent the standard deviation over 10 random throws of CNTs. The sensitivity is normalized to the sensitivity observed for a concentration of 120 CNT/μm² (represented in red).

The results of the rigid CNT model are very consistent with our own result (high reproducibility for a network high above the percolation threshold; see Section 2.3) and a more general result of the experimental literature on CNT networks (for instance [Hu 10] [Li 14]): sensitivity decreases and reproducibility increases when the density of CNT increases above the percolation threshold (Figure 31 right).

Consistently with our experiments (see Section 2.2.2), the model reproduces the linearity at low strain. However, the gauge factor is significantly too low compared with experiments (even accounting for experimental and numerical variability) (Figure 32). It also does not reproduce the non-linearity at large strain which is observed experimentally.

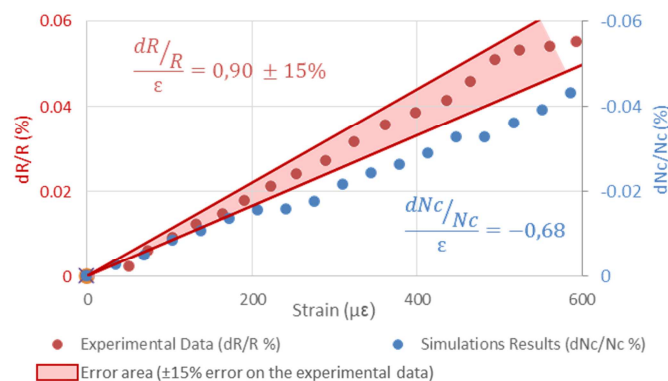


Figure 32 : Comparison between model (relative variation of the number of contacts divided by strain) and experimental (relative variation of the resistance divided by strain) gauge factor.

To account for this, we developed a model for wavy nanotubes with varying curvature and length [Fisher 03] which is much more consistent with SEM images of our deposition. The problems we encountered in building this improved model were two-fold: how to parametrize the waviness of CNTs, and how to count the number of contacts (as the traditional analytical method becomes completely impractical).

To parametrize the waviness of the CNTs, we proceeded by manual counting on SEM images (Figure 33); this process should definitely be automatized in a next stage, possibly using the algorithms developed for CNT recognition in [Lebental 11]

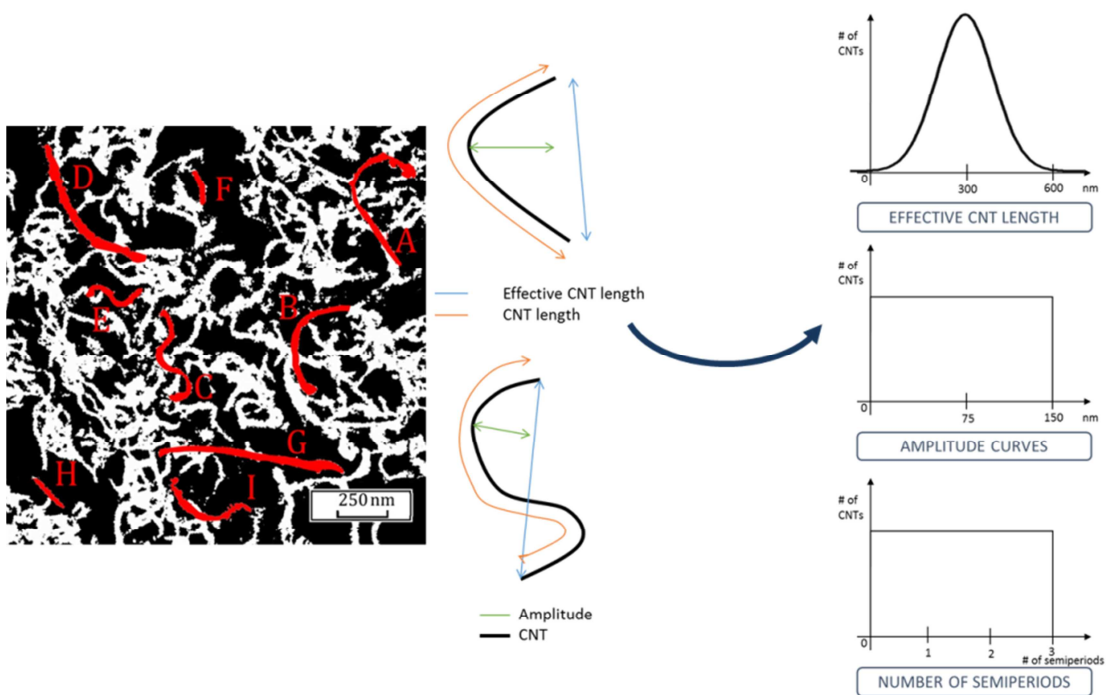


Figure 33 : Left) Naked-eye extraction of CNT and estimation waveness parameters (effective length, amplitude of curves, number of semiperiods) on a SEM image of the CNT network Middle) Definition of CNT waveness parameters Right) Distribution of CNT parameters used in the model

To count the number of contacts, we completely bypassed the analytical approach and now represent each CNT as a Boolean matrix. The structure of a layer is calculated by achieving the Boolean operation OR between matrices of randomly created CNT matrices, while the number of contacts is derived by the Boolean operation AND, as depicted in Figure 34.

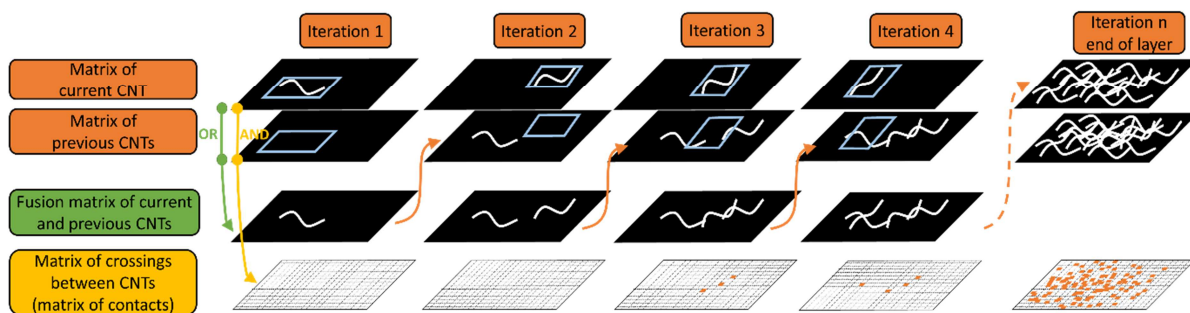


Figure 34: Iterative method of construction for the CNT layer and for the derivation of the number of contacts.

The SEM images of the real deposition of one layer of CNTs were compared with a simulated layer. The simulation represents better the deposition than the rigid model, with surface coverage by CNTs very similar to the real deposition. Most importantly, the relative change in number of contacts fits well the experimental data up to large strains (0,2%), and the gauge factor in the small strain regime (1.1) is now much closer to experimental data ($0.9 \pm 0.15\%$, that is 0.77 to 1.04) (Figure 35).

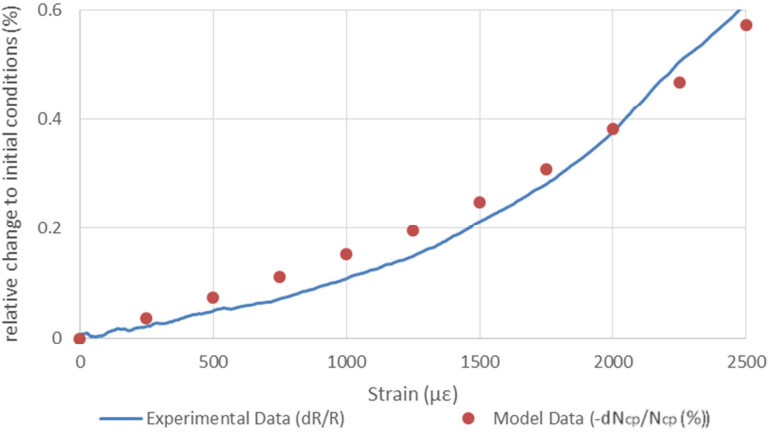


Figure 35: Comparison between model and experimental data for large deformation (2500 με).

Though a lot of work should still be carried out to finalize this method (automatization of CNT shape recognition, conversion of the number of contacts into resistivity value, deformation of the CNTs themselves), the closeness of its output with experimental data is remarkable and provide us with ideas for optimization. For instance, to improve the gauge factor without losing reproducibility, and to improve the linear range of operation, it suggests the use of more rigid CNTs (Figure 36).

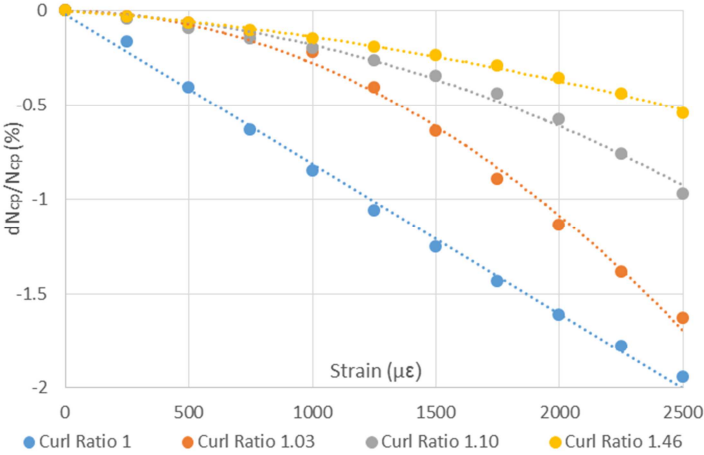


Figure 36: Simulation results showing the relationship between variation of number of contacts (dN_{cp}/N_{cp}) and applied strain for different curl ratios. Curl ratio=(CNT length)/(effective CNT length) [Li 2007]

In view of the reliability topic, the next stage on this model, beyond the above-mentioned improvements required for peer-reviewed publication (the work is already planned with a 2016-2017 research project by two Ecole Polytechnique students), is to use this method to derive a compact parametric model of the CNT strain sensors. Then the evolution of the parameters upon cycling could be analyzed, yielding a model for sensor drift upon cycling.

3.5. Conclusions

To summarize, the nanoreliability topic has been a consistent driver of my activities in the last few years. A keystone toward technology transfer of nanosensor technologies, it requires a strong multidisciplinary and the use of a variety of advanced methodologies and characterizations tools. Presently, we are at the start of the story, where we develop the tools that will be later assembled to provide a complete lifetime analysis of nanodevices. We are developing an original experimental platform dedicated to Multiphysics loadings with in-situ characterization, while building the data analysis tools enabling quantitative analysis of high-resolution characterization tools. We are starting to use these data to provide fine models of our nanodevices, which we will later exploit to establish lifetime predictions. Progressing toward a complete proof of concept of our idea, we have already had early results, for instance on CNT strain sensors characterizations and advanced modelling, or on laser annealing of textured carbon.

4. Conclusion and prospects

4.1. Reproducibility and reliability of nanosensors: from the nanoparticle up to deployment level

With the goal to investigate the potential of nanosensors for sustainable city applications, we have developed, and are still developing, a repertoire of nanosensors for strain, humidity and chemical sensing. Each of those could, and some of those will, find its use in one or more urban monitoring applications.

One of our main scientific contributions in this field to this day is the promotion of sensitivity reproducibility as the key to both mechanisms understanding and subsequent electronic integration. We have actually made the state of the art in terms of reproducibility of CNT network-based flexible sensors. Besides its scientific impact, this result was significant because it enabled us to proceed to deployment of our CNT sensor technology in the field.

Hence, we proposed and realized a RFID-based wireless sensor node dedicated to embedded microstrain monitoring within concrete. This node is currently the smallest available in the field of structural health monitoring, and it integrates our CNT sensor technology. We used this system to deploy our nanosensors within the foundation slab of one of Sense-City houses, and showed by this experiment that our embedded nanosensors have a better resilience for this application than commercial sensors.

Based on feedbacks from our industrial partners, it however appeared that “better resilience” may not be enough for the actual technology transfer of our prototypes. We thus proposed to develop the concept of nanoreliability, namely by developing nanodevice-compatible tools to understand the ageing and predict the lifetime of nanodevices. This approach having been highly successful to leverage collaborative funding, we are currently in the process of developing the experimental and numerical tools needed to achieve our goals.

We are building (and have started using) an experimental platform enabling to carry out multiphysics loadings under in-situ characterizations in order to determine fatigue behavior of the devices and identify at the microscale weak spots that foster ageing. High resolution characterization tools complemented with data processing tools are then used to understand the nanoscale mechanisms of operation and of ageing. The outputs of both approaches are gathered to build accurate device models, which will be later use to predict lifetime.

4.2. What about nanosensors for greener cities?

I consider that these results, jointly with my current project portfolio, show convincingly that nanosensors are really worthwhile for urban applications. This work, which started out during my PhD as a highly academic research with a 10 to 20 year roadmap, is now of direct interest for our industrial partners. It is notably the case of our work on weigh-in-motion (startup project), water quality (H2020 project with industrial exploitation) and embedded monitoring of construction materials (Smarti project with Eiffage).

We will see the outcomes of this technology transfer approach in the next few years, while in the mean time we improve on our methodologies for nanoreliability, to be able to address the needs of our industrial partners, when the time will come for them to address these issues.

What this means on the longer term is that nanosensors will actually reach the market and get disseminated in the civil society, contributing to a more sustainable approach to urbanization.

Thus, in the next few years, we need to ensure that the benefits of nanosensors in terms of sustainability are not overcome by the health and environmental risks nanoparticles may present.

We are starting on this topic within the Proteus project, where four reports on CNT-related health risk issue are due (two of those already available). Putting aside the issue of worker exposure during fabrication and manipulation of nanodevices (because the methodological tools are now well in place [NIOSH 13], though still imperfect and imperfectly applied) the main concern with nanoparticle-based sensors lies in the potential release of nanomaterials from the nanosensor [Yi 13] during its lifecycle (including recycling operations and/or waste storage [Cuchiella 15]).

Though the volume of nanoparticles will remain small compared to the volume of nanoparticles involved in nanocomposite products (bulk materials with nanoparticle fillers, now widely on the market), the potential release in the environment and exposure of the public should not be neglected without proper investigation. Such investigation could probably start by building lifecycle analysis tools for nanoelectronic devices, a topic which I believe to be completely unexplored at this time.

4.3. Personal Roadmap for the future

Based on these considerations on the status, benefits and risks of nanosensors, I have been able to devise a tentative roadmap for my upcoming research activities. Regarding to the next 2 to 3 years, my main topics are already well defined by my current project portfolio:

- Finalize the promising preliminary results on selective chemical sensing in liquid via functionalized CNT sensors (Proteus project), and arrange the subsequent technology transfer.
- Derive fatigue compliant models for selected nanodevices based on Multiphysics in-situ and ex-situ characterizations, and use them for lifetime prediction (Platine project, and its follow up “Environnements Intelligents”).
- Achieve the technology transfer for our strain sensors for road applications, with the startup-to-come SmartR (SmartR project) and with Eiffage (Smarti project, potential I-Street program).

On a more exploratory level, during this first phase, I plan to tackle in more depths several topics that have arisen in the last few years:

- Apply big data analysis techniques to the outputs of nanosensors data, with the main goal to improve sensor performances, notably via Sense-City project
- Explore the applications of nanosensors for health-related wearable devices, notably via student projects.
- Propose methodologies for life-cycle-analysis of nanosensors, in view of minimizing their health impact.

On the longer term, there is of course no certainty regarding to where these different topics will lead me, depending on both the research and the funding contexts. But here are two likely possibilities:

- NanoCAD: Computer-assisted design of wireless nanosensor node for urban applications.
- NanoWSN: Advanced miniaturization in wireless nanosensor nodes.

Though their formulations are very much application-oriented here, both these topics involve pluri-disciplinary upstream research, which I want to pursue more intensely in the future.

5. Bibliography

- [Allen 09] Matthew J Allen, Vincent C Tung & Richard B Kaner. Honeycomb carbon : a review of graphene. *Chemical reviews*, vol. 110, no. 1, pages 132–145, 2009.
- [Angelescu 08] Dan E Angelescu, Hua Chen, Jacques Jundt, Helene Berthet, Bruno Mercier & Frederic Marty. Highly integrated microfluidic sensors. In *MOEMS-MEMS 2008 Micro and Nanofabrication*, pages 688607–688607. International Society for Optics and Photonics, 2008.
- [Basset 09] P Basset, D Galayko, A Mahmood Paracha, F Marty, A Dudka & T Bourouina. A batch-fabricated and electretfree silicon electrostatic vibration energy harvester. *Journal of Micromechanics and Microengineering*, vol. 19, no. 11, page 115025, 2009.
- [Becher 10] Christopher Becher, Peter Kaul, Jan Mitrovics & Johannes Warmer. The detection of evaporating hazardous material released from moving sources using a gas sensor network. *Sensors and Actuators B : Chemical*, vol. 146, no. 2, pages 513–520, 2010.
- [Bertolino 07] G Bertolino, A Constantinescu, Mohamed Ferjani & Philippe Treiber. A multiscale approach of fatigue and shakedown for notched structures. *Theoretical and Applied Fracture Mechanics*, vol. 48, no. 2, pages 140–151, 2007.
- [Bondavalli 09] P. Bondavalli, P. Legagneux & D. Pribat. Carbon nanotubes based transistors as gas sensors : State of the art and critical review. *Sensors and Actuators B*, vol. 140, pages 304–318, 2009.
- [Burgess 08] Jacquelin Burgess & Michael Nye. Re-materialising energy use through transparent monitoring systems. *Energy policy*, vol. 36, no. 12, pages 4454–4459, 2008.
- [Cao 08] Qing Cao, Hoon-sik Kim, Ninad Pimparkar, Jaydeep P Kulkarni, Congjun Wang, Moonsub Shim, Kaushik Roy, Muhammad A Alam & John A Rogers. Medium-scale carbon nanotube thin-film integrated circuits on flexible plastic substrates. *Nature*, vol. 454, no. 7203, pages 495–500, 2008.
- [CDC 11] Joan M. Brunkard ; Elizabeth Ailes ; Virginia A. Roberts ; Vincent Hill ; Elizabeth D. Hilborn ; Gunther F. Craun ; Anu Rajasingham ; Amy Kahler ; Laurel Garrison ; Lauri Hicks ; Joe Carpenter ; Timothy J. Wade ; Michael J. Beach ; Jonathan S. Yoder ;. Surveillance for waterborne disease outbreaks associated with drinking water, United States, 2007-2008. In *Surveillance Summaries*, volume 12, pages 38–68. Centers for Disease Control and Prevention (CDC), September 2011.
- [Chen 09a] Po-Chiang Chen, Fumiaki N Ishikawa, Hsiao-Kang Chang, Kounghmin Ryu & Chongwu Zhou. A nanoelectronic nose: a hybrid nanowire/carbon nanotube sensor array with integrated micromachined hotplates for sensitive gas discrimination. *Nanotechnology*, vol. 20, no. 12, page 125503, 2009.
- [Chen 09b] Yu Chen & Zhaoyu Liu. Distributed intelligent city street lamp monitoring and control system based on wireless communication chip nRF401. In *Networks Security, Wireless Communications and Trusted Computing, 2009. NSWCTC'09. International Conference on*, volume 2, pages 278–281. IEEE, 2009.
- [Chen 10] Lei Chen, Shuang Yang & Ying Xi. Based on ZigBee wireless sensor network the monitoring system design for chemical production process toxic and harmful gas. In *2010 International*

Conference on Computer, Mechatronics, Control and Electronic Engineering, volume 4, pages 425–428. IEEE, 2010.

[Cho 07] Taeg Sang Cho, Kyeong-Jae Lee, Jing Kong & Anantha P Chandrakasan. A low power carbon nanotube chemical sensor system. In 2007 IEEE Custom Integrated Circuits Conference, pages 181–184. IEEE, 2007.

[Clark 03] Clifford G Clark, Lawrence Price, Rafiq Ahmed, David L Woodward, Pasquale L Melito, Frank G Rodgers, Frances Jamieson, Bruce Ciebin, Aimin Li & Andrea Ellis. Characterization of waterborne outbreak-associated *Campylobacter jejuni*, Walkerton, Ontario. *Emerging infectious diseases*, vol. 9, no. 10, page 1232, 2003.

[Clarke 02] JA Clarke, J Cockroft, S Conner, JW Hand, NJ Kelly, R Moore, T O'Brien & P Strachan. Simulation-assisted control in building energy management systems. *Energy and buildings*, vol. 34, no. 9, pages 933–940, 2002.

[Cojocar 11] C. S. Cojocar, B. Lebental, F. Z. Bouanis & E. D. Norman. Méthode de détection d'analytes utilisant des réseaux de transistors à effet de champ à base de nanotubes/nanofils et dispositif électronique associé, 2011.

[Cucchiella 15] Federica Cucchiella, Idiano D'Adamo, SC Lenny Koh & Paolo Rosa. Recycling of WEEEs: An economic assessment of present and future e-waste streams. *Renewable and Sustainable Energy Reviews*, vol. 51, pages 263–272, 2015.

[Cui 01] Yi Cui, Qingqiao Wei, Hongkun Park & Charles M Lieber. Nanowire nanosensors for highly sensitive and selective detection of biological and chemical species. *Science*, vol. 293, no. 5533, pages 1289–1292, 2001.

[Dang-Van 93] K Dang-Van. Macro-micro approach in high-cycle multiaxial fatigue. In *Advances in multiaxial fatigue*. ASTM International, 1993.

[David 15] Chavez M David, Quispe T River, Rojas M Jorge, Jacoby K Andres & Garayar L Guillermo. A low-cost, rapid deployment and energy-autonomous wireless sensor network for air quality monitoring. In 2015 9th International Conference on Sensing Technology (ICST), pages 122–127. IEEE, 2015.

[De Volder 13] Michael FL De Volder, Sameh H Tawfick, Ray H Baughman & A John Hart. Carbon nanotubes : present and future commercial applications. *science*, vol. 339, no. 6119, pages 535–539, 2013.

[DEFRA 15] DEFRA. Emissions of air pollutants in the UK, 1970 to 2014. Rapport technique, Defra National Statistics Release, December 2015.

[Derx 12] F. Derx, B. Lebental, T. Bourouina, F. Bourquin, C.-S. Cojocar, E. Robin & H. Van Damme. The Sense-City project. In XVIIIth Symposium on Vibrations, Shocks and Noise and ASTELAB, EDF Clamart research center, France, July 3-5, 2012.

[Dharap 04] Prasad Dharap, Zhiling Li, Satish Nagarajaiah & EV Barrera. Nanotube film based on single-wall carbon nanotubes for strain sensing. *Nanotechnology*, vol. 15, no. 3, page 379, 2004.

[EC 10] Water Scarcity and Drought in the European Union. Rapport technique, European Commission, August 2010.

[ECR 10] European Competitiveness Report. Rapport technique, European Commission - Enterprise and Industry, 2010.

[EEA 15] Report No 5/2015 : Air quality in Europe. Rapport technique, European Environmental Agency, 2015.

[Efron 86] Bradley Efron & Robert Tibshirani. Bootstrap methods for standard errors, confidence intervals, and other measures of statistical accuracy. *Statistical science*, pages 54–75, 1986.

[EPA 16] 1990-2014 National Level US Greenhouse Gas Inventory, Fast Facts. Rapport technique, Environmental Protection Agency, April 2016.

[EPOSS 13] Strategic research Agenda. Rapport technique, EPoSS - The European Technology Platform on Smart Systems Integration, September 2013.

[ERS 03] Asthma Burden. In *European Lung White Book*, volume 2, chapitre 1. European Respiratory Society, 2003.

[Ferrari 00] Andrea C Ferrari & Jf Robertson. Interpretation of Raman spectra of disordered and amorphous carbon. *Physical review B*, vol. 61, no. 20, page 14095, 2000.

[Ferrari 04] Andrea Carlo Ferrari & John Robertson. Raman spectroscopy of amorphous, nanostructured, diamond-like carbon, and nanodiamond. *Philosophical Transactions of the Royal Society of London A : Mathematical, Physical and Engineering Sciences*, vol. 362, no. 1824, pages 2477–2512, 2004.

[Ferrari 06] AC Ferrari, JC Meyer, V Scardaci, C Casiraghi, Michele Lazzeri, Francesco Mauri, S Piscanec, Da Jiang, KS Novoselov, S Roth et al. Raman spectrum of graphene and graphene layers. *Physical review letters*, vol. 97, no. 18, page 187401, 2006.

[Fisher 03] FT Fisher, RD Bradshaw & LC Brinson. Fiber waviness in nanotube-reinforced polymer composites – I: Modulus predictions using effective nanotube properties. *Composites Science and Technology*, vol. 63, no. 11, pages 1689–1703, 2003.

[Frégonèse 08] Sébastien Frégonèse, Hugues Cazin d'Honincthun, Johnny Goguet, Cristell Maneux, Thomas Zimmer, Jean-Philippe Bourgoïn, Philippe Dollfus & Sylvie Galdin-Retailleau. Computationally efficient physics-based compact CNTFET model for circuit design. *IEEE Transactions on Electron Devices*, vol. 55, no. 6, pages 1317–1327, 2008.

[Fregonese 13] Sebastien Fregonese, Maura Magallo, Cristell Maneux, Henri Happy & Thomas Zimmer. Scalable electrical compact modeling for graphene FET transistors. *IEEE Transactions on Nanotechnology*, vol. 12, no. 4, pages 539–546, 2013.

[Ghaddab 14] Boutheina Ghaddab, Vincent Gaudefroy, Fulvio Michelis, Eduardo Ruiz-Hitzky, Pilar Aranda, Cristina Ruiz-Garcia & Bérengère Lebental. A Novel Weigh-In Motion Sensor Using An Asphalt-Embedded Thin Film of Graphene-On-Clay and Carbon-Nanotubes. In *International*

Conference & Exhibition on Advanced & NanoMaterials, 2014, August 11-13, Calgary, Alberta, Canada, 2014.

[GINA 15] Pocket guide for asthma management and prevention. Rapport technique, Global Initiative for Asthma, 2015.

[Gohier 12] Aurélien Gohier, Barbara Laiik, Ki-Hwan Kim, Jean-Luc Maurice, Jean-Pierre Pereira-Ramos, Costel Sorin Cojocaru & Pierre Tran Van. High-Rate Capability Silicon Decorated Vertically Aligned Carbon Nanotubes for Li-Ion Batteries. *Advanced Materials*, vol. 24, no. 19, pages 2592-2597, 2012.

[Gong 14] Shen Gong & Zheng H Zhu. On the mechanism of piezoresistivity of carbon nanotube polymer composites. *Polymer*, vol. 55, no. 16, pages 4136–4149, 2014.

[Greer 05] Julia R Greer & William D Nix. Size dependence of mechanical properties of gold at the sub-micron scale. *Applied Physics A*, vol. 80, no. 8, pages 1625–1629, 2005.

[Heine 69] V Heine & RO Jones. Electronic band structure and covalency in diamond-type semiconductors. *Journal of Physics C : Solid State Physics*, vol. 2, no. 4, page 719, 1969.

[Broquereau 13] Broquereau ; L (HiKob). Urban traffic management and winter services: wireless sensor networks power smarter decisions. In 9th ITS European Congress. Dublin, Ireland, June 2013.

[Hoffheins 96] Barbara Hoffheins. Solid state, resistive gas sensors. Philadelphia : Institute of Physics, 1996.

[Hu 08] Ning Hu, Yoshifumi Karube, Cheng Yan, Zen Masuda & Hisao Fukunaga. Tunneling effect in a polymer/carbon nanotube nanocomposite strain sensor. *Acta Materialia*, vol. 56, no. 13, pages 2929–2936, 2008.

[Hu 10] Ning Hu, Yoshifumi Karube, Masahiro Arai, Tomonori Watanabe, Cheng Yan, Yuan Li, Yaolu Liu & Hisao Fukunaga. Investigation on sensitivity of a polymer/carbon nanotube composite strain sensor. *Carbon*, vol. 48, no. 3, pages 680–687, 2010.

[Iijima 91] Sumio Iijima et al. Helical microtubules of graphitic carbon. *Nature*, vol. 354, no. 6348, pages 56–58, 1991.

[INSEE 11] Le nouveau zonage en aires urbaines de 2010. Rapport technique 1374, INSEE Première, 10 2011.

[IPCC 14] C.B. Field, V.R. Barros, D.J. Dokken, K.J. Mach, M.D. Mastrandrea, T.E. Bilir, M. Chatterjee, K.L. Ebi, Y.O. Estrada, R.C. Genova, B. Girma, E.S. Kissel, A.N. Levy, S. MacCracken, P. R. Mastrandrea & L.L. (eds.) White. IPCC, 2014 : Summary for policymakers. In *Climate Change 2014 : Impacts, Adaptation, and Vulnerability. Part A : Global and Sectoral Aspects. Contribution of Working Group II to the Fifth Assessment Report of the Intergovernmental Panel on Climate Change*, pages 1–32. Cambridge University Press, Cambridge, United Kingdom and New York, NY, USA, 2014.

[Jain 12] PC Jain & Rajesh Kushwaha. Wireless gas sensor network for detection and monitoring of harmful gases in utility areas and industries. In *Sensing Technology (ICST), 2012 Sixth International Conference on*, pages 642–646. IEEE, 2012.

[Jeng 07] Shuen-Lin Jeng, Jye-Chyi Lu & Kaibo Wang. A review of reliability research on nanotechnology. *IEEE Transactions on Reliability*, vol. 56, no. 3, pages 401–410, 2007.

[Kang 94] WP Kang & CK Kim. Performance and detection mechanism of a new class of catalyst (Pd, Pt, or Ag)-adsorptive oxide (SnO_x or ZnO)-insulator-semiconductor gas sensors. *Sensors and Actuators B : Chemical*, vol. 22, no. 1, pages 47–55, 1994.

[Karbashi 12] Golnaz Karbashi, Francoise Sailhan & Stephane Rovedakis. Towards a Fault-Tolerant Wireless Sensor Network Using Fault Injection Mechanisms : A Parking Lot Monitoring Case. In *Green Computing and Communications (GreenCom), 2012 IEEE International Conference on*, pages 783–787. IEEE, 2012.

[KET 11] Final Report. Rapport technique, European Commission, High-level Expert Group on Key-Enabling Technologies, June 2011.

[Kim 06] S-W Kim, Andreas Heckel, SA McKeen, GJ Frost, E-Y Hsie, MK Trainer, Andreas Richter, JP Burrows, SE Peckham & GA Grell. Satellite-observed US power plant NO_x emission reductions and their impact on air quality. *Geophysical Research Letters*, vol. 33, no. 22, 2006.

[Kroto 85] HaroldWKroto, James R Heath, Sean C O'Brien, Robert F Curl, Richard E Smalley et al. C₆₀: buckminsterfullerene. *Nature*, vol. 318, no. 6042, pages 162–163, 1985.

[Kumar 05] S Kumar, JY Murthy & MA Alam. Percolating conduction in finite nanotube networks. *Physical review letters*, vol. 95, no. 6, page 066802, 2005.

[Laheurte 16] Jean-Marc Laheurte, Aladdin Kabalan, Houssam Retima, Eric Piedallu, Fulvio Michelis & Bérengère Lebental. Embedded UHF RFID Tag for Durability Monitoring in Concrete. *Wireless Sensor Network*, vol. 8, no. 07, page 137, 2016.

[Lebental 10] B. Lebental. Instrumentation immergée des matériaux cimentaires par des micro-transducteurs ultrasoniques à nanotubes de carbone : Perspectives pour le contrôle nondestructive in-situ de durabilité. PhD thesis, Université Paris Est, 2010.

[Lebental 11] Bérengère Lebental, Pierre Chainais, Pascale Chenevier, Nicolas Chevalier, Eric Delevoye, Jean-Marc Fabbri, Sergio Nicoletti, Philippe Renaux & Anne Ghis. Aligned carbon nanotube based ultrasonic microtransducers for durability monitoring in civil engineering. *Nanotechnology*, vol. 22, page 395501, 2011.

[Lebental 14a] Bérengère Lebental, Boutheina Ghaddab, Vincent Gaudefroy, Eduardo Ruiz-Hitzky, Pilar Aranda, Cristina Ruiz-Gracia & Birger Henning. Dispositif d'acquisition, procédé de fabrication de celui-ci, procédé de mesure de force, 2014.

[Lebental 14b] Bérengère Lebental, Heechul Woo, Evgeny Norman, Fatima Zahra Bouanis, Aurélien Gohier & Costel-Sorin Cojocar. Multi-mode humidity sensitivity of carbon nanotubes field-effect transistors (poster). In *Nanotech 2014, Washington DC, USA, June 15-19, 2014*.

[Lebental 15a] B. Lebental. Des nanocapteurs pour une ville durable. *Les Clés de Demain*, May 2015.

[Lebental 15b] B. Lebental & N. Hautière. Innovation et villes durables, repères pour l'action., Note d'approfondissement sur l'évaluation des territoires d'innovation urbaine. 2015.

[Lebental 15c] F. Michelis ; L. Bodelot ; Y. Bonnassieux ; B. Lebental. Highly reproducible, hysteresis-free, flexible strain sensors by inkjet printing of carbon nanotubes. Carbon, vol. 95., pages 1020-1026, 2015.

[Lee 12] Chang Seok Lee, Costel Sorin Cojocar, Waleed Moujahid, Bérengère Lebental, Marc Chaigneau, Marc Châtelet, François Le Normand & Jean-Luc Maurice. Synthesis of conducting transparent few-layer graphene directly on glass at 450°C. Nanotechnology, vol. 23, pages 265603–265608, 2012.

[Li 07] Chunyu Li & Tsu-Wei Chou. Continuum percolation of nanocomposites with fillers of arbitrary shapes. Applied Physics Letters, vol. 90, no. 17, page 174108, 2007.

[Li 08] Chunyu Li, Erik T Thostenson & Tsu-Wei Chou. Effect of nanotube waviness on the electrical conductivity of carbon nanotube-based composites. Composites Science and Technology, vol. 68, no. 6, pages 1445–1452, 2008.

[Lin 10] Chuan Lin, Hongtao Wang & Wei Yang. Variable percolation threshold of composites with fiber fillers under compression. Journal of Applied Physics, vol. 108, no. 1, page 013509, 2010.

[Liu 12] Yuxin Liu, Xiaochen Dong & Peng Chen. Biological and chemical sensors based on graphene materials. Chemical Society Reviews, vol. 41, no. 6, pages 2283–2307, 2012.

[Liu 13] Jing Liu, Jung Hwan Seo, Yubo Li, Di Chen, Katsuo Kurabayashi & Xudong Fan. Smart multi-channel two dimensional micro-gas chromatography for rapid workplace hazardous volatile organic compounds measurement. Lab on a Chip, vol. 13, no. 5, pages 818–825, 2013.

[Liu 15] Xiaofeng Liu, Bin Li, Aimin Jiang, Shixin Qi, Chaosheng Xiang & Ning Xu. A bicycle-borne sensor for monitoring air pollution near roadways. In Consumer Electronics- Taiwan (ICCE-TW), 2015 IEEE International Conference on, pages 166–167. IEEE, 2015.

[Llatser 12] Ignacio Llatser, Christian Kremers, Albert Cabellos- Aparicio, Josep Miquel Jornet, Eduard Alarcón & Dmitry N Chigrin. Graphene-based nano-patch antenna for terahertz radiation. Photonics and Nanostructures-Fundamentals and Applications, vol. 10, no. 4, pages 353–358, 2012.

[Llobet 13] Eduard Llobet. Gas sensors using carbon nanomaterials: A review. Sensors and Actuators B : Chemical, vol. 179, pages 32–45, 2013.

[Loisel 15] Loïc Loisel, Marc Châtelet, Guillaume Giudicelli, Mathias Lebihain, Yi Yang, Costel-Sorin Cojocar, Andrei Constantinescu, Beng Kang Tay & Bérengère Lebental. Controlled Amorphization and graphitization of Nano-Crystalline Graphite Using High-Energy Nanosecond Laser Pulses for phase-change memory applications. Carbon, vol. 105, pages 227-232, 2015.

[Loisel 16a] Loïc Loisel. Optical and electrical breakdown of carbon allotropes: mechanisms and applications for data storage, 2016. PhD Thesis. Nanyang Technological University and Ecole Polytechnique

[Loisel 16b] Loïc Loisel, Ileana Florea, Costel-Sorin Cojocaru, Beng Kang Tay & Bérengère Lebental. Oxidation-Based Continuous Laser Writing in Vertical Nano-Crystalline Graphite Thin Films. Scientific reports, vol. 6, 2016.

[Loisel 16c] Loïc Loisel, Ange Maurice, Stefano Vezzoli, Costel-Sorin Cojocaru, Beng Kang Tay & Bérengère Lebental. In-plane electro-mechanical motion in resistive graphene memories. Under revision for resubmission.

[Lundström 75] I Lundström, S Shivaraman, C Svensson & L Lundkvist. A hydrogen- sensitive MOS field- effect transistor. Applied Physics Letters, vol. 26, no. 2, pages 55–57, 1975.

[Maffucci 08] Antonio Maffucci, Giovanni Miano & Fabio Villone. Performance comparison between metallic carbon nanotube and copper nano-interconnects. IEEE Transactions on Advanced Packaging, vol. 31, no. 4, pages 692–699, 2008.

[Manes 12] Gianfranco Manes, Giovanni Collodi, Rosanna Fusco, Leonardo Gelpi & Antonio Manes. A wireless sensor network for precise volatile organic compound monitoring. International Journal of Distributed Sensor Networks, vol. 2012, 2012.

[MEDDE 14] Bilan de la qualité de l'air en France en 2013 et principales tendances observées sur la période 2000-2013. Rapport technique, MEDDE, 2014.

[Michelis 15a] Fulvio Michelis. Wireless Nano Sensors for Embedded Durability Monitoring in Concrete. PhD thesis, Ecode doctorale de l'Ecole Polytechnique (EDX); IFSTTAR-Institut Français des Sciences et Technologies des Transports, de l'Aménagement et des Réseaux, 2015.

[Michelis 15b] Fulvio Michelis, Laurence Bodelot, Jean-Marc Laheurte, Fadi Zaki, Yvan Bonnassieux & Bérengère Lebental. Wireless Nanosensors for Embedded Measurement in Concrete Structures. In Nanotechnology in Construction, pages 389–396. Springer, 2015.

[Mitra 12] Saurav Mitra, Siddhartha P Duttagupta, Kushal Tuckley & Samsul Ekram. Wireless sensor network based localization and threat estimation of hazardous landfill gas source. In Industrial Technology (ICIT), 2012 IEEE International Conference on, pages 349–355. IEEE, 2012.

[Mochalin 12] Vadym N Mochalin, Olga Shenderova, Dean Ho & Yury Gogotsi. The properties and applications of nanodiamonds. Nature nanotechnology, vol. 7, no. 1, pages 11–23, 2012.

[Muhlstein 04] CL Muhlstein, RT Howe & RO Ritchie. Fatigue of polycrystalline silicon for microelectromechanical system applications: crack growth and stability under resonant loading conditions. Mechanics of Materials, vol. 36, no. 1, pages 13–33, 2004.

[Munoz-Sandoval 14] Emilio Munoz-Sandoval. Trends in nanoscience, nanotechnology, and carbon nanotubes : a bibliometric approach. Journal of nanoparticle research, vol. 16, no. 1, pages 1–22, 2014.

[Nachef 12] Kinda Nachef, Frédéric Marty, Eric Donzier, Bertrand Bourlon, Kamran Danaie & Tarik Bourouina. Micro gas chromatography sample injector for the analysis of natural gas. Journal of Microelectromechanical Systems, vol. 21, no. 3, pages 730–738, 2012.

[Nastos 10] Panagiotis T Nastos, Athanasios G Paliatsos, Michael B Anthracopoulos, Eleftheria S Roma & Kostas N Priftis. Outdoor particulate matter and childhood asthma admissions in Athens, Greece: a time-series study. *Environmental Health*, vol. 9, no. 1, page 1, 2010.

[NIOSH 13] NIOSH. Occupational Exposure to Carbon Nanotubes and Nanofibers. *Current Intelligence Bulletin* 65. National Institute for Occupational Safety and Health, April 2013.

[Norman 11] E. D. Norman, L. Gorintin, B. Lebental, P. Bondavalli & C. S. Cojocar. Carbon nanotube based humidity sensor. In GDR-I Nanotubes and Graphene 2011, Dourdan, France, Feb; 11th-15th, 2011.

[Novoselov 04] Kostya S Novoselov, Andre K Geim, Sergei V Morozov, D Jiang, Y_ Zhang, Sergey V Dubonos, Irina V Grigorieva & Alexandr A Firsov. Electric field effect in atomically thin carbon films. *science*, vol. 306, no. 5696, pages 666–669, 2004.

[OEMP 04] OEMP. 20 ans de chauffage dans les résidences principales en France de 1982 à 2002. *Observatoire de l’Energie et des Matières Premières*, 2004.

[Olsen 02] Sonja J Olsen, Gayle Miller, Thomas Breuer, Malinda Kennedy, Charles Higgins, Jim Walford, Gary McKee, Kim Fox, William Bibb & Paul Mead. A waterborne outbreak of *Escherichia coli* O157 : H7 infections and hemolytic uremic syndrome : implications for rural water systems. *Emerging infectious diseases*, vol. 8, no. 4, page 370, 2002.

[O’Sullivan 04] D. O’Sullivan, MM Keane, Dennis Kelliher & Robert J Hitchcock. Improving building operation by tracking performance metrics throughout the building lifecycle (BLC). *Energy and buildings*, vol. 36, no. 11, pages 1075–1090, 2004.

[Palmgren 07] Finn Palmgren, Ruwim Berkowicz, Matthias Ketzel & Morten Winther. Elevated NO₂ pollution in Copenhagen due to direct emission of NO₂ from road traffic. In *2nd ACCENT Symposium*, Urbino, Italy, 2007.

[PBD 15] PBD. *Rapport d’Activité. Plan Bâtiment Durable*, 2015.

[Qi 03] Pengfei Qi, Ophir Vermesh, Mihai Grecu, Ali Javey, Qian Wang, Hongjie Dai, Shu Peng & KJ Cho. Toward large arrays of multiplex functionalized carbon nanotube sensors for highly sensitive and selective molecular detection. *Nano letters*, vol. 3, no. 3, pages 347–351, 2003.

[Reddy 12] Karthik Reddy, Yunbo Guo, Jing Liu, Wonsuk Lee, Maung Kyaw Khaing Oo & Xudong Fan. Rapid, sensitive, and multiplexed on-chip optical sensors for micro-gas chromatography. *Lab on a Chip*, vol. 12, no. 5, pages 901–905, 2012.

[Ruiz-Hitzky 11] Eduardo Ruiz-Hitzky, Margarita Darder, Francisco M Fernandes, Ezzouhra Zatile, Francisco Javier Palomares & Pilar Aranda. Supported graphene from natural resources: easy preparation and applications. *Advanced Materials*, vol. 23, no. 44, pages 5250–5255, 2011.

[Sagnard 16] Florence Sagnard, Christophe Norgeot, Xavier Derobert, Vincent Baltazart, Erick Merliot, François Derkx & Bérengère Lebental. Utility detection and positioning on the urban site Sense-City using Ground-Penetrating Radar systems. *Measurement*, vol. 88, pages 318–330, 2016.

- [Sargent Jr 13] John F Sargent Jr. The National Nanotechnology Initiative: overview, reauthorization, and appropriations issues. DTIC Document, 2013.
- [Schütze 04] Manfred Schütze, Alberto Campisano, Hubert Colas, Wolfgang Schilling & Peter A Vanrolleghem. Real time control of urban wastewater systems: “where do we stand today?”. *Journal of hydrology*, vol. 299, no. 3, pages 335–348, 2004.
- [Sivaraman 13] Vijay Sivaraman, James Carrapetta, Ke Hu & Blanca Gallego Luxan. HazeWatch : A participatory sensor system for monitoring air pollution in Sydney. In *Local Computer Networks Workshops (LCN Workshops)*, 2013 IEEE 38th Conference on, pages 56–64. IEEE, 2013.
- [Slonczewski 58] JC Slonczewski & PR Weiss. Band structure of graphite. *Physical Review*, vol. 109, no. 2, page 272, 1958.
- [Smalley 03] Richard E Smalley, Mildred S Dresselhaus, Gene Dresselhaus & Phaedon Avouris. *Carbon nanotubes : synthesis, structure, properties, and applications*, volume 80. Springer Science & Business Media, 2003.
- [Stieb 09] David M Stieb, Mieczyslaw Szyszkowicz, Brian H Rowe & Judith A Leech. Air pollution and emergency department visits for cardiac and respiratory conditions : a multi-city time-series analysis. *Environmental Health*, vol. 8, no. 1, page 1, 2009.
- [Stieb 12] David M Stieb, Li Chen, Maysoon Eshoul & Stan Judek. Ambient air pollution, birth weight and preterm birth : a systematic review and meta-analysis. *Environmental research*, vol. 117, pages 100–111, 2012.
- [Taillade 11] Frédéric Taillade, Marc Quiertant, Karim Benzarti & Christophe Aubagnac. Shearography and pulsed stimulated infrared thermography applied to a nondestructive evaluation of FRP strengthening systems bonded on concrete structures. *Construction and Building Materials*, vol. 25, no. 2, pages 568–574, 2011.
- [UN 14] *World Urbanization Prospects : The 2014 Revision, Highlights (ST/ESA/SER.A/352)*. United Nations, Department of Economic and Social Affairs, Population Division, 2014.
- [Vlasov 12] Yurii A Vlasov. Silicon CMOS-integrated nano-photonics for computer and data communications beyond 100G. *IEEE Communications Magazine*, vol. 50, no. 2, pages s67–s72, 2012.
- [WEC 13] WEC 2013 Survey. Rapport technique, World Energy Council, 2013.
- [Wen 13] Tzai-Hung Wen, Joe-Air Jiang, Chih-Hong Sun, Jehn-Yih Juang & Tzu-Shiang Lin. Monitoring Street-Level Spatial-Temporal Variations of Carbon Monoxide in Urban Settings Using a Wireless Sensor Network (WSN) Framework. *International journal of environmental research and public health*, vol. 10, no. 12, pages 6380–6396, 2013.
- [Werner-Allen 05] Geoffrey Werner-Allen, Jeff Johnson, Mario Ruiz, Jonathan Lees & Matt Welsh. Monitoring volcanic eruptions with a wireless sensor network. In *Proceedings of the Second European Workshop on Wireless Sensor Networks*, 2005., pages 108–120. IEEE, 2005.

[WFD 00] Water Framework Directive : Directive 2000/60/EC of the European Parliament and of the Council establishing a framework for the Community action in the field of water policy. European Commission, 2000.

[WHO 11] Guidelines for Drinking-water Quality, 4th edition. World Health Organization, 2011.

[WHO 16] Protecting Surface Water for Health : Identifying, assessing and managing drinking-water quality risks in surface-water catchments. World Health Organization, 2016.

[Wong 05] Johnny KW Wong, Heng Li & SW Wang. Intelligent building research : a review. *Automation in construction*, vol. 14, no. 1, pages 143–159, 2005.

[Wunderle 09] Bernhard Wunderle & B Michel. Lifetime modelling for microsystems integration: from nano to systems. *Microsystem technologies*, vol. 15, no. 6, pages 799–812, 2009.

[Xu 12] Naiyun Xu, Hang Tong Edwin Teo, Maziar Shakerzadeh, Xincai Wang, Chee Mang Ng & Beng Kang Tay. Electrical properties of textured carbon film formed by pulsed laser annealing. *Diamond and Related Materials*, vol. 23, pages 135–139, 2012.

[Yang 10] Wenxian Yang, Peter J Tavner, Christopher J Crabtree & Michael Wilkinson. Cost-effective condition monitoring for wind turbines. *IEEE Transactions on industrial electronics*, vol. 57, no. 1, pages 263–271, 2010.

[Yang 15] Ning Yang, Xianping Chen, Tianling Ren, Ping Zhang & Daoguo Yang. Carbon nanotube based biosensors. *Sensors and Actuators B : Chemical*, vol. 207, pages 690–715, 2015.

[Yi 13] Peng Yi & Kai Loon Chen. Influence of solution chemistry on the release of multiwalled carbon nanotubes from silica surfaces. *Environmental science & technology*, vol. 47, no. 21, pages 12211–12218, 2013.

[Yu 13] Yong Yu, Shuangqi Song, Zhixiang Bu, Xiaofeng Gu, Gangbing Song & Li Sun. Influence of filler waviness and aspect ratio on the percolation threshold of carbon nanomaterials reinforced polymer nanocomposites. *Journal of Materials Science*, vol. 48, no. 17, pages 5727–5732, 2013.

Appendices

Appendix 1: Personal bibliography, August 2016

The highlighted papers are provided in the following appendices.

PEER-REVIEWED ARTICLES²³

	Under revision	<i>A high performance non-volatile graphene memory by planar electro-mechanical switching.</i> Loïc Loisel, Ange Maurice, Stefano Vezzoli, Costel-Sorin Cojocaru, Beng Kang Tay, <u>Béregère Lebental</u>
10	Wireless sensor networks 2016, 8(7), 137	<i>Embedded UHF RFID Tag for Nanosensor-based Durability Monitoring in Concrete.</i> Laheurte, J. M.; Kabalan, A.; Retima, H.; Piedallu, E.; Michelis, F. & Lebental, B.
9	Scientific Reports 2016, 6, 26224	<i>Phase Change, Oxidation and Matter Removal in Vertical Nano-Crystalline Graphite Films by Continuous Laser Writing.</i> Loïc Loisel, <u>Béregère Lebental</u> , Ileana Florea, Costel-Sorin Cojocaru, Beng Kang Tay
8	Carbon 2016, 105, 227-232	<i>Graphitization and amorphization of textured carbon using high-energy nanosecond laser pulses.</i> Loïc Loisel, , Marc Châtelet, Yi Yang, Costel-Sorin Cojocaru, Beng Kang Tay, <u>Béregère Lebental</u> . DOI:10.1016/j.carbon.2016.04.026
7	Measurement 2016, 88, 318-330	<i>Utility detection and positioning on the urban site Sense-City using Ground-Penetrating Radar systems.</i> Florence Sagnard; Christophe Norgeot; Xavier Derobert; Vincent Baltazart; Erick Merliot; François Derckx ; <u>Béregère Lebental</u> . DOI:10.1016/j.measurement.2016.03.044
6	Carbon 2015, 95, 1020-1026	<i>Highly reproducible, hysteresis-free, flexible strain sensors by inkjet printing of carbon nanotubes.</i> F. Michelis; L. Bodelot ; Y. Bonnassieux; <u>B. Lebental</u> . DOI: 10.1016/j.carbon.2015.08.103
5	App. Phys. Lett 2013, 103, 051907	<i>Electrostatic method to estimate the mechanical properties of suspended membranes applied to nickel-coated graphene oxide.</i> Nawres Sridi, <u>Béregère Lebental</u> , Joel Azevedo, Jean Christophe P. Gabriel and Anne Ghis. DOI: 10.1063/1.4817301
4	Nanotechnology 2012, 23, 265603	<i>Synthesis of conducting transparent few-layer graphene directly on glass at 450°C.</i> C. S. Lee, C. S. Cojocaru, W. Moujahid, <u>B. Lebental</u> , M. Chaigneau, M. Châtelet, F. Le Normand and J.-L. Maurice. DOI: 10.1088/0957-4484/23/26/265603
3	JSV 2012, 31, 1870-1886	<i>Elasto-acoustic modelling of a vibrating plate interacting with water confined in a domain of micrometric size.</i> <u>B. Lebental</u> and F. Bourquin. DOI:10.1016/j.jsv.2011.12.016
2	EJECE 2011, 15, 649-662	<i>Capacitive ultrasonic micro-transducer made of carbon nanotubes: prospects for the in-situ embedded non-destructive testing of durability in cementitious materials.</i> <u>B. Lebental</u> , A. Ghis, E. Delevoye, J.-M. Caussignac, F. Bourquin. DOI:10.1080/19648189.2011.9693353
1	Nanotechnology 2011, 22, 395501	<i>Aligned carbon nanotubes based ultrasonic microtransducers for durability monitoring in civil engineering.</i> <u>B. Lebental</u> , P. Chainais, P. Chenevier, N. Chevalier, E. Delevoye, J.-M. Fabbri, S. Nicoletti, P. Renaux, A. Ghis. http://dx.doi.org/10.1088/0957-4484/22/39/395501

²³ The first author (sometimes jointly with the second author) is the main writer while the last author is head of the group. Other authors are sorted by alphabetical order or by intensity of involvement.

PATENTS

5	2014 FR 14 52842 PCT en cours	<i>Dispositif d'acquisition, procédé de fabrication de celui-ci, procédé de mesure de force, <u>B. Lebental</u>, B. Ghaddab, V. Gaudefroy, E. Ruiz Hitzky, P. Aranda, C. Ruiz Gracia, B. Hennings</i>
4	2012 FR 1252861	<i>Détecteur d'analytes utilisant un inverseur logique réalisé à partir de deux transistors. C. Sorin-Cojocar, <u>B. Lebental</u>, F. Z. Bouanis, E. Norman</i>
3	2010 FR 10 52050	<i>Transmission acoustique d'informations dans un matériau poreux. A. Ghis, <u>B. Lebental</u></i>
2	2008 N° EN 08 57928	<i>Cellule CMUT formée d'une membrane de nanotubes ou de nanofils ou de nanopoutres et dispositif d'imagerie acoustique ultra haute fréquence comprenant une pluralité de telles cellules. <u>B. Lebental</u>, A. Ghis</i>
1	2008 N° EN 08 57927	<i>Procédé et dispositif d'analyse acoustique de microporosites dans un matériau tel que le béton à l'aide d'une pluralité de transducteurs CMUTS incorporés dans le matériau. <u>B. Lebental</u>, A. Ghis, E. Delevoye</i>

CHAPTER

1	Feb. 2015	<i>Innovation et Villes Durables, repères pour l'action. Note d'approfondissement sur l'évaluation des territoires d'innovation urbaine. <u>B. Lebental</u>, N. Hautière. Sous la coordination de M. Ray, Advancity</i>
---	-----------	---

CONFERENCES WITH PROCEEDINGS²⁴

18	TNT, Fribourg, Switzerland, Sept. 2016	<i>Nanosensors and sustainable cities: prototyping, integration and reliability. <u>B. Lebental</u>, Yvan Bonnassieux, Fulvio Michelis, Laurence Bodelot</i>
17	IEEE NEMS, Sendai, Japan April 2016	<i>An autonomous, wireless carbon nanotube strain sensor embedded in concrete for crack monitoring. F. Michelis, L. Bodelot, J.-M. Laheurte, F. Zaki, Y. Bonnassieux and <u>B. Lebental</u></i>
16	IEEE NEMS, Sendai, Japan April 2016	<i>Robust Multi-Parameter Sensing Probe for Water Monitoring Based on ALD-Coated Metallic Micro-patterns. Poster. Massimo Pellegrino, William Cesar, <u>Frederic Marty</u>, Martine Capo-Chichi, Bérengère Lebental and Tarik Bourouina</i>
15	SPIE Nanoscience & Engineering 2 (San Diego, USA) August 2015	<i>A graphene-based non-volatile memory, <u>L. Loisel</u>, A. Maurice, B. Lebental, S. Vezzoli, C-S. Cojocar, B.K. Tay. Proceedings SPIE 9552, Carbon Nanotubes, Graphene, and Emerging 2D Materials for Electronic and Photonic Devices VIII</i>
14	NICOM 5 (Chicago, USA) May 2015	<i>Nanosensors for embedded monitoring of construction materials: the "2D conformable" route. <u>B. Lebental</u>, B. Ghaddab, F. Michelis</i>
13	NICOM 5 (Chicago, USA) May 2015	<i>Wireless nanosensors for embedded measurement in concrete structures. <u>F. Michelis</u>, L. Bodelot, J.-M. Laheurte, F. Zaki, Y. Bonnassieux, B. Lebental</i>
12	ICANM (Calgary, Canada) August 2014	<i>A novel weigh-in motion sensor using an asphalt-embedded thin film of graphene-on-clay and carbon-nanotubes. <u>B. Ghaddab</u>, V. Gaudefroy, F. Michelis, E. Ruiz Hitzky, P. Aranda, C. Ruiz Gracia, B. Lebental</i>
11	EWSHM (Nantes, France) July 2014	<i>An innovative nanosensor for weigh-in-motion applications. <u>B. Ghaddab</u>, V. Gaudefroy, F. Michelis, E. Ruiz Hitzky, P. Aranda, C. Ruiz Gracia, B. Lebental</i>

²⁴ For conferences with or without proceedings, the underlined name is the name of the presenter.

10	EWSHM (Nantes, France) July 2014	<i>Wireless flexible strain sensor based on Carbon Nanotube piezoresistive networks for embedded measurement of strain in concrete.</i> <u>F. Michelis</u> , B. Lebental, C.-S. Cojocaru, J.-L. Sorin, Y Bonnassieux
9	EGU 2013	<i>The Sense-City equipment project: insight into the prototyping and validation of environmental micro-and nanosensors for a sustainable urbanization.</i> Poster. B. Lebental, D. Angelescu, T. Bourouina, F. Bourquin, C. S. Cojocaru, F. Derkx, <u>J. Dumoulin</u> , T. L. Ha, E. Robine, H. Van Damme
8	NICOM 4 Agios Nikolaos, Crete, Grees May 2012	<i>Graphene-based resistive humidity sensor for in-situ monitoring of drying shrinkage and intrinsic permeability in concrete</i> <u>B. Lebental</u> , W. Moujahid, C.-S. Lee, J.-L. Maurice and C.S. Cojocaru.
7	ASTELAB Clamart, France July 2012	<i>The Sense-City project.</i> <u>F. Derkx</u> , B. Lebental, T. Bourouina, F. Bourquin, C.-S. Cojocaru, E. Robine, H. Van Damme
6	Acoustics (Nantes, France) July 2012	<i>Carbon nanotubes and graphene-based microsonar for embedded monitoring of microporosity.</i> <u>B. Lebental</u> , N. Sridi, F. Bouanis, C.S. Cojocaru, F. Bourquin, A. Ghis
5	GRETSI (Bordeaux) Sept. 2011	<i>Caractérisation statistique d'une assemblée de nanotubes en imagerie microscopique.</i> <u>P. Chainais</u> , B. Lebental
4	NANOSPAIN (Bilbao, Spain) Avril 2011	<i>Nanosensors for structural monitoring in civil engineering: New insight on promising carbon nanotubes devices.</i> <u>B. Lebental</u> , E. Norman, L. Gorintin, P. Renaux, P. Bondavalli, C. S. Cojocaru, A. Ghis
3	C2I (Le Mans) Jan. 2010	<i>Micro-transducteur ultrasonique capacitif à membrane de nanotubes de carbone.</i> <u>B. Lebental</u> , A. Ghis, F. Bourquin, J.-M. Caussignac, P. Chenevier, N. Chevalier, E. Delevoye, J.-M. Fabbri, A. Meguekam Sado, S. Nicoletti
2	CFM 09 (Marseille) Aout 09	<i>Micro-transducteur ultrasonique à base de nanotubes de carbone pour l'instrumentation immergée des matériaux cimentaires.</i> <u>B. Lebental</u> , F. Bourquin, J.-M. Caussignac, E. Delevoye, P. Chenevier, A. Ghis
1	NDTCE 09 (Nantes) Juin 09	<i>In-situ non-destructive testing of cementitious materials via embedded ultrasonic transducers made up of carbon nanotubes.</i> <u>B. Lebental</u> , F. Bourquin, J.-M. Caussignac, L. Acauan, S. Sanaur, A. Ghis

CONFERENCES WITHOUT PROCEEDINGS

23	MCD Nantes, France June 2016	<i>A mobile nanosensor mat for detection of traffic patterns and overweight vehicles.</i> <u>Bérengère Lebental</u> , Cécile Villette Océane Antoine, Edoardo Milana, John David Roth. Invited Paper.
22	Innov Days Marne La Vallée, France May 2016	<i>Sense-City, Smart Technologies for Sustainable Cities.</i> <u>B. Lebental</u> . Invited paper.
21	3rd CoE Technology Domain Workshop NTU, Singapore March 2016	<i>Sense-City, Smart technologies for sustainable cities.</i> Keynote. <u>B. Lebental</u>
20	GDR-I CNT& Graphene (Aussois, France) Dec 2015	<i>Carbon nanotubes sensors for sustainable city applications: prototyping, integration and reliability analysis.</i> Invited paper. <u>Bérengère Lebental</u> , Yvan Bonnassieux, Fulvio Michelis, Laurence Bodelot
19	Orgagec 2015 (Champs s/ Marne, France) Nov 2015	<i>Sense-City, realistic demonstration of innovative technologies for sustainable cities.</i> Invited paper. <u>B. Lebental</u> .

18	Efficacity Workshop (Champs s/ Marne, France) Nov 2015	<i>Sense-City, Prototypage et Validation de Micro et Nanocapteurs pour la Ville Durable.</i> Invited paper. B. Lebental .
17	MNBS 2015 (Leuven, Belgium) Oct 2015	<i>Project PROTEUS: Smart System integration for Smart Water Monitoring. General overview and technology transfer.</i> Invited paper. B. Lebental
16	Int. Workshop Nanomaterials for Energy and Environment, Orsay, France, March 2015	<i>Nanosensors and sustainable cities: prototyping, integration and reliability.</i> Invited paper. B. Lebental , Yvan Bonnassieux, Fulvio Michelis, Laurence Bodelot
15	French-Singaporean workshop on THz nanosystems (NTU, Singapore) October 2014	<i>Smart technologies for sustainable cities.</i> Invited paper. B. Lebental
14	Nanotech 2014 (Washington, USA) June 2014	<i>The Sense-City equipment project: 9M€ for prototyping and validation of nanosensors for sustainable cities.</i> B. Lebental
13	Nanotech 2014 (Washington, USA) June 2014	<i>Multi-mode humidity sensitivity of carbon nanotubes field-effect transistors.</i> Poster. B. Lebental , H. Woo, E. D. Norman, F. Z. Bouanis, A. Gohier, C. S. Cojocar
12	Nanotech 2014 (Washington, USA) June 2014	<i>Wireless flexible strain sensor based on Carbon Nanotube piezoresistive networks for embedded measurement of strain in concrete.</i> F. Michelis , B. Lebental, C.-S. Cojocar, J.-L. Sorin, Y Bonnassieux
11	E-MRS 2014 Spring meeting (Lille, France) May 2014	<i>Nanosecond-laser-induced graphitization and amorphization of thin nano-crystalline graphite films.</i> Loïc Loisel , Bérengère Lebental, Majid Kabiri Samani, Chong Wei Tan, Costel Sorin Cojocar, Dominique Baillargeat, Beng Kang Tay
10	Journées Ville Numérique (Villeurbanne, France) Dec 2013	<i>Equipex Sense-City, an experimental platform dedicated to networked micro and nanosensors for sustainable cities.</i> Invited paper. B. Lebental
9	CAFFEET Berkeley, France Nov 2012	<i>Sense-City: Sensor networks toward city resilience.</i> B. Lebental
8	Nanotech 2012 (Santa Clara, CA, USA) June 2012	<i>Mechanical properties of suspended few layers graphene sheets.</i> N. Sridi , B. Lebental, E. Merliot, C. S. Cojocar, J. Azevedo, A. Nowodzinski, J.C. Gabriel and A. Ghis
7	GDR-I CNT& Graphene (Ecully, France) Jan. 2012	<i>Developing low-cost graphene devices.</i> C. S. Lee , W. Moujahid, B. Lebental, M. Châtelet, F. Le Normand, J.-L. Maurice, C. S. Cojocar
6	ECND-PdL (Nantes, France) Nov. 2011	<i>Nanosensors for the smart city: new insight on promising carbon nanotubes devices.</i> Invited paper. B. Lebental
5	NDCM 12 (Blacksburg, VA, USA) June 2011	<i>Nanosensors for nanoscale structural health monitoring in civil engineering: new insight on carbon nanotubes devices.</i> B. Lebental , F. Bourquin, A. Ghis and C. S. Cojocar
4	GDR-I CNT& Graphene (Dourdan, France) Feb. 2011	<i>Carbon nanotube based humidity sensor.</i> E. D. Norman , L. Gorintin, B. Lebental, P. Bondavalli and C. S. Cojocar

3	NT 2010 Montréal, Canada July 2010	<i>Ultra-thin membranes of well-aligned single-walled carbon nanotubes.</i> Poster. Bérengère Lebental, Nicolas Chevalier, Pierre Chainais, Pascale Chenevier, Anne Ghis
2	CFMP (Paris, France) 2010	<i>Nanotechnologies et Génie Civil, comment coopérer pour innover ?</i> Invited paper. <u>B. Lebental</u>
1	GDR-I CNT& Graphene (Coma Ruga, Spain) 2009	<i>Carbon nanotubes based ultrasonic transducer for the instrumentation of cementitious materials.</i> <u>B. Lebental</u> , P. Chainais, P. Chenevier, N. Chevalier, A. Meguekam Sado, S. Nicoletti and A. Ghis

DISSEMINATION AND VULGARIZATION²⁵

17	CPU.fr Apr. 2016	Interview sur Sense-City. Laure Marot
16	PCM Mars. 2016	Interview sur Sense-City. Christine Del Papa
15	EPAMARNElavallee.fr Dec. 2015	Interview video sur Sense-City. Anne Schneidel
14	Les héros du climat, France 2, Nov. 2015	Interview video sur Sense-City. Allain Bougrain Dubourg
13	Trajectoires, n° 41 Sept. 2015	Interview sur Sense-City, Marie-Sophie Gauthier
12	ICUBE, n°26 2015	<i>Sense-City.</i> E. Vidal, B. Lebental
11	Journal du Grand Paris, Mai 2015	Interview sur Sense-City : « <i>la ville sous capteurs se matérialise à Marne La Vallée</i> ». Géraldine Bouton
10	Les clés de demain, Mai 2015	<i>Des nanocapteurs pour une ville durable.</i> B. Lebental
9	Environnement magazine Avril 2015	Interview sur Sense-City, Cécile Michaut
8	Le Parisien, édition Seine-et-Marne Mars 2015	Interview sur Sense-City : « <i>la ville du futur sera communicante</i> ». Gilles Cordillot
7	Canal Coquelicot Mars 2015	Interview video sur Sense-City.
6	Les Echos Mars 2015	Interview sur Sense-City: « <i>une ville intelligente en miniature</i> ». Frank Niedercom
5	DIXIT 2014	<i>Des réseaux de capteurs pour la résilience et l'attractivité urbaine.</i> <u>B. Lebental</u>
4	Green City Champs s/ Marne, France Oct. 2013	<i>Expérimentation et démonstrateurs, une priorité pour l'accélération des cycles d'innovation en milieu urbain, Atelier 3.</i> Table ronde. L. Actman, S. Anders, J.-M. Barbier, <u>B. Lebental</u> , J. Soula, T. Bodirot, R. Vicari, J. Dumonteil

²⁵ For interviews, the provided name is the name of the journalist.

3	Cycle des Rencontres du Café des techniques, CNAM, Paris, France 2013	<i>Écologie urbaine : l'avenir de la ville sera durable.</i> Table ronde. Laure Heland, <u>Béregère Lebental</u> , Bernard Matyja, Eric Vidalenc
2	Futurs en Seine, 104-Paris, France June 2013	<i>How R\&D improves Sustainability and Quality of Life in Smart Cities, Paris Region Economic Development Agency. Panel on Cities Issues, the points of view of ICT, Telecommunication and Environmental Services Corporates.</i> Hervé Rannou, Ger Baron, <u>Béregère Lebental</u> , Nathalie Leboucher, Philippe Sajhau, François Grosse
1	Hippocampe 2012	<i>Sense-city : prototypage et validation en milieu réaliste de micro et nanocapteurs pour la ville durable.</i> B. Lebental

Appendix 2: State of the art on carbon nanotube sensors

The following sections present a sample of the wide state of the art (SOTA) on carbon nanotube sensors. These texts were written for ANR or H2020 projects between 2010 and 2015, and have NOT been actualized with the more recent literature.

1) Humidity sensors

State of the art from December 2010, extracted from unsuccessful ANR proposal Nympheco: Carbon-nanotubes based pH and humidity sensors for the non-destructive testing of cementitious materials

Most existing humidity sensors are based on capacitive, resistive, gravimetric or optical effects. Features of the sensors are their sensitivity over a large range of humidity and temperature, their response time, the measurement reproducibility, their durability, their cost [Rittersma 2002]. Carbon nanotubes are commonly used as coating material to improve the sensitivity of the devices to vapour water, for example for capacitive [Bruzzi 2004; Yeow 2006; Chen, 2009], resistive [Huang 2004; Jiang 2007] or mechanical [Zhang 2005; Jaruwongrungrunsee 2008; Su 2009] sensors.

Carbon nanotubes have also demonstrated very promising properties as the active channel of FET based gas sensors [Bondavalli 2009]: they are ultra-compact, effective at room temperature; they have low power consumption, very fast response time and a good versatility. Typical gas sensed are NH₃, NO or CO. The sensing of gas by CNTFET devices seems to rely on a variation of the metal electrode work function upon gas adsorption. It leads to changes in the properties of the Schottky junctions formed by the metal-CNT contacts. The technique of gas fingerprinting, based on arrayed CNTFET devices with different metal electrodes, is used to discriminate different gaz. In this context, CNTFET-based gas sensors can be adapted for humidity (vapour H₂O) sensing: in [Star 2004], a Nafion-coated, single SWNT-based FET is shown to be sensitive to relative humidity in the 12% to 93 % range.

However, single SWNTs devices are expensive to produce and poorly reproducible. Moreover SWNTs are always obtained as a mixture of 1/3 metallic and 2/3 semiconducting nanotubes independently from the growth technique, so that a very complex step of sorting of the semiconducting SWNTs is often required to produce single-SWNT-FET devices. On the other hand, by wisely exploiting a percolation effect in random SWNTs networks (SWNT mats) overall semiconductor behaviour can be obtained for carefully controlled SWNT (surface) densities [Snow, 2004]. Devices made from such films exhibit stunning characteristics (especially considering their relatively simple processing conditions), although such characteristics (carrier mobility, subthreshold slope...) are not as good as those of counterpart devices obtained with individual SWNT specimens.

Sensitivity to humidity of SWNTs-mats based FET devices has not been systematically studied, although it is well known that the hysteresis observed in CNTFET devices depends strongly on humidity [Kim 2003; Zahab 2000; Na 2005]. This hysteresis contributes to uncertainty of measurement in CNTFET gas sensors.

Bibliography

[Bondavalli 2009] Bondavalli P., et al., "Carbon nanotubes based transistors as gas sensors: State of the art and critical review", *Sensors and Actuators B*, vol. 140, p. 304-318, 2009

- [Bruzzi 2004] Bruzzi M., et al., "First study of humidity sensors based on nanostructured carbon films produced by supersonic cluster beam deposition", *Sensors and Actuators B*, vol. 100, p. 173-176, 2004.
- [Chen 2005] Chen H.-W., et al., "The application of CNT/Nafion composite material to low humidity sensing measurement", *Sensors and Actuators B*, vol. 104, p. 80-84, 2005
- [Huang 2004] Huang X., et al., "Carboxylation multi-walled carbon nanotubes modified with LiClO₄ for water vapour detection", *Nanotechnology*, vol. 15, p. 1284-1288, 2004
- [Jaruwongrungrongsee 2008] Jaruwongrungrongsee K., et al., "Humidity sensor utilizing multiwalled carbon nanotubes coated quartz microbalance", 2nd IEEE International Nanoelectronics Conference, 2008
- [Jiang 2007] Jiang W. F., et al., "Resistive humidity sensitivity of arrayed multi-wall carbon nanotube nests grown on arrayed nanoporous silicon pillars", *Sensors and Actuators B*, vol. 125, p. 651-655, 2007
- [Kim 2003] Kim W., et al., "Hysteresis Caused by Water Molecules in Carbon Nanotube Field-Effect Transistors", *Nano Letters*, vol. 3, p. 193-198, 2003
- [Na 2005] Na P. S., et al., "Investigation of the humidity effect on the electrical properties of single-walled carbon nanotube transistors", *Applied Physics Letters*, vol. 87, p. 093101, 2005
- [Rittersma 2002] Rittersma Z. M., "Recent achievements in miniaturised humidity sensors – a review of transduction techniques", *Sensors and Actuators A: Physical*, vol. 96, p. 196-210, 2002.
- [Star 2004] Star A., et al., "Sensing with Nafion Coated Carbon Nanotube Field-Effect Transistors", *Electroanalysis*, vol. 16, p. 108-112, 2004
- [Su 2009] Su P.-G., Tsai J.-F., "Low-humidity sensing properties of carbon nanotubes measured by a quartz crystal microbalance", *Sensors and Actuators B*, vol. 135, p. 506-511, 2009
- [Yeow 2006] Yeow J. T.W., She J. P. M., "Carbon nanotube-enhanced capillary condensation for a capacitive humidity sensor", *Nanotechnology*, vol. 17, p. 5441-5448, 2006
- [Zahab 2000] Zahab A., et al., "Water-vapor effect on the electrical conductivity of a single-walled carbon nanotube mat", *Physical Review B*, vol. 62, p. 10000, 2000.

2) Gas sensors (SOTA 2013, extract from ANR INCAS)

State of the art from March 2013, extracted from unsuccessful ANR proposal INCAS: Integrated carbon-based gas sensors for urban air quality monitoring

Generalities on CNT-based gas sensing

Four main uses of carbon nanotubes (CNT) for gas sensing have been reported since 2000 [Wang 2009]:

- Sensitizing coatings in various electronic devices, such as resistances and capacitances [Varghese 2001], resonating disks [Chopra 2002] or surface acoustic wave devices [Penza 2004, Sivaramakrishnan 2008].
- Vertically aligned field emitters in low pressure environment [Modi 2003, Hou 2006].
- Resistive thin films of randomly organized nanotubes [Li 2003, Valentini 2003, Wong 2003, Ueda 2008, Lorwongtragool 2012].
- Semi-conducting channel of a field effect transistor (CNTFET) [Bondavalli 2009], including early work where the transistor channel is an isolated single walled carbon nanotubes (SWNT) [Kong 2000] and later work where it is an (usually) random network of single walled carbon nanotubes [Snow 2006].

Both multi-walled and single-walled CNT are used (except for the CNTFET route), and the CNTs are either deposited by a liquid route (sometime by self-assembly) on SiO₂, plastics or glass or grown by

CVD on SiO₂ (and sometimes transferred onto other substrates). Most of these devices are operable at room temperature, although increased performances may be observed at higher temperature (150°C-200°C).

The first gases detected with carbon nanotubes were NO₂ and NH₃, as they are respectively strong electron-acceptor and electron-donor gases [Kong 2000]. Detected concentrations ranged from 2ppm to 10,000ppm. Today, the gas compounds tested for sensing by carbon nanotubes-based devices are quite diverse: O₂, O₃, NO₂, NO, NH₃, H₂, H₂S, H₂O, DMMP, TNT, acetone, ethanol, nitrotoluene, and various volatil organic compounds, in particular formaldehyde, hydrocarbons...

The effectiveness of CNT-based gas sensing devices is mainly ascribed to the charge-transfer-enabling (effective doping) physisorption of gas molecules (especially NO₂ and NH₃) on the surface of carbon nanotubes [Chang 2001] as well as to the alteration of the Schottky barrier at the CNT/metal and CNT/CNT interfaces (especially in CNTFETs and random thin films) [Bondavalli 2009]. The presence of defects on the CNTs seems to enhance sensitivity [Salehi-Khojin 2011].

Non functionalized graphene is used similarly to carbon nanotubes and displays pretty much the same behaviour as carbon nanotubes regarding to gas sensing. The following devices have been reported since a 2007 paper by Novoselov and Geim's team [Schedin 2007]:

- Sensitizing coating in various electronic devices, including CMOS integrated capacitance [Zhao 2011], RFID antennas [Le 2012] or surface acoustic wave devices [Arsat 2009].
- Resistive films of individual large scale sheets [Varezhnikov 2012] or micro scale sheets [Schedin 2007, Lu 2009] or assembled microsheets [Robinson 2008, Fowler 2009] on various substrates including polymeric and/or flexible substrates.
- Semi-conducting channel of a field effect transistor (G-FET) [Rumyantsev 2012].

It is most important to note that most devices rely on graphene oxide (GO) or reduced graphene oxide (RGO), and rarely on pristine graphene (transferred or not). It stems not only from technological issues (GO and RGO are easier to manipulate, as they are solution-processable) but also from the fact that GO and RGO, being more defective than pristine graphene, are expected to be more sensitive to gases (although they have less interesting electronic transport properties).

As with carbon nanotubes, the first detected gases were NO₂, NH₃ [Schedin 2007], but H₂, CO, H₂O, ethanol, isopropanol and methanol, tetrahydrofuran, chloroform, hydrazine hydrate or dinitrotoluene quickly followed. Theoretical works mainly attribute the strong sensitivity to charge-transfer-enabling physisorption of gas molecules on graphene surface [Leenaerts 2008]. The advantage of graphene with respect to carbon nanotubes is that every atom of graphene can be considered a surface atom, capable of interacting even with a single molecule of the target gas or vapor species. It eventually results in the ultrasensitive (single molecule detection [Schedin 2007]) sensor response.

CNT-based gas sensing via CNT functionalization

The general problem of previously described carbon nanotubes and graphene devices is their cross sensitivity to almost all gases [Cantalini 2003], which prevents any selective measurement. Although some techniques based on arraying devices with different metal electrodes and using data processing algorithms (artificial neural networks) [Bondavalli 2009; Varezhnikov 2012] have been proposed both for graphene and CNTFET (the electronic nose approach), the most common

approach by far to selectivity (and which can be coupled with the electronic nose approach) is to functionalize carbon nanotubes and graphene by chemical compounds sensitive to specific gases [Zhang 2008].

The first route consists in functionalizing (covalently or not) CNT or graphene by polymeric compounds such as PEI, Nafion, PMMA [Santhanam 2005, Wei 2006]. This solution is attractive but most of the proposed polymers are also highly sensitive to moisture, so that for practical use, the dominant response is that of the air moisture content. Another route consists in functionalizing the material by different, selected DNA sequences [Staji 2005, Johnson 2006, Lu 2010]; this route (as well as similar routes relying on functionalization by biological compounds) is also very promising for selectivity to an unlimited number of gases (because the DNA sequences can be tuned to infinity) but the DNA sequences cannot withstand environmental aggression such as high temperature (>80°C), exposure to high or low pH or chemical agents [Bauer 2003], which strongly limit their relevance for use in long-span outdoor applications with exposure to various climatic conditions (heat wave, acid rains...)

The most promising strategy for “generic-use” gas sensing devices consists in functionalizing (covalently or not) the sp² materials by metal and metal oxides nanoparticles (Pt, Pd, Au, Ti, Sn, Rh, ZnO, SnO₂) [Kong 2001, Starr 2006, Penza 2007; Kauffmann 2007, Pumera 2010, Chu 2011, Shafiei 2009, Ko 2010, Nomani 2010, Wu 2011, Singh 2012, Sharma 2012]. The metal nanoparticles may be residual growth catalysts or may be deposited by a variety of methods, including sputtering and electrochemistry. In [Lo 2010], it is reported that the sensitivity reaches the parts-per-billion level with 10 ppb rms noise in presence of commonly interfering gases like CO₂, H₂O, NH₃ and O₂. Similarly to the DNA and the polymer approaches, there are numerous degrees of freedom to improve selectivity, namely the composition (pure metal, alloys), size, density, morphology of the nanoparticles [Penza 2009, Mubeen 2011]. Operation of the devices has been reported up to 250°C [Penza 2007, 2009].

Two sensing mechanisms have been proposed: gas-environment sensitive charge transfer at the sp² carbon/metal interface [Penza 2007, 2009] associated to oxydo-reduction reactions between metal and targeted gases in presence of oxygen [Lupan 2008] and nano Schottky junctions at the sp²-carbon/metal interface [Mubeen 2011] (in other words, energy band displacements and discontinuities around the nanoparticles); Joule self-heating of the sp²-materials enhanced by thermal resistance at the sp² carbon/nanoparticles interfaces [Rouxinol 2010].

Despite the success of the metal-decoration approach, selectivity remains lower than expected; for instance the influence of (non-selective) Joule heating is found to be larger than that of the charge transfer by [Rouxinol 2010]: it is attributed to the fact that the charge transfer remains small between metal and sp² carbon, especially when functionalization is non-covalent, which is preferred to covalent bonding to avoid degrading the sp²-carbon outstanding electronic transport properties (covalent bonds may introduce electron scattering centers [Park 2006]).

To improve drastically selectivity, instead of direct functionalization by metal or metal oxides nanoparticles, an alternative approach relies on non-covalent functionalization of sp²-carbon materials by metal complexes enabling a strong interaction of the metal core with the π system of the nanotube or graphene. A few examples (describing Pt complexes on SWNTs) support the validity of this approach for gas sensing [Albrecht 2001, Cid 2009].

The non-covalent functionalization of SWCNTs with metal complexes has been carried out since the beginning of years 2000 mainly using porphyrin and phtalocyanin metal-based complexes [Li 2004, Ehli 2006, Rahman 2006, D'souza 2010, Ho 2010, Hijazi 2012]. However, because of the lack of large extended π -system within these complexes, the electronic interaction of the metal center present in the ligand cavity and the nanotubes is usually relatively weak. Indeed, in many cases the phtalocyanin or the porphyrin units need to be functionalized by pyrene or long alkyl chains groups or be included within a polymer in order to enhance their interaction with the nanotubes [Li 2004, Hijazi 2012, Maligaspe 2010]. Apart from phtalocyanin or porphyrin complexes, metal tetraazannulene based complexes were reported but again no evidence of a large interaction of the metal ion with the carbon material was evidenced [Basiuk 2002, 2013]. Bisalophen based complexes, with an organic ligand made of an extended π -system, feature enhanced interaction with nanotubes; evidenced by a charge transfer between metal and nanotubes [Magadur 2012] attributed to large electronic withdrawing effect that affects the organic part in contact with the nanotube.

Toward integrated gas sensing

Literature shows than once some kind of sensitivity is achieved (with or without selectivity), devices can be integrated, which is mandatory for further applicative use. In general, integration comprises several successive levels: 1. signal conditioning to obtain analog (typically 3V to 5V) voltage or 2. digital outputs acquired by the user via wired connections on work stations; integration into 3. passive RFID nodes or 4. active wireless sensor nodes (WSN). 5. Packaging to protect the sensing device from non-desired outside perturbations. The following table summarizes the few existing results, most of them very recent, none of them in France:

Tableau 1 : 2013 state of the art on integration of CNT sensors

Ref.	Sensing material and device structure	Gas sensed	Integration level	Validation level
Cho 2009	As grown (900°C) CNTFET (CNT mats) used as resistive devices	NO ₂	CMOS based, low power (<32 μ W) signal conditioning up to wired digital output	Single integrated prototype, lab validation, Repeatability of devices tested (>400 devices) but not satisfying (6 orders of magnitude variability)
Le 2012	Ink-jet printed RGO with no additional functionalization Resistive thin film configuration	NH ₃	Integration into passive RFID node without packaging.	Single integrated prototype, lab validation
Feng	Spray-coated CNT forming a resistive thin	H ₂ O	Integration into passive RFID node without	Single integrated prototype, lab

2012	film		packaging.	validation
Occhiuzzi 2012	CNT coating a RFID passive tag	NH ₃	Coating of conventional RFID tag	Single prototype, lab validation
Penza 2012	Pt decorated CNT thin films described in [Penza 2007, 2009]	NO _x	Not detailed; at least signal conditioning; final system is car-portable	20 days continuous urban monitoring (from a mobile lab) with comparison with reference NO _x sensor, (displaying strong discrepancies)
Kim 2012	Ink-jet printed CNT on Pt electrodes with Pd decorations Resistive operation	NO ₂	Packaged sensor including numeric display of readings and USB connectivity	Several prototypes (6) with superposable outputs, lab validation
Liu 2013	Dielectrophoresis-deposited, DNA functionalized CNT in resistive configuration	DNT, DMMP	CMOS based signal conditioning Integration into ZigBee based WSN	Single integrated prototype, lab validation

The previous table shows that, to this day, although there are numerous papers on CNT/graphene gas sensing devices, the devices are almost never integrated (7 reports only over hundreds²⁶ of papers on this issue since 2000). It is mostly attributed to the lack of repeatability of the devices fabrication process: dispersion in device features and in device sensitivity is usually huge. For instance, 6 orders of magnitude in the I_{on}²⁷ of over 400 CNTFET devices are reported in [Cho 2009], 5 orders of magnitude variations in the I_{off} of 90 CNTFET devices are reported in [Gorintin 2011], even after optimization of the I_{on} parameter (less than 1 decade variation on I_{on}). It hinders or even forbids signal conditioning, as it is very complicated to provide an integrated acquisition chain with large acquisition dynamics. It is all the more true when one requires ultra-low power conditioning, as is the case for autonomous wireless sensing. As a consequence, devices are integrated only as proof of concept at the prototype level, without regards for further integration, future up-scaling of the process or potential industrial transfer

Bibliography

[Albrecht 2001] M. Albrecht et al., Chem. Commun. 2001, 1874-1875

[Arsat 2009] R. Arsat et al., Chemical Physics Letters, vol. 467, 2009, pp. 344-347

[Basiuk 2002] E. V. Basiuk et al., Nano Lett. 2002, 2, 1249-1252

[Basiuk 2013] V. A. Basiuk et al., Appl. Surf. Sci. 2013, <http://dx.doi.org/10.1016/j.apsusc.2013.01.106>

²⁶www.sciencedirect.com: 282 entries with keys 'carbon nanotubes' & 'gas sensitivity', 82 with keys 'graphene' & 'gas sensitivity'

²⁷ I_{on} : Closed circuit drain source current ; I_{off} : Open circuit drain source current

- [Bauer 2003] T. Bauer et al., *Eur Food Res Technol* (2003) 217:338–343
- [Bondavalli 2009] P. Bondavalli et al., *Sens. Actuators, B*, 2009, 140, 304–318
- [Cantalini 2003] C. Cantalini et al., *Sensors and Actuators B: Chemical*, vol. 95, 2003, pp. 195-202(8)
- [Chang 2001] H. Chang et al., *Appl. Phys. Lett.* 79, 3863 (2001)
- [Cho 2009] T. S. Cho et al., *Solid-State Circuits, IEEE Journal of* , vol.44, no.2, pp.659,669, Feb. 2009
- [Chopra 2002] S. Chopra et al., *Appl. Phys. Lett.* 80, 4632 (2002)
- [Chu 2011] B.H. Chu et al., *Sensors and Actuators B* 157 (2011) 500–503
- [Cid 2009] C. C. Cid et al., *Sensor Actuat. B-Chem.* 2009, 141, 97-103
- [D'souza 2010] F. D'souza et al., *J. Phys. Chem. A* 2010, 114, 10951-10959
- [Ehli 2006] C. Ehli et al., *J. Am. Chem. Soc.* 2006, 128, 11222-11231
- [Feng 2012] Y. Feng et al. *Sensors Journal, IEEE* , vol.12, no.9, pp.2844,2850, Sept. 2012
- [Fowler 2009] J. D. Fowler et al. *ACS Nano*, 2009, 3 (2), 301-306
- [Gorintin 2011] Gorintin L, *Etude et réalisation de transistors à nanotubes de carbone pour la détection sélective de gaz*, PhD thesis for Ecole Polytechnique, 2011, TRT, Supervisors : P. Bondavalli, M. Chatelet
- [Hijazi 2012] I. Hijazi et al., *J. Mater. Chem.* 2012, 22, 20936-20942.
- [Ho 2010] K. H. L. Ho et al., *Chem. Commun.* 2010, 46, 8731-8733
- [Hou 2006] Z. Hou et al., *Appl. Phys. Lett.*, vol. 89, no. 21, 2006
- [Johnson 2006] A.T. Johnson et al., *Semicond. Sci. Technol.*, 21 (2006), pp. S17–21
- [Kauffmann 2007] D.R. Kauffmann, A. Starr, *Nano Lett.* 7 (7) (2007) 1863–1868
- [Kim 2012] J. Kim, *J. Nanomaterials*, January 2012, Article ID 741647
- [Ko 2010] G. Ko, et al., *Current Applied Physics* 10 (2010) 1002–1004
- [Kong 2000] J. Kong et al., *Science*, 287 (2000), pp. 622–625
- [Kong 2001] J. Kong et al., *Adv. Mat.* 13 (18) (2001)
- [Le 2012] T. Le et al., *IEEE Sensors 2012*, pp.1-4, 28-31 Oct. 2012
- [Le 2012] T. Le et al., *Microwave Conference (EuMC), 42nd European* , pp.412,415, 2012
- [Leenaerts 2008] O. Leenaerts et al., *Phys. Rev. B* 77, 125416 (2008)
- [Li 2003] J. Li et al., *Nanoletters*, 3 (7) (2003), pp. 929–933
- [Li 2006] H. P. Li et al. *J. Am. Chem. Soc.* 2004, 126, 1014-1015
- [Lorwongtragool 2012] P. Lorwongtragool et al., *ECTI-CON, 9th International Conference*, pp.1-4, 16-18 May 2012
- [Lu 2009] G. Lu et al., *2009 Nanotechnology* 20 445502
- [Lu 2010] Y. Lu et al., *Appl. Phys. Lett.* 97, 083107 (2010)
- [Lupan 2008] O. Lupan et al., *Thin Solid Films* 2008; 516:3338–45
- [Magadur 2012] G. Magadur et al., *J. Am. Chem. Soc.*, 2012, 134, 7896-7901
- [Maligaspe 2010] E. Maligaspe et al., *J. Am. Chem. Soc.* 2010, 132, 8158-8164
- [Modi 2003] A. Modi et al., *Nature*, vol. 424, no. 6945, pp. 171–174, 2003
- [Mubeen 2011] S. Mubeen et al., *Electroanalysis* 2011, 23, No. 11, 2687 – 269
- [Nomani 2010] M.W.K. Nomani et al., *Sensors and Actuators B* 150 (2010) 301–307
- [Occhiuzzi 2012] C. Occhiuzzi et al., *Microwave Theory and Techniques, IEEE Transactions on*, vol.59, 2674, 2011
- [Park 2006] H. Park et al., *Nano letters* 6.5 (2006): 916-919
- [Penza 2004] M. Penza et al., *Sensors and Actuators B: Chemical*, vol. 100, 2004, pp. 47-59
- [Penza 2007] M. Penza et al. *Appl. Phys. Lett.* 90, 173123 (2007)
- [Penza 2009] M. Penza et al., *Sensors and Actuators B: Chemical*, vol. 140, 2009, pp. 176-184

- [Penza 2012] Penza, Michele et al. 14th International Meeting on Chemical Sensors (2012): 1767-1770
- [Pumera 2010] M. Pumera et al., Trends in Analytical Chemistry 29 (2010) 954–965
- [Rahman 2006] G. M. A. Rahman et al., J. Mater. Chem. 2006, 16, 62-65
- [Robinson 2008] J. T. Robinson et al., Nano Letters 2008 8 (10), 3137-3140
- [Rouxinol 2010] F. P. Rouxinol et al. (2010) ISBN: 978-953-307-054-4, InTech, DOI: 10.5772/39434
- [Rumyantsev 2012] S. Rumyantsev et al., Nano Letters 2012 12 (5), 2294-2298
- [Salehi-Khojin 2011] A. Salehi-Khojin et al., ACS Nano 2011 5 (1), 153-158
- [Santhanam 2005] K. S. V. Santhanam et al., 2005 Sensors Actuators B, 106, 766–71
- [Schedin 2007] F. Schedin et al., Nat. Mater., 6 (2007) 652–655.
- [Schedin 2007] F. Schedin et al., Nat. Mater., 6 (2007) 652–655.
- [Shafiei 2009] M. Shafiei et al., 8th IEEE SENSORS Conference (2009), 25–28 October 2009
- [Sharma 2012] A. Sharma et al., Journal of Materials Chemistry (2012)
- [Singh 2012] G. Singh et al., Carbon, vol. 50, 2012, pp. 385-394
- [Sivaramakrishnan 2008] S. Sivaramakrishnan et al., Sensors and Actuators B: Chemical, Vol. 132, 2008, pp. 296-304
- [Snow 2006] E.S. Snow et al., Chem. Soc. Rev., 35 (2006), pp. 790–798
- [Staji 2005] C. Staii et al., Nano Lett., 5 (9) (2005), pp. 1774–1778
- [Starr 2006] A. Starr et al., J. Phys. Chem. B 110 (2006) 21014–21020
- [Ueda 2008] T. Ueda et al., Diamond and Related Materials, vol. 17, 2008, pp. 1586-1589
- [Valentini 2003] L. Valentini et al., Applied Physics Letters, vol.82, no.6, pp.961-963, Feb 2003
- [Varezhnikov 2012] A. Varezhnikov et al., P2.9.24, 14th International Meeting on Chemical Sensors - IMCS 2012
- [Varghese 2001] O.K. Varghese et al., Sensors and Actuators B: Chemical, Vol. 81, 2001, pp. 32-41
- [Wang 2009] Y. Wang and John T. W. Yeow, Journal of Sensors, vol. 2009, Article ID 493904, 24 pages, 2009
- [Wei 2006] C. Wei et al., 2006 J. Am. Chem. Soc. 128 1412–3
- [Wong 2003] Y. M. Wong et al, Sensors and Actuators B, vol. 93, no. 1–3, pp. 327–332, 2003
- [Wu 2011] B. Wu, et al. Nano Today 6.1 (2011): 75-90
- [Zhang 2008] T. Zhang et al., 2008 Nanotechnology 19 332001
- [Zhao 2011] C. L. Zhao et al., Solid-State Sensors, Actuators and Microsystems Conference, 16th International, pp.1954-1957, 2011

3) Liquid phase sensing

State of the art from April 2015, extracted from successful H2020 proposal PROTEUS: Adaptive microfluidic and nano-enabled smart systems for water quality Sensing

Focus on pH sensing: State of the art from December 2010, extracted from unsuccessful ANR proposal Nympheco: Carbon-nanotubes based pH and humidity sensors for the non-destructive testing of cementitious materials

For permanent, autonomous, integrated monitoring of chemicals in liquid, there is a need for robust sensitive, low cost materials that can be integrated into simple electronic devices. Sp²-carbon based nanomaterials (carbon nanotubes and graphene derivatives) have been heavily studied as promising candidates, because they can be integrated in a wide range of electronic devices (resistances,

transistors, voltammetric electrodes) and withstand a wide range of chemical attacks and because their high surface-to-volume ratio is a promise for exceptional sensitivity and highly compact devices.

However, the bulk of the effort has focused on gas [Llobet 2013] and biological [Jacobs 2010, Wang 2011] sensing and the monitoring of inorganic analytes has been mostly limited to pH, with only punctual research on Cl_2 [Dong 2012] or dissolved O_2 [Zheng 2011]. Regarding to pH sensing, issues such as integration into wireless [Gou 2014] or microfluidic [Li 2014] systems, time stability [Li 2011], process yield and device reproducibility are progressively getting addressed at the lab stage, but results are far from satisfactory for long term use. For other analytes, cross sensitivity is a major issue usually solved by chemical functionalization; time stability, reproducibility and integration are not addressed yet.

Focusing now on pH sensing only, CNT are used in various categories of devices. The most common are electrodes for voltammetric measurements [Keampgen 2005; Weber 2006], resistors [Kwon 2006; Morato 2007] and transistors [Rosenblatt 2002; Wang 2004]. CNT are either employed raw [Keampgen 2005] or additionally sensitized to pH by functionalization [Weber 2006], polymer- or enzyme-coating [Wang 2005] or integration in a polymer-CNT composite [Keampgen 2006].

CNTFET based aqueous sensors present various advantages over other types of sensors, ultra compactness and high sensitivity [Kaufman 2008] among others. CNTFET devices for pH measurements are often electrolyte gated [Krüger 2001; Rosenblatt 2002; Kaufman 2008]: the device itself consists only in the Source-Channel(CNT)-Drain part of the FET, which is immersed in an electrolyte solution, whereas the FET gate is formed by an external electrode plunged in the solution. Such technique is hardly applicable for embedded monitoring.

FET devices with integrated gate have also been often reported [Wang 2005; Allen 2007]. They are most often based on functionalized SWNTs. However, functionalization is detrimental for the nanotubes atomic structure and thus for their conducting properties as FET channel material. To our knowledge, only Takeda in [Takeda 2007] reports on a non-functionalized-SWNTs-based FET for pH sensing. In this device, the upper bound for the studied pH is 8, way below the range of pH of interest for the monitoring of cementitious materials. More generally, CNT based pH sensors have not been experimented above pH 10 to 12, because there was no identified application out of the biological sphere.

Bibliography

[Allen 2007] Allen B. L., et al., "Carbon Nanotube Field-Effect-Transistor-Based Biosensors", *Advanced Materials*, vol. 19, p. 1439-1451, 2007

[Dong 2012] Dong et al. (2012) *Analytical chemistry*, 84(19), 8378-8382

[Gou 2014] Gou et al. (2014) *Scientific reports*, 4, 4468

[Jacobs 2010] Jacobs et al. (2010). *Analytica Chimica Acta*, 662(2), 105-127.

[Kaempgen 2005] Kaempgen M., Roth S., "Ultra microelectrodes from MWCNT bundles", *Synthetic Metals*, vol. 152, p. 353-356, 2005

[Kaempgen 2006] Kaempgen M., Roth S., "Transparent and flexible carbon nanotube/polyaniline pH sensors", *Journal of Electroanalytical Chemistry*, vol. 586, p. 72-76, 2006

- [Kauffman 2008] Kauffman D. R., Star A., "Electronically monitoring biological interactions with carbon nanotube field-effect transistors", *Chemical Society Reviews*, vol. 37, p. 1197-1206, 2008
- [Kruger 2001] Krüger M., et al., "Electrochemical carbon nanotube field-effect transistor", *Applied Physics Letters*, vol. 78, p. 1291-1293, 2001
- [Kwon 2006] Kwon J.-H., et al., "Single-Wall Carbon Nanotube-Based pH Sensor Fabricated by the Spray Method", *Electrochemical and Solid-State Letters*, vol. 9, p. H85-H87, 2006
- [Li 2014] Li et al. (2014) *Analyst*, 139(8), 2011-2015.
- [Llobet 2013] Llobet, E. (2013) *Sensors and Actuators B: Chemical*, 179, 32-45
- [Maroto 2007] Maroto A., et al., "Functionalized Metallic Carbon Nanotube Devices for pH Sensing", *ChemPhysChem*, vol. 8, p. 220-223, 2007
- [Rosenblatt 2002] Rosenblatt S., et al., "High Performance Electrolyte Gated Carbon Nanotube Transistors", *Nano Letters*, vol. 2, p. 869-872, 2002
- [Takeda 2007] Takeda M., et al., "A pH sensor based on electric properties of nanotubes on a glass substrate", *Nanoscale Research Letters*, vol. 2, p. 207-212, 2007
- [Wang 2005] Wang J., "Carbon-Nanotube Based Electrochemical Biosensors: A Review", *Electroanalysis*, vol. 17, p. 7-14, 2005
- [Wang 2011] Wang et al. (2011) *Trends in biotechnology*, 29(5), 205-212
- [Weber 2006] Weber J., et al., "Novel lactate and pH biosensor for skin and sweat analysis based on single walled carbon nanotubes", *Sensors and Actuators B*, vol. 117, p. 308-313, 2006
- [Zheng 2011] Zheng et al. (2011) *Sensors and Actuators B: Chemical*, 157(2), 488-493
- Li et al. (2011) *Biosensors*, 1(1), 23-35.

Appendix 3: State of the art of reproducibility in carbon nanotube network-based sensors

Tableau 2 : 2015 State of the art of reproducibility of sensors based on networks of CNT

Ref	Observables	Year	Fabrication	Substrate	Device-to-device variability on fabrication	Device-to-device variability on sensitivity
Inkjet-printed sensors with study of variability						
[1]	Strain	2012	Ink-jet printing	PET	3 set of 3 sensors compared Best std dev 3.5%	No
[2]	Gas (NO ₂ , CO)	2009	Ink-jet printing	4in. Si/SiO ₂ wafer	6 sensors compared No std dev provided Std dev < 4%	4 sensors compared No std dev provided
[3]	pH	2009	Ink-jet printing	glass	5.6% over 10 sensors	No
[4]	Anti-oxidant power	2014	Inkjet printing	Kapton polyimide	Overlaid plots of amperometric response for batches of 6 and 4 sensors Std dev : 7% and 20% on the two parameters extracted from amperometric response	Two sets of two devices compared
Inkjet printing with study of variability						
[5]	Strain	2012	Inkjet printing	PDMS	No	No
[6]	Relative humidity	2013	Inkjet printing	Kapton polyimide	No	No
[7]	Gas (CO ₂)	2013	Inkjet printing	Flexible laminate	No	No
[8]	Gas (Ammonia)	2012	Inkjet printing	Paper	No	No
[9]	Electrochemical sensor	2013	Ink-jet printing	PVP	No	No
[10]	Light	2014	Inkjet printing	Si/SiO ₂	No	No
[11]	Infrared	2011	Inkjet printing	Kapton Polyimide	No	No
Other liquid phase based approach Insight into variability						
[12]	Chemical (Hg ²⁺ and NH ₄ ⁺)	2011	Self assembly	Si/SiO ₂	Dispersion plot provided. 21 sensors. Conductance range	Dispersion plot provided. 21 sensors. Sensitivity range spanning 2

					spanning 2 orders of magnitude	orders of magnitude
[13]	Gas (NO ₂ ; nitrotoluene)	2003	Drop casting	Si/SO ₂	Yes	3 devices compared 7% variability on the slope (DY/DX) 25% variability on the Y-intercept
[14]	Gas	2010	Vacuum filtration and transfer	Si/SiO ₂	Yes (Resistances of 23 devices provided)	No
[15]	Relative humidity	2012	Spray-coating	PPE	3 resistance values provided (160% std dev)	No
[16]	Strain	2007	Direct drying	Epoxy over Steel	Range of resistances provided	No
Other liquid phase based approach- Strain sensors No insight into variability						
[17]	Strain	2012	Filtration and contact transfer	SiO ₂	No	No
[18]	Strain	2010	Vacuum filtration and transfer	PDMS	No	No
[19]	Strain	2004	Filtration and drying	PVC on brass	No	No
[20]	Strain	2008	Filtration	Aluminium	No	No
[21]	Strain Pressure	2011	Spray coating	PDMS	No	No
Other liquid phase based approach – Chemical sensors No insight into variability						
[22]	Relative humidity	2012	Spray coating	PET	No	No
[23]	Humidity	2009	Dielectrophoresis	Si/SiO ₂	No	No
[24]	Gas (O ₂)	2012	Drop casting Self assembly	Glass	No	No
[25]	Gas (H ₂)	2014	Drop casting	Glass	No	No
[26]	Gas (H ₂)	2012	Aerosol-jet printing	Si/SiO ₂	No	No
[27]	Gas (Ammonia)	2014	Drop casting	Kapton Polyimide	No	No
[28]	Gas (Ammonia)	2014	Drop casting	Unspecified plastics	No	No
[29]	Gas	2013	Paint brush	Cotton	No	No

	(Ammonia)					
[30]	Gas (NO ₂ , NH ₃ , EtOH and acetone)	2014	Screen printer	Alumina	No	No
[31]	Water	2013	Direct casting	Glass	No	No
Methods based on mechanical compression to form films						
[32]	Strain	2012	Press-tablets	PMMA	Range of resistance between 6 and 9 (std dev<25%)	Gauge factor for 2 sensors provided (GF=60 ; 70) (std dev 11%)
[33]	Gas	2013	Pellet compression	Paper	Yes	Comparison between 3 devices displayed but no std deviation provided
Methods based on direct growth (with or without transfer)						
[34]	Chemical (Dopamine)	2013	Direct growth	Si/SO ₂	No	No
[35]	Strain	2011	Direct growth and transfer	PDMS	No	3 devices compared. Strong device to device differences

- [1] A. Benchirouf, E. Sowade, A. Al-Hamry, T. Blaudeck, O. Kanoun and R. Baumann, "Investigation of RFID passive strain sensors based on carbon nanotubes using inkjet printing technology," in 9th IEEE Int. Multiconference on Systems, Signals and Devices, 2012.
- [2] J. Kim, J.-H. Yun, J.-W. Song and C.-S. Han, "The spontaneous metal-sitting structure on carbon nanotube arrays positioned by inkjet printing for wafer-scale production of high sensitive gas sensor units," *Sensors and Actuators B: Chemical*, vol. 135, pp. 587-591, 2009.
- [3] M. O'Toole, R. Shepherd, G. G. Wallace and D. Diamond, "Inkjet printed LED based pH chemical sensor for gas sensing," *Analytica Chimica Acta*, vol. 652, pp. 308-314, 2009.
- [4] A. Lesch, F. Cortés-Salazar, M. Prudent, J. Delobel, S. Rastgar, N. Lion, J.-D. Tissot, P. Tacchini and H. H. Girault, "Large scale inkjet-printing of carbon nanotubes electrodes for antioxidant assays in blood bags," *Journal of Electroanalytical Chemistry*, Vols. 717-718, pp. 61-68, 2014.
- [5] T. Kim, J. Byun, H. Song and Y. Hong, "Inkjet-printed SWCNT films for stretchable electrode and strain sensor applications," in IEEE 70th Annual Device Research Conference (DRC), University Park, TX, USA, 2012.
- [6] Y. Feng, L. Xie, M. Mäntysalo, Q. Chen and L.-R. Zheng, "Electrical and humidity-sensing characterization of inkjet-printed multi-walled carbon nanotubes for smart packaging," in IEEE Sensors, Baltimore, MD, USA, 2013.
- [7] A. Vena, L. Sydänheimo, M. M. Tentzeris and L. Ukkonen, "A Novel Inkjet Printed Carbon Nanotube-Based Chipless RFID Sensor for Gas Detection," in 43rd European Microwave Conference, Nuremberg, Germany, 2013.
- [8] H. Lee, G. Shaker, V. Lakafosis, R. Vyas, T. Thai, S. Kim and X. Yi, "Antenna-based "Smart Skin" Sensors for Sustainable, Wireless Sensor Networks," in IEEE ICIT, 2012.
- [9] R. P. Tortorich, E. Song and a. J.-W. Choi, "Inkjet-Printed Carbon Nanotube Electrodes for Electrochemical Sensor Applications," in 224th ECS Meeting, 2013.

- [10] E. Katzir, S. Yochelis, Y. Paltiel, S. Azoubel, A. Shimoni and S. Magdassi, "Tunable inkjet printed hybrid carbon nanotubes/nanocrystals light sensor," *Sensors and Actuators B: Chemical*, vol. 196, pp. 112-116, 2014.
- [11] A. Gohier, A. Dhar, L. Gorintin, P. Bondavalli, Y. Bonnassieux and C. Cojocar, "All-printed infrared sensor based on multiwalled carbon nanotubes," *Applied Physics Letters*, vol. 98, p. 063103, 2011.
- [12] B. Y. Lee, M. G. Sung, J. Lee, K. Y. Baik, Y.-K. Kwon, M.-S. Lee and S. Hong, "Universal Parameters for Carbon Nanotube Network-Based Sensors: Can Nanotube Sensors Be Reproducible?," *ACS Nano*, vol. 5, pp. 4373-4379, 2011.
- [13] J. Li, Y. Lu, Q. Ye, M. Cinke, J. Han and M. Meyyappan, "Carbon Nanotube Sensors for Gas and Organic Vapor Detection," *Nano Letters*, vol. 3, pp. 929-933, 2003.
- [14] C. R. Field, J. Yeom, A. Salehi-Khojin and R. I. Masel, "Robust fabrication of selective and reversible polymer coated carbon nanotube-based gas sensors," *Sensors and Actuators B: Chemical*, vol. 148, pp. 315-322, 2010.
- [15] Y. Feng, A. L. Cabezas, Q. Chen, L.-R. Zheng and Z.-B. Zhang, "Flexible UHF Resistive Humidity Sensors Based on Carbon Nanotubes," *IEEE Sensors Journal*, vol. 12, pp. 2844-2950, 2012.
- [16] C. Cao, C. Hu, Y. Xiong, X. Han, Y. Xi and J. Miao, "Temperature dependent piezoresistive effect of multi-walled," *Diamond and Related materials*, vol. 16, pp. 388-392, 2007.
- [17] D. J. Cohen, D. Mitra, K. Peterson and M. M. Maharbiz, "A Highly Elastic, Capacitive Strain Gauge Based on Percolating Nanotube Networks," *Nano Letters*, vol. 12, pp. 1821-1825, 2012.
- [18] "Carbon nanotube film piezoresistors embedded in polymer membranes," *Applied Physics Letters*, vol. 96, p. 013511, 2010.
- [19] P. Dharap, Z. Li and S. Nagarajaiah, "Nanotube film based on single-wall carbon nanotubes for strain sensing," *Nanotechnology*, vol. 15, pp. 379-382, 2004.
- [20] X. Li, C. Levy and L. Elaadil, "Multiwalled carbon nanotube film for strain sensing," *Nanotechnology*, vol. 19, p. 045501, 2008.
- [21] D. J. Lipomi, M. Vosgueritchian, B. C.-K. Tee, S. L. Hellstrom, J. A. Lee, C. H. Fox and a. Z. Bao, "Skin-like pressure and strain sensors based on transparent elastic films of carbon nanotubes," *Nature Nanotechnology*, vol. 6, pp. 788-792, 2011.
- [22] V. Scardaci, R. Coull, J. N. Coleman, L. Byrne and G. Scott, "Carbon nanotube network based sensors," in *12th IEEE Intl Conference on Nanotechnology*, Birmingham, UK, 2012.
- [23] L. Liu, X. Ye, K. Wu, R. Han, Z. Zhou and a. T. Cui, "Humidity Sensitivity of Multi-Walled Carbon Nanotube Networks Deposited by Dielectrophoresis," *Sensors*, vol. 9, pp. 1714-1721, 2009.
- [24] C. Cava, R. Salvatierra, D. Alves, A. Ferlauto, A. Zarbin and L. S. Roman, "Self-assembled films of multi-wall carbon nanotubes used in gas sensors to increase the sensitivity limit for oxygen detection," *Carbon*, vol. 50, pp. 1953-1958, 2012.
- [25] J. Garcia-Aguilar, I. Miguel-Garcia, A. Berenguer-Murcia and D. Cazorla-Amoros, "Single wall carbon nanotubes loaded with Pd and NiPd nanoparticles for H₂ sensing at room temperature," *Carbon*, vol. 66, pp. 599-611, 2014.
- [26] R. Liu, H. Ding, J. Lin, F. Shen, Z. Cui and T. ZHANG, "Fabrication of platinum-decorated single-walled carbon nanotube based hydrogen sensors by aerosol jet printing," *Nanotechnology*, vol. 23, p. 505301, 2012.
- [27] Y. Ling, H. Zhang, G. Gu, X. Lu, V. Kayastha, C. S. Jones, W.-S. Shih and D. C. Janzen, "A Printable CNT-Based FM Passive Wireless Sensor Tag on a Flexible Substrate With Enhanced Sensitivity," *IEEE Sensors journal*, vol. 14, pp. 1193 - 1197, 2014.
- [28] F. Rigoni, G. Drera, S. Pagliara and A. Goldoni, "High sensitivity, moisture selective, ammonia gas sensors based on single-walled carbon nanotubes functionalized with indium tin oxide nanoparticles," *Carbon*, vol. 80, pp. 356-363, 2014.
- [29] J.-W. Han, B. Kim, J. L and M. Meyyappan, "A carbon nanotube based ammonia sensor on cotton textile," *Applied Physics Letters*, vol. 102, p. 193104, 2013.

- [30] G. P. Evans, D. J. Buckley, N. T. Skipper and I. P. Parkin, "Single-walled carbon nanotube composite inks for printed gas sensors: enhanced detection of NO₂, NH₃, EtOH and acetone," *RCS Advanced*, vol. 4, pp. 51395-51403, 2014.
- [31] H. Qi, E. Mäder and J. Liu, "Unique water sensors based on carbon nanotube–cellulose composites," *Sensors and Actuators B: Chemical*, vol. 185, pp. 225-230, 2013.
- [32] K. S. Karimov, F. A. Khalid and M. T. S. Chani, "Carbon nanotubes based strain sensors," *Measurement*, vol. 45, pp. 918-921, 2012.
- [33] K. A. Mirica, J. M. Azzarelli, J. G. Weis, J. M. Schnorr and T. M. Swager, "Rapid prototyping of carbon-based chemiresistive gas sensors on paper," *PNAS*, pp. 3265-3270, 2013.
- [34] S. Sansuk, E. Bitziou, M. B. Joseph, J. A. Covington and M. G. Boutelle, "Ultrasensitive Detection of Dopamine Using a Carbon Nanotube," *Analytical chemistry*, vol. 85, pp. 163-169, 2013.
- [35] T. Yamada, Y. Hayamizu, Y. Yamamoto, Y. Yomogida, A. Izadi-Najafabadi, D. N. Futaba and K. Hata, "A stretchable carbon nanotube strain sensor for human-motion detection," *Nature Nanotechnology*, vol. 6, pp. 296-301, 2011.

Highly reproducible, hysteresis-free, flexible strain sensors by inkjet printing of carbon nanotubes

Fulvio Michelis^{1,2}, Laurence Bodelot³, Yvan Bonnassieux², Bérengère Lebental^{1,2}²⁸

¹ Université Paris-Est, IFSTTAR, COSYS/LISIS, Paris, France

² Laboratoire de Physique des Interfaces et Couches Minces (LPICM), UMR 7647, Ecole Polytechnique-CNRS, Palaiseau, France

³ Laboratoire de Mécanique des Solides (LMS), UMR 7649, Ecole Polytechnique-CNRS, Palaiseau, France

Abstract

In order to build upon the exceptional interest for flexible sensors based on carbon nanotube networks (CNNs), the field requires high device-to-device reproducibility. Inkjet printing has provided outstanding results for flexible ohmic sensors in terms of reproducibility of their resistance. However, the reproducibility of the sensitivity, the most critical parameter for sensing application, has been only marginally assessed. In the present paper, CNN-based resistive strain sensors fabricated by inkjet-printing on flexible Ethylene Tetrafluoroethylene (EFTE) sheets are presented. The variability on the device initial resistance is studied for 5 different batches of sensors from 3 to 72 devices each. The variability ranges between 8.4% and 43% depending on the size of the batches, with a 20% average. An 8-device batch with 15% variability on initial resistance is further studied for variability on the strain and thermal sensitivity. Standard deviation values are found to be as low as 16% on the strain sensitivity and 8% on the temperature sensitivity. Moreover, the devices are hysteresis free, a rare achievement for CNT strain sensors on plastics.

1. Introduction

Owing to their very large specific surface area [1], carbon nanotubes (CNTs) have been of utmost interest for sensing applications since the early days of CNT research [2]. Ohmic or transistor devices using CNTs deposited or grown on rigid substrates have demonstrated exceptional sensitivity to their environment, leading to various examples of analytical (humidity, pH, gas, chemical or biological species) [3], mechanical (strain, pressure) [4] or radiation (thermal or infrared, UV) [5] sensors. Following the quick rise of CNT-based flexible electronics [6], a wide range of flexible CNT sensors was proposed [7], with the goal of providing the next generation of wearable devices [8] for human welfare monitoring or wireless sensor networks [9] for infrastructure [10] or environmental monitoring [11]. With their mechanical robustness (high Young's modulus, low bending rigidity, low buckling properties, high tensile strength [2] [12]) flexible CNT sensors are expected to provide long-lasting, reliable devices compatible with industrial requirements.

The active component of these sensors most often consists of wet-processed carbon nanotube networks (CNNs) [13]. CNNs are films of randomly or partially organized CNTs and their thickness ranges from a few tens of nanometers to a few tens of micrometers. Their fabrication methods include filtration and extraction of buckypaper [14], spray coating [15], layer-by-layer assembly [10] as well as contact (roll to roll [16] or transfer based [17]) and non contact (aerosol [18] or inkjet [19] printing techniques. Except for the buckypaper approach, all these methods rely on deposition over a

²⁸ Corresponding author. Tel: +33 1 81 66 81 18. E-mail: berengere.lebental@ifsttar.fr (Bérengère Lebental)

substrate. Studies have yielded strain gauges [18] [20], gas sensors [21], photodetectors [22] and chemistors [23]. Table 1 in Supplementary information 1 provides an extensive study of the state of the art of CNN rigid and flexible sensors.

A long standing, acute challenge for industrial applications of flexible CNN sensors lies in their low device to device reproducibility [24]. Reproducibility specifically addresses two factors, firstly, the standard deviation in initial device resistance, secondly, the standard deviation in device sensitivity. Device to device variability has been discussed repeatedly with regard to CNN based flexible resistors [18] and transistors [25] and various causes have been reported, including liquid-phase dispersion issues of CNTs [26], variability in CNT properties within a batch (semiconducting versus metallic, diameter, length, sidewall defects) [24], quality of the CNT to electrode contacts or surface roughness of the flexible substrates [13].

In spite of this, reports on CNN sensors (either rigid or flexible) rarely provide standard deviation on the resistance level (see Table 1, SI1). Lowest reported standard deviations have been achieved via inkjet-printing: Benchirouf et al. [27] reports 3.5% standard deviation on the resistance level of 3-device-batches (strain sensors) while Lesch et al. [19] reports 7% and 20% standard deviation on the two fitting parameters of the amperometric cycle of antioxidant power sensors, for a 6-device batch.

Regarding to studying variability on sensitivity, Lesch et al. [19] and Karimov et al [28] provide the response of respectively 2 sets and 1 set of 2 devices. Kim et al. [29], Mirica et al [30], Takeo et al [31] compare respectively 4, 3 and 3 sensors from the same batch, but provide no standard deviation on the sensitivity. Beyond this, Li et al. [31] provide the standard deviation on the benchmarking parameters (slope/sensitivity and Y-intercept, respectively 7% and 25%) of a 3-device batch of gas sensors on SiO₂. Finally, the most statistically relevant results stem from Lee et al. [24]. Lee et al. provide the full dispersion plot of the sensitivity of a batch of 21 sensors on SiO₂, which spans two orders of magnitude. No comparable study is presently available for devices on flexible sensors.

In the present paper, we provide a detailed study on resistance and sensitivity variability in batch-fabricated inkjet-printed CNN-based flexible sensors. The study focuses on strain sensors based on multi-walled CNTs (MWCNTs) printed on Ethylene Tetrafluoroethylene (ETFE) sheets. After describing the fabrication process, we prove the high device-to-device reproducibility in terms of strain and temperature sensitivity. We also present the sensing performance, including exceptional cyclability and hysteresis-free operation.

2. Methods

2.1. Materials

MWCNTs Graphistrenth C100 are purchased from Arkema. The solvents 1,2-Dichlorobenzene (Dichlorobenzene hereafter), Acetone and Methanol and the surfactant Sodium Dodecyl Benzene Sulphonate (SDBS) are purchased from Sigma-Aldrich. The substrate is a 0.125 mm thick, 30 cm by 30 cm foil of Ethylene Tetrafluoroethylene (ETFE) with 90 nm roughness (calculated as in [33], see formula in Supplementary Information (SI) 1) supplied by Goodfellow.

2.2. Carbon nanotube ink preparation

The MWCNTs are dispersed in dichlorobenzene at 0.02 wt.% using an ultrasonic probe (Bioblock Scientific VibraCell 75043) operated at 150 W for 20 min followed by centrifugation at 10 kG for 4 h. In order to increase ink-wettability on ETFE and improve homogeneity of the deposition, SDBS at 0.3 wt.% is added to the supernatant using a 20 min sonication bath (see details in SI2) [13]. The resulting dispersion, called ink in the rest of the paper, is stable for over 3 months.

2.3. Device fabrication

The device structure is shown in Figure 1a and b. The ETFE foils are first cleaned with acetone and dried under nitrogen flow. Pairs of 100 nm thin, 5 mm x 5 mm gold electrodes spaced by 7 mm are deposited using thermal evaporation under vacuum (10^{-7} mbar). The MWCNTs are then deposited by inkjet printing using the customizable Dimatix Material Inkjet Printer 2800 with DMP-11601 cartridges. The cartridge is kept at room temperature during printing and the substrate is heated to 55 °C. The printing pattern is a 17 mm x 5 mm rectangle positioned to fully cover both electrodes of each device, in order to ensure proper electrical contact. Several layers can be printed successively depending on the properties targeted for the devices. Residual dichlorobenzene and surfactant are rinsed away by immersion and slight agitation in methanol and acetone for 8s each, followed by drying under nitrogen flow.

The number of layers and the rinsing periodicity strongly impact the final device resistance (see details in SI.3). We optimized these parameters in order to reach device resistances below 1 M Ω (threshold value required for compatibility with commercial acquisition cards; see next section 2.4) while keeping the fabrication time manageable. Devices presented here are obtained from 20 printed layers rinsed every two layers. They are produced by batches of either 8 or 144 sensors on ETFE foils (Figure 1c). The time required for the production of 8 or 144 devices with 20 layers and rinsing every 2 layers is 3 and 5 days respectively.

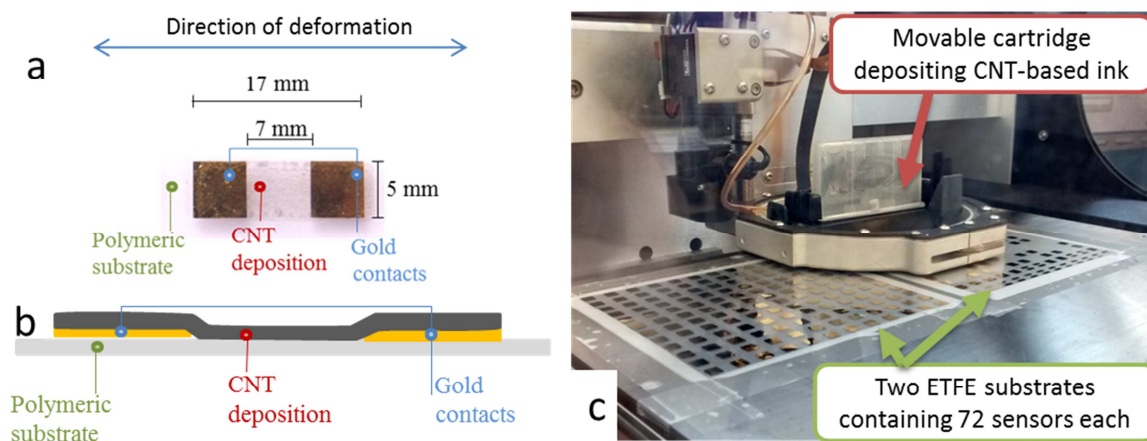


Figure 1 a) Image of a CNT-based device printed on ETFE (top view) with device size and direction of deformation. b) Cross-sectional diagram of the device. c) Ink-jet printing of a 144-device batch on side-by-side ETFE foils. Each substrate contains 72 sensors.

2.4. Physical and electrical characterizations

The devices are observed via optical and scanning electron microscopy SEM (Hitachi S 4800). The deposition thickness is measured via profilometry (Dektak 150). For resistance measurements, electrical contacting is achieved by gluing thin copper wires to the gold electrodes with silver paste. The resistance is measured in a 4-probe configuration to limit the impact of contact resistances: a Keithley 2612 source measurement unit imposes a constant, continuous current in the μ A range (from 4 to 7 μ A) while a National Instrument NI9212 acquisition card measures the output voltage at a frequency of 6.7 Hz. All electrical characterizations are performed within a Faraday cage providing electromagnetic shielding.

2.5. Strain sensing

To characterize the devices as strain gauges, variations in resistance are measured while applying longitudinal deformation to the substrate (deformations applied along the main axis, see Figure 1a).

Deformations are applied by gluing the two opposite sides of a substrate to two clamps mounted on force-controlled motors (Figure). Forces up to 8N are applied. The force is measured using Althen ALF328 load cells. A CCD camera is used to determine the resulting deformation of the substrate: the displacement of surface patterns is tracked during deformation and then converted into strain. Strain levels reach up to 2500 $\mu\epsilon$.

Devices are characterized either separately or by series of 4 sensors on the same substrate. During characterization of the piezoresistive response, the temperature is not controlled but is monitored by a thermocouple.

2.6. Temperature sensitivity

The temperature sensitivity of the resistance is also measured. The devices are placed on a hot plate controlled by the Thermoelectric Temperature Controller LFI 3751 by Wavelength Electronics. The resistance is measured with a Keithley S4200 using a 4-probe configuration. During temperature characterization, the samples are positioned in a shielded environment under nitrogen flow to ensure that relative humidity remains constant at 0.8 % during the duration of the measurement.

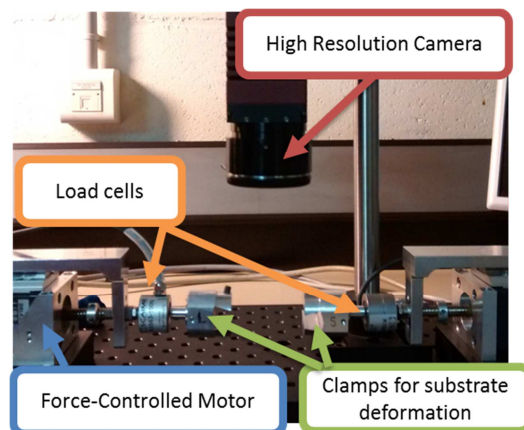


Figure 2 Extensometric bench used for electromechanical characterization.

3. Results and interpretation

3.1. Morphology of the carbon nanotube network

SEM images of a single layer deposition (Figure a) show that CNTs overlap each other and are spread randomly on the surface, with a surface density of 240 CNT/ μm^2 as obtained by visual counting on high resolution images (see SI5 for more details). Numerous micrometric holes are observed, probably due to loss of material during rinsing. When increasing the number of layers, the homogeneity of the deposition improves and the surface coverage increases. At 20 depositions, the surface is entirely covered (Figure b and c).

Up to 20 layers, the thickness of the deposition increases quadratically for each additional layer and reaches 1100 nm for a 20-layer deposition (Figure 3d). As expected from the SEM images, the film surface is very rough. The roughness (error bars in Figure 3d) increases with the number of layers, from 110 nm for 3 layers up to 720 nm for 20 layers. The substrate itself contributes to the overall roughness by only 90 nm. The faster than linear rise of the thickness (clear despite the large roughness/error bars) suggests that the film porosity increases with increasing number of layers, probably due to the imperfect filling of the holes (Figure 3a).

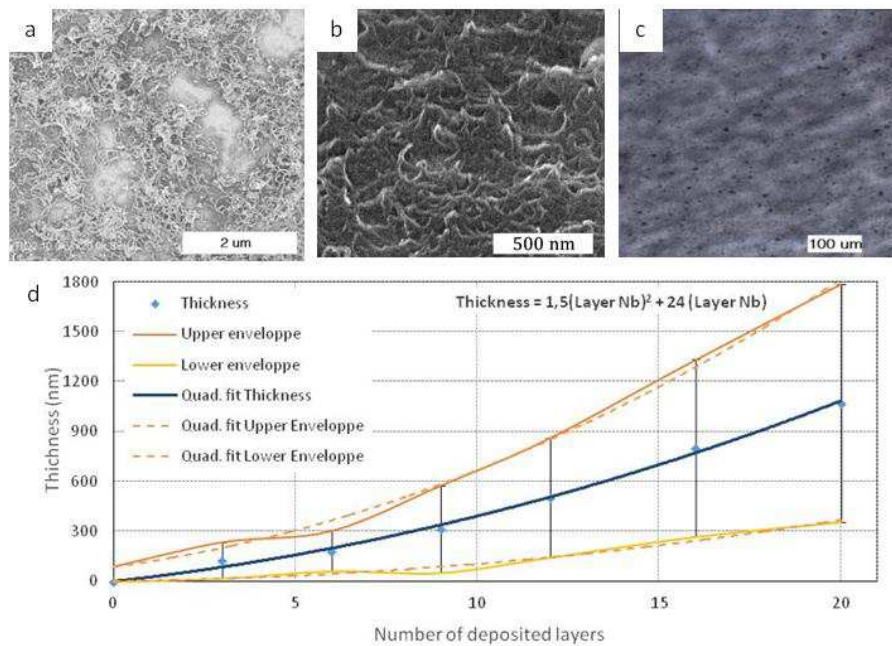


Figure 3 a) SEM image of 1-layer deposition. Micrometric holes are observed in the layer; they are attributed to loss of matter during rinsing. b) SEM image of 20-layer deposition. A uniform coverage can be observed. c) Optical microscopy image of a 20-layer deposition, showing homogeneity and uniformity at a micro scale. d) Thickness of the deposition with respect to number of layers. The rise is roughly quadratic. The error bars represent the surface roughness (the error bar for 0 layer is the roughness of the substrate, 90nm). They are used to define the envelope of the thickness curve. Both upper and lower envelopes also rise quadratically.

3.2. Device resistance

A single layer has a resistance in the $G\Omega$ range, too high for sensing applications. As expected, the resistance decreases as the number of layers increases, in accordance with the literature on CNTs percolated networks[34]. It reaches the $1 M\Omega$ range at 15 layers, the $150 k\Omega$ range at 20 layers and the $100 k\Omega$ range at 30 layers (Figure). The lowest resistance reached is $104 k\Omega$ ($87 k\Omega/sq$) for a 30-layer deposition. This range of magnitude of resistance, though quite high compared to CNN-based inkjet-printed flexible transparent conducting layers [35], is fully compatible with sensing applications. The decrease of resistance as a function of the thickness is much faster than for homogeneous thin films (see for instance Fuchs model [36]). It is attributed to the decrease of the roughness-to-thickness ratio of the films when the number of layer increases (as predicted by Namba model for rough thin films [37]).

Standard deviations for 3- to 72-device-batches of 20-layer devices were found to range from 8.4 % (3 devics) to 43 % (72 devices) with an average at 20%. (Details on the standard deviations of the different batches are provided in SI6). The larger standard deviation for the large batch is attributed to a degraded homogeneity in the gold deposition over the full area of the ETFE sheet. For smaller batches (3 to 8 devices; standard deviations ranging from 8.4% to 18%), the differences in variability are attributed to slight variations in the ink quality.

In the rest of the paper, we discuss a 20-layer, 8-sensor batch with average resistance $156 k\Omega$ and 15 % ($23 k\Omega$) standard deviation. This batch was selected as it featured the lowest average resistance and was of sufficient size for further sensitivity analysis. The batch with lowest standard deviation had only 3 devices and thus appeared too small for standard deviation calculation.

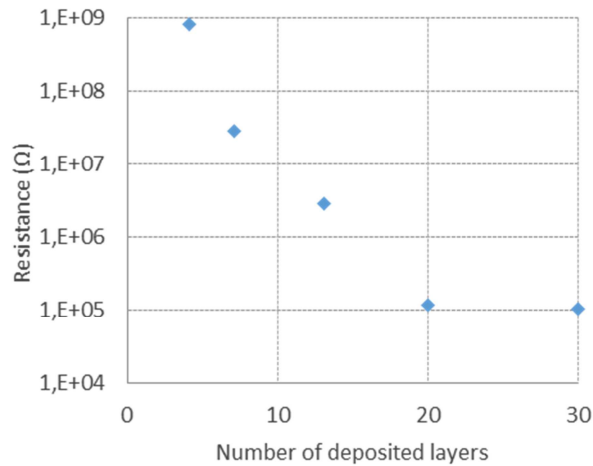


Figure 4 Resistance of the deposition with respect to number of layers.

3.3. Reproducibility of strain sensing performances

As expected from the literature on CNNs strain sensitivity [15] [18], the resistance of the devices varies when they are subjected to longitudinal strains of up to 2500 $\mu\epsilon$ (Figure 1a). In this range of strain, the strain-stress relationship of the substrate is linear (see SI7 for details on the mechanical properties of the film). For large strains up to 2500 $\mu\epsilon$ (1 $\mu\epsilon$ strain corresponds to an extension ΔL of the device initial length L by $\Delta L=10^{-6}L$), the resistance increases quadratically with strain, reaching up to 0.6 % (about 900 Ω) of the initial resistance (Figure a), in accordance with [38] (see SI 8). The resistance variation measured on the gold electrodes when they are subjected to strain of up to 2500 $\mu\epsilon$ is 10 Ω , over 10 times smaller than the resistance variation for the whole sensing element. Consequently, we can deduce that the piezoresistive effect is not due to the electrodes only.

All devices feature a linear behavior in the small strain regime. The linear range exceeds 400 $\mu\epsilon$ for all the devices. 75 % have a linear range of over 600 $\mu\epsilon$ and 50 % above 800 $\mu\epsilon$. The strain sensitivity, also called gauge factor (GF), is defined as the slope of $\Delta R/R$ vs ϵ curve in the linear regime. It is found to be 0.90 ± 0.14 for an 8-device batch, corresponding to 16% standard deviation on the GF. The 0.9 GF value is the only reported GF for printed CNT resistive strain sensors [39]. This is the first quantitative evaluation of the variability in sensitivity for batch-produced CNT-based flexible sensors.

This GF value is comparable to the GF of commercially available strain gauges (between 1 and 2), though the standard deviation on the resistance and on the gauge factor are still higher than the dispersion reported in the datasheets of commercial devices (respectively 2% and 5% standard deviation on the resistance and on the GF) [40] [41]. Much higher GF values can be achieved in devices with oriented CNT [8] or closer to the CNN's percolation threshold, including buckypaper-based devices (for instance [42]). However operation close to the percolation threshold has a detrimental impact on device-to-device reproducibility [18].

3.4. Reproducibility of temperature sensitivity

Temperature is known to strongly influence both the conductivity of CNNs [43] and the mechanical response of polymer foils [44]. Hence, we studied the dependence of the devices on temperature (Figure b). The results show that the resistance decreases linearly with temperature, in accordance with other studies [43] [45]. The temperature sensitivity, defined as the slope of the $\Delta R/R$ versus temperature curve, is equal to $-1.0 \times 10^{-3} \text{ K}^{-1}$. This coefficient is comparable to those published in [43] and [46] for CNT devices fabricated respectively on silicon and PET. The thermal sensitivity cannot be explained by the thermal expansion of the substrate ($0.9\text{-}1.7 \times 10^{-4} \text{ K}^{-1}$) [47]), as the effect would be a

positive thermal sensitivity in the range of $+0.8-1.5 \times 10^{-4} \text{ K}^{-1}$. Dehghani et al. [43] proposes that the thermal sensitivity is mostly due to thermal variation in the CNT resistivity.

The standard deviation in the temperature sensitivity is as low as 8 % over 7 devices, even lower than the standard deviation over resistance (15%) and over gauge factor (16%). The possibility of compensating for temperature is critical for future applications of this strain gauge.

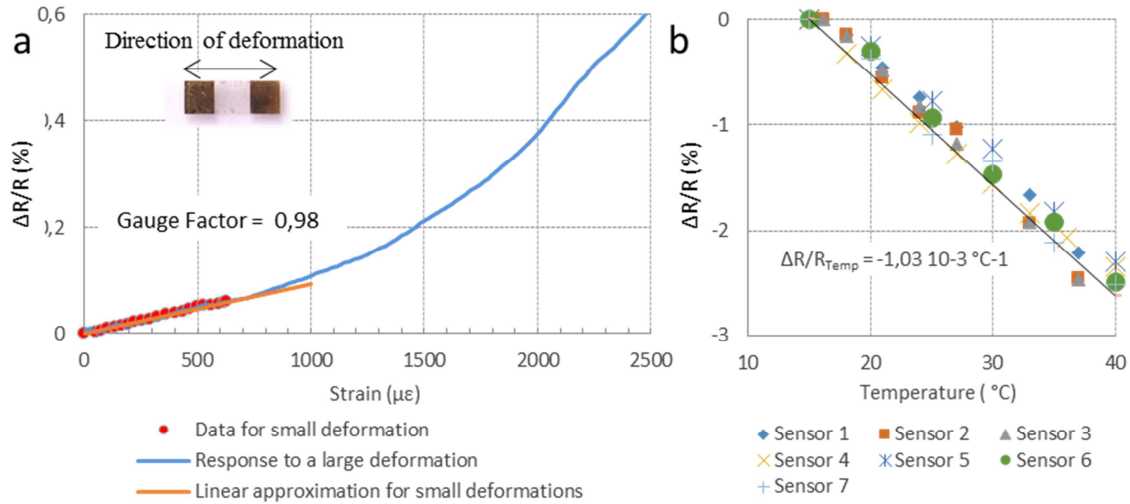


Figure 5 a) Resistance variation with respect to strain. The linear regime reaches up to 700 $\mu\epsilon$ for this device. The gauge factor of the device presented here is 0,98. Overall, the response up to large strains is roughly quadratic. b) Linear dependence of resistance on temperature. The temperature sensitivity is equal to $-1.0 \times 10^{-3} \text{ K}^{-1}$.

3.5. Response time

We assessed the device response time, defined here as the time to reach 95 % of the expected value once the target strain is reached (Figure a and b). The strain is increased linearly over 5 s to reach its target (see Figure a). The response time was found to be 3.6 s for a 500 $\mu\epsilon$ strain (within the linear regime of the device). This suggests that the devices should preferably be used for static or quasi-static applications (frequencies well below 0.3 Hz/period well over 3.6 s).

As expected, out of the linear range, the response time is much higher. For a 1600 $\mu\epsilon$ strain, the response time is as high as 19 s; it appears that from about 1200 $\mu\epsilon$, the device cannot follow the increase in strain, thus suggesting a settling effect in the CNN at larger strain levels.

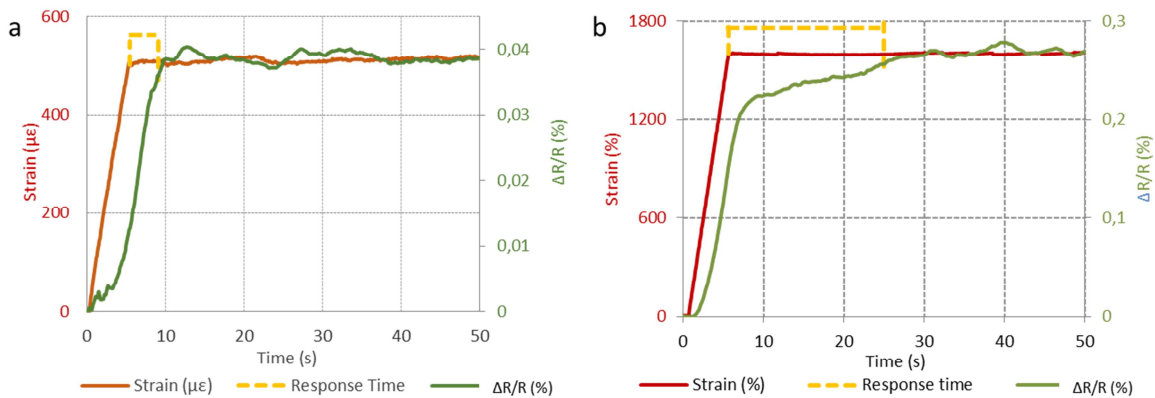


Figure 6 Measurement of device response time: a) 3.6 s under small strains (500 $\mu\epsilon$). b) 19 s under large strains (1500 $\mu\epsilon$).

3.6. Quasi-static cyclability and hysteresis-free operation in quasi-static mode

We evaluated the quasi-static cyclability of the devices in the linear regime. The devices are submitted to cyclic loadings (20 cycles over 3 hours) in the linear regime ($800 \mu\epsilon$) with 9 minutes periodicity (2 mHz, well below the frequency limit defined using the response time). The device response is acquired at 6.7 Hz (3600 measurements per period).

Over 3 hours and 20 cycles, the devices display remarkable cyclability and hysteresis-free operation (Figure 25a and b). The discrepancy between gauge factor measured during loading and the one measured during unloading is only 2.7 % (figure 7a), which underlines the high reversibility of the devices compared to the state of the art [48] [49]. As can be observed in Figure 7a, there is no significant a baseline drift, though there is a significant variability in the cycle min and max values (Figure 7b). The standard deviation over the maximum resistance value (0.58×10^{-2}) is 4.7% over 20 cycles (range $0.55-0.61 \times 10^{-2}$). Based on the thermal sensitivity of the devices (-1.0×10^{-3}), a relative resistance variation of 6×10^{-4} can be explained by only 0.6°C of thermal variation. This is the range of magnitude of temperature variations (between 0.3°C and 1°C) measured in the climate-controlled room where the experiments were carried out. Hence, the variability in the resistance/strain curves is attributed to temperature variations.

Hysteresis free operation is possible only in the linear regime of the devices. Additional resistance-stress curves are provided in SI9 for strains up to $2500 \mu\epsilon$ and up to $4000 \mu\epsilon$. In this range of strain, the devices clearly display hysteresis and creep effects. The creep effect on the resistance can be attributed to the creep of the substrate, estimated at $27 \mu\epsilon$ by cycle for 8N load cycles with 5 min periodicity.

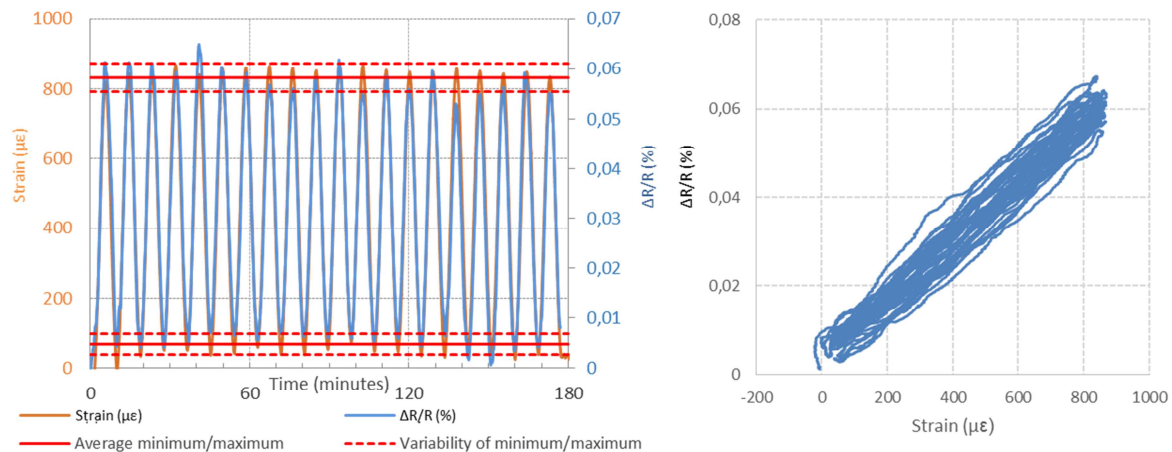


Figure 7 a) Response of a device to 20 cycles of strains between 0 and $800 \mu\epsilon$. No evident hysteresis or baseline drift is observed. b) Corresponding resistance-strain plot. The extent of the bundle of resistance-strain curve is due to a slight variability (4.7%) in min and max resistance value. It is attributed to temperature variations in the range of approx. $\pm 0.3^\circ\text{C}$.

4. Conclusions

In this paper, we study for the first time the sensitivity variability of CNN-based flexible ohmic sensors. We focus on CNN-based strain gauges on Ethylene Tetrafluoroethylene sheets achieved by inkjet printing of MWCNTs dispersed in Dichlorobenzene with SDBS as a surfactant. The use of inkjet printing produces highly reproducible devices with low variability in resistance (best standard deviation 8.4 % for a 3-device batch; 20% standard deviation averagely between 5 batches between 3 and 72 devices), gauge factor (16 % standard deviation for a 8-device batch with 15% standard deviation on the resistance), and temperature sensitivity (8 % standard deviation for a 8-device batch with 15% standard deviation on the resistance). Compared to the state of the art of CNN strain

gauges, the devices demonstrate remarkable cyclability and hysteresis-free operation. These results open the road towards the use of the proposed sensors in real-life applications.

Acknowledgments

The authors acknowledge support from ANR (France) for project Sense-City (ANR-10-EQPX-48). The authors also thank Costel –Sorin Cojocaru, Denis Tondelier, Eléonor Caristan and Jean-Luc Sorin from LPICM and IFSTTAR laboratories for their help and support.

Bibliography

- [1] A. Peigney, C. Laurent, E. Flahaut, R. Bacsa and A. Rousset, "Specific surface area of carbon nanotubes and bundles of carbon nanotubes," *Carbon*, vol. 39, no. 4, pp. 507-514, 2001.
- [2] R. H. Baughman, A. A. Zakhidov and W. A. d. Heer, "Carbon Nanotubes—the Route Toward Applications," *Science*, vol. 297, p. 787, 2002.
- [3] J. Kong, N. R. Franklin, C. Zhou, M. G. Chapline, S. Peng, K. Cho and H. Dai, "Nanotube Molecular Wires as Chemical Sensors," *Science*, vol. 287, p. 622, 2000.
- [4] Y. Li, Y. Zhao, Y. Zhu, J. Rodriguez, J. Morante, E. Mendozac, C. Poa and S. Silva, "Mechanical and NH₃ sensing properties of long multi-walled carbon nanotube ropes," *Carbon*, vol. 44, no. 9, pp. 1821-1825, 2006.
- [5] P. W. Barone, S. B. D. A. Heller and M. S. Strano, "Near-infrared optical sensors based on single-walled carbon nanotubes," *Nature Materials*, vol. 4, pp. 86-92, 2005.
- [6] K. Bradley, J.-C. P. Gabriel and G. Grüner, "Flexible Nanotube Electronics," *Nano Letters*, vol. 3, no. 10, pp. 1353-1355, 2003.
- [7] M. Mabrook, C. Pearson, A. Jombert, D. Zeze and M. Petty, "The morphology, electrical conductivity and vapour sensing ability of inkjet-printed thin films of single-wall carbon nanotubes," *Carbon*, vol. 47, no. 3, pp. 752-757, 2009.
- [8] T. Yamada, Y. Hayamizu, Y. Yamamoto, Y. Yomogida, A. Izadi-Najafabadi, D. N. Futaba and K. Hata, "A stretchable carbon nanotube strain sensor for human-motion detection," *Nature Nanotechnology*, vol. 6, pp. 296-301, 2011.
- [9] S. Laflamme, M. Kolloosche, J. Connor and G. Kofod, "Robust Flexible Capacitive Surface Sensor for Structural Health Monitoring Applications," *Journal of Engineering Mechanics*, vol. 139, no. 7, pp. 879-885, 2013.
- [10] K. J. Loh, J. Kim, J. P. Lynch, N. W. S. Kam and N. A. Kotov, "Multifunctional layer-by-layer carbon nanotube–polyelectrolyte thin films for strain and corrosion sensing," *Smart Materials and Structures*, vol. 16, pp. 429-438, 2007.
- [11] M. S. Mauter and M. Elimelech, "Environmental Applications of Carbon-Based Nanomaterials," *Environmental Science and Technology*, vol. 42, no. 16, pp. 5843-5859, 2008.
- [12] M.-F. Yu, O. Lourie, M. J. Dyer and K. Moloni, "Strength and Breaking Mechanism of Multiwalled Carbon Nanotubes Under Tensile Load," *Science*, vol. 287, p. 637, 2000.
- [13] A. Saha, C. Jiang and A. A. Martí, "Carbon nanotube networks on different platforms," *Carbon*, vol. 79, pp. 1-18, 2014.
- [14] Y. Li and M. Kröger, "A theoretical evaluation of the effects of carbon nanotube entanglement and bundling on the structural and mechanical properties of buckypaper," *Carbon*, vol. 50, no. 5, pp. 1793-1806, 2012.
- [15] D. J. Lipomi, M. Vosgueritchian, B. C.-K. Tee, S. L. Hellstrom, J. A. Lee, C. H. Fox and Z. Bao, "Skin-like pressure and strain sensors based on transparent elastic films of carbon nanotubes," *Nature Nanotechnology*, vol. 6, pp. 788-792, 2011.
- [16] J. Noh, M. Jung, K. Jung, G. Lee, S. Lim, D. Kim, S. Kim, J. M. Tour and G. Cho, "Integrable single walled carbon nanotube (SWNT) network based thin film transistors using roll-to-roll gravure and inkjet," *Organic Electronics*, vol. 12, no. 12, pp. 2185-2191, 2011.

- [17] P. H. Lau, K. Takei, C. Wang, Y. Ju, J. Kim, Z. Yu, T. Takahashi, G. Cho and A. Javey, "Fully Printed, High Performance Carbon Nanotube Thin-Film Transistors on Flexible Substrates," *Nano Letters*, vol. 13, no. 8, pp. 3864-3869, 2013.
- [18] S. Li, J. G. Park, S. Wang, R. Liang, C. Zhang and B. Wang, "Working mechanisms of strain sensors utilizing aligned carbon nanotube network and aerosol jet printed electrodes," *Carbon*, vol. 73, pp. 303-309, 2014.
- [19] A. Lesch, F. Cortés-Salazar, M. Prudent, J. Delobel, S. Rastgar, N. Lion, J.-D. Tissot, P. Tacchini and H. H. Girault, "Large scale inkjet-printing of carbon nanotubes electrodes for antioxidant assays in blood bags," *Journal of Electroanalytical Chemistry*, Vols. 717-718, pp. 61-68, 2014.
- [20] D. J. Cohen, D. Mitra, K. Peterson and M. M. Maharbiz, "A Highly Elastic, Capacitive Strain Gauge Based on Percolating Nanotube Networks," *Nano Letters*, vol. 12, pp. 1821-1825, 2012.
- [21] F. Rigoni, G. Drera, S. Pagliara and A. Goldoni, "High sensitivity, moisture selective, ammonia gas sensors based on single-walled carbon nanotubes functionalized with indium tin oxide nanoparticles," *Carbon*, vol. 80, pp. 356-363, 2014.
- [22] A. Gohier, A. Dhar, L. Gorintin, P. Bondavalli, Y. Bonnassieux and C. S. Cojocaru, "All-printed infrared sensor based on multiwalled carbon nanotubes," *Applied Physics Letters*, vol. 98, p. 063103, 2011.
- [23] J. M. A. Katherine A. Mirica, J. G. Weis, J. M. Schnorr and T. M. Swager, "Rapid prototyping of carbon-based chemiresistive gas sensors on paper," *PNAS*, pp. 3265-3270, 2013.
- [24] B. Y. Lee, M. G. Sung, J. Lee, K. Y. Baik, Y.-K. Kwon, M.-S. Lee and S. Hong, "Universal Parameters for Carbon Nanotube Network-Based Sensors: Can Nanotube Sensors Be Reproducible?," *ACS Nano*, vol. 5, no. 6, pp. 4373-4379, 2011.
- [25] C. Wang, J.-C. Chien, K. Takei, T. Takahashi and J. Nah, "Extremely Bendable, High-Performance Integrated Circuits Using Semiconducting Carbon Nanotube Networks for Digital, Analog, and Radio-Frequency Applications," *Nano Letters*, vol. 12, pp. 1527-1533, 2012.
- [26] S. Kim, T. Kim, Y. Kim, H. Choi, H. Lim, S. Yang and C. Park, "Surface modifications for the effective dispersion of carbon nanotubes in solvents and polymers," *Carbon*, vol. 50, no. 1, pp. 3-33, 2012.
- [27] A. Benchirouf, E. Sowade, A. Al-Hamry, T. Blaudeck, O. Kanoun and R. Baumann, "Investigation of RFID passive strain sensors based on carbon nanotubes using inkjet printing technology," in *9th IEEE Int. Multiconference on Systems, Signals and Devices*, 2012.
- [28] K. S. Karimov, F. A. Khalid and M. T. S. Chani, "Carbon nanotubes based strain sensors," *Measurement*, vol. 45, pp. 918-921, 2012.
- [29] J. Kim, J.-H. Yun, J.-W. Song and C.-S. Han, "The spontaneous metal-sitting structure on carbon nanotube arrays positioned by inkjet printing for wafer-scale production of high sensitive gas sensor units," *Sensors and Actuators B: Chemical*, vol. 135, pp. 587-591, 2009.
- [30] K. A. Mirica, J. M. Azzarelli, J. G. Weis, J. M. Schnorr and T. M. Swager, "Rapid prototyping of carbon-based chemiresistive gas sensors on paper," *PNAS*, pp. 3265-3270, 2013.
- [31] J. Li, Y. Lu, Q. Ye, M. Cinke, J. Han and M. Meyyappan, "Carbon Nanotube Sensors for Gas and Organic Vapor Detection," *Nano Letters*, vol. 3, pp. 929-933, 2003.
- [32] B. Y. Lee, M. G. Sung, J. Lee, K. Y. Baik, Y.-K. Kwon, M.-S. Lee and S. Hong, "Universal Parameters for Carbon Nanotube Network-Based Sensors: Can Nanotube Sensors Be Reproducible?," *ACS Nano*, vol. 5, pp. 4373-4379, 2011.
- [33] E. P. DeGarmo, J. T. Black and R. A. Kohser, *Materials and Processes in Manufacturing*, Wiley, 2003.
- [34] P. Slobodian, P. Riha, A. Lengalova, R. Olejnik and D. Kimmer, "Effect of compressive strain on electric resistance of multi-wall carbon nanotube networks," *Journal of Experimental Nanoscience*, vol. 6, no. 3, p. 294-304, 2011.
- [35] O.-S. Kwon, H. Kim, H. Ko, J. Lee, B. Lee and C.-H. Jung, "Fabrication and characterization of inkjet-printed carbon nanotube electrode patterns on paper," *Carbon*, vol. 58, pp. 116-127, 2013.
- [36] A. A. Cottrey, "The electrical conductivity of thin metal films with very smooth surfaces," *Thin Solid Films*, vol. 1, no. 4, p. 297-307, 1938.

- [37] H. Hoffmann and J. Vancea, "Critical assessment of thickness-dependent conductivity of thin metal films," *Thin Solid Films*, vol. 85, no. 2, p. 147–167, 1981.
- [38] F. J. Baeza, O. Galao, E. Zornoza and E. Garcés, "Multifunctional Cement Composites Strain and Damage Sensors Applied on Reinforced Concrete Structural Elements," *Materials*, vol. 6, pp. 841-855, 2013.
- [39] T. Kim, J. Byun, H. Song and Y. Hong, "Inkjet-printed SWCNT films for stretchable electrode and strain sensor applications," in *Device Research Conference*, 2012.
- [40] E. Omega, "Strain gauge technical data sheet".
- [41] I. Tokyo Sokki Kenkyujo Co., "Strain Gauge Performance Characteristics," 2011.
- [42] N. Hu, Y. Karube, M. Arai, T. Watanabe and C. Yan, "Investigation on sensitivity of a polymer/carbon nanotube composite strain sensor," *Carbon*, vol. 48, pp. 680-687, 2010.
- [43] S. Dehghani, M. K. Moravvej-Farshi and M. H. Sheikhi, "Temperature Dependence of Electrical Resistance of Individual Carbon Nanotubes and Carbon Nanotubes Network," *Modern Physics Letters B*, vol. 26, no. 21, 2012.
- [44] Fisher | Moore, "Ethylene tetrafluoroethylene (ETFE) Technical Information," 1999.
- [45] W. S. Bao, S. A. Meguid, Z. Z. H. and G. Zeng, "Tunneling resistance and its effect on the electrical conductivity of carbon nanotube nanocomposites," *Journal of Applied Physics*, vol. 111, no. 093726, 2012.
- [46] V. Scardaci, R. Coull, J. Coleman, L. Byrne and G. Scott, "Carbon Nanotube network based sensors," in *Conference on Nanotechnology IEEE-Nano*, Birmingham, 2012.
- [47] "Copolymère d'Éthylène-tetrafluoroéthylène (ETFE) - Informations Matériau," [Online]. Available: <http://www.goodfellow.com/F/Copolymere-d'Ethylene-tetrafluoroethylene.html>.
- [48] R. Zhang, H. Deng, R. Valenca, J. Jin, Q. Fu, E. Bilotti and T. Peijs, "Strain sensing behaviour of elastomeric composite films containing carbon nanotubes under cyclic loading," *Composites Science and Technology*, vol. 74, no. 24, pp. 1-5, 2013.
- [49] R. K. Srivastava, V. S. M. Vemuru, Y. Zeng, R. Vajtai, S. Nagarajaiah, P. M. Ajayan and A. Srivastava, "The strain sensing and thermal–mechanical behavior of flexible multi-walled carbon nanotube/polystyrene composite films," *Carbon*, vol. 49, no. 12, pp. 3928-3936, 2011.
- [50] A. Benchirouf, E. Sowade, A. Al-Hamry, T. Blaudeck, O. Kanoun and R. Baumann, "Investigation of RFID passive strain sensors based on carbon nanotubes using inkjet printing technology," in *9th International Multiconference on Systems, Signals and Devices*, 2012.

Oxidation-Based Continuous Laser Writing in Vertical Nano-Crystalline Graphite Thin Films

Loïc Loisel^{1,2,3,*}, Ileana Florea³, Costel-Sorin Cojocaru³, Beng Kang Tay^{1,2}, Bérengère Lebental^{3,4}

¹CINTRA CNRS/NTU/Thalès, UMI 3288, 50 Nanyang Drive, Singapore

²School of Electrical and Electronics Engineering, Nanyang Technological University, 50 Nanyang Avenue, Singapore

³LPICM, CNRS, Ecole Polytechnique, Université Paris Saclay, 91128, Palaiseau, France

⁴Université Paris-Est, IFSTTAR, 14-20 Bd Newton, Champs-sur-Marne, F-77447, Marne-la-Vallée, France

*Corresponding author. Tel: +337 82 02 42 40. E-mail: loic.loisel@polytechnique.edu (Loïc Loisel)

Email addresses (in order):

loic.loisel@polytechnique.edu

lenuta-ileana.florea@polytechnique.edu

costel-sorin.cojocaru@polytechnique.edu

ebktay@ntu.edu.sg

berengere.lebental@ifsttar.fr

Nano and femtosecond laser writing are becoming very popular techniques for patterning carbon-based materials, as they are single-step processes enabling the drawing of complex shapes without photoresist. However, laser writing may require a costly pulsed laser source. As compared to pulsed lasers, continuous-wave lasers are cheap, stable and enable deposition of energy in a more controlled manner. Here, we use a continuous-wave laser to pattern vertical nano-crystalline graphite thin films. Continuous laser annealing results in amorphization and matter removal at the center of the beam, and sp^2 clustering at its periphery. Oxygen doping is observed, suggesting that amorphization and matter removal are controlled by carbon oxidation. The simultaneous occurrence of oxidation and hole doping results in a unique evolution of the Raman spectra as a function of annealing time, with a decrease of the I(D)/I(G) values but an upshift of the G peak frequency. The resulting annealed matter features very few macroscale defects, which is promising for high quality laser writing applications.

Introduction

As silicon transistors can no longer follow Moore's law¹, carbon is considered one of the most promising material for replacing or complementing silicon-based electronics^{2,3}. Therefore, it is of primary interest to master the fabrication of carbon-based electronic chips that can achieve the desired data computing, storing and transmitting functions. Though short-wavelength (13.5 nm) laser-based lithography will be one of the most critical processes for the mass fabrication of high-performance transistors⁴ at resolutions below 10 nm⁵, a wide range of applications of carbon materials do not require such small features (thin-film transistors⁴ or sensors).

In this case, laser light may be used directly (without a mask) to draw patterns onto carbon allotropes without using photoresist. It rids the fabrication process of a well-known contaminating agent for carbon-based electronics (*e.g.* contamination of graphene by photoresist⁶⁻⁸).

Despite being costly, pulsed lasers are the most frequent choice for carbon writing: they can locally transform insulating amorphous carbon into electrically conducting graphitic carbon^{9,10}. They have also been used to obtain patterns of reduced graphene-oxide from graphene-oxide¹¹⁻¹⁸. The resulting material has potential beyond electronics, for instance for gas-sensing¹⁹. Though the capability to amorphize graphitic carbon is also of interest, for instance to draw insulating lines in graphitic carbon, or to fabricate heat and radiation-resistant optical memories²⁰, no reports on amorphization is presently available. Moreover, due to the very short duration of the pulses (several nanosecond to several femtoseconds), power densities are large, which lead to undesired surface degradations such as sputtering²¹ or phase explosion^{15,22,23}. At such short timescales, the light-matter interactions enabling energy dissipation are difficult to predict and optimize²⁴.

By comparison, the physics behind slow thermal annealing are more easily modeled²⁵⁻²⁹. Because they enable the deposition of energy in a slow manner, continuous-wave (CW) lasers can be used to locally transform matter in a similar manner as thermal annealing^{30,31}. CW lasers are also cheap. They might thus be a preferable option to pulsed lasers.

CW lasers have already been used to draw graphitic patterns in amorphous carbon³⁰⁻³². Moreover, at least one report³⁰ mentions CW-based carbon amorphization, which opens up the way toward the patterning of either conductive or insulating designs. Like their pulsed counterparts, CW lasers may also be used to reduce graphene oxide^{15,19} or to induce matter removal³⁰. These capabilities are relevant for applications such as monolayer graphene synthesis³³, field emission³⁴, light trapping³⁵, or the drawing of micro-ribbons for plasmonic applications³⁶.

Despite these various studies, the literature on CW laser annealing of carbon does not provide a clear description of the mechanisms behind these phase change and matter removal processes. It is not clear whether the graphitization and amorphization processes occur in the solid-state or after melting, or what role the atmosphere plays in the patterning. In particular, it is well known that oxygen reacts strongly with carbon at temperatures below the melting point, resulting in carbon etching: the literature on carbon oxidation in an oven (slow annealing) is abundant³⁷⁻³⁹.

On the other hand, the literature on carbon laser-annealing seldom if ever mentions oxidation as a modification mechanism (see Supplementary Table S1), probably because most reports focus on

pulsed-laser annealing for which the modifications (*e.g.* melting) occur too fast for oxidation phenomena to be significant.

Moreover, though it is expected that CW-laser induced graphitization increases the electrical conductivity, there is no direct evidence for it. It is also unclear whether degradations are induced in the areas surrounding the annealing region, or if the process leaves a smooth surrounding surface, which could be critical for some applications.

These questions must be answered if one wants to assess the capabilities of CW lasers as low-cost tools to draw patterns on carbon, and use those patterns for applications.

Here, we use a CW laser to anneal a thin film of vertical nano-crystalline graphite (vnC-G). vnC-G is ideal for an assessment of the phenomena related to CW-laser annealing because it contains both crystalline and amorphous domains, enabling the probing of both graphitization and amorphization processes; moreover, its non-zero thickness (as compared to 2D graphene) enables to estimate the kinetics of matter removal and the spatial distribution of the phase changes in the depth of the film.

We find that three main processes occur in carbon during CW laser annealing: at low power densities, sp^2 clusters form, leading to an increase in the electrical conductivity. At higher power densities, oxidation starts, leading to both a degradation of the crystalline order in the depth and a removal of matter at the surface.

We provide definitive evidence that oxidation plays an important role during the CW-laser annealing of carbon.

Hence, CW-laser writing enables the writing of electrically conductive or insulating patterns as well as patterns made of holes. The gentle deposition of energy leads to very few undesired surface defects, as evidenced by atomic force microscopy.

Results and Discussion

Crystalline structure of pristine vertical nano-crystalline graphite

Figure 1 (a) presents a dark-field HR-STEM micrograph of the as-deposited carbon film. The carbon layer is ≈ 140 nm thin, and comprises two sublayers: a graphitic layer of thickness ≈ 100 nm directly on top of the Ti layer (labeled “G” for graphitic) and, resting on it, an amorphous layer of thickness ≈ 40 nm (labeled “A” for amorphous). “G” consists of neighboring amorphous and crystalline regions, with graphite crystals as large as 50 nm being frequently observed (Figure 37 (a)), with a measured interplanar distance of ≈ 0.33 nm (Figure 37 (b)). It is comparable to the interplanar distance of pristine graphite (0.34 nm). On the other hand, no trace of crystalline content is observed in the top “A” layer.

Raman spectroscopy on the pristine vnC-G layer yields $I(D)/I(G) \approx 1.02 \pm 0.03$, $x_G \approx 1557 \pm 2$ cm^{-1} and $\text{FWHM}_G \approx 254 \pm 6$ cm^{-1} . The large G peak FWHM suggests average crystal sizes much smaller than 2 nm⁴⁰ which is consistent with the properties of the “A” layer observed by TEM. Considering the penetration depth of the Raman photons in carbon (≈ 38 nm), the “G” layer is not probed much (Supplementary Information S1). However, graphitic crystals deeper than 35 nm can still have an impact on Raman spectra due to the large cross section of graphitic carbon³⁰.

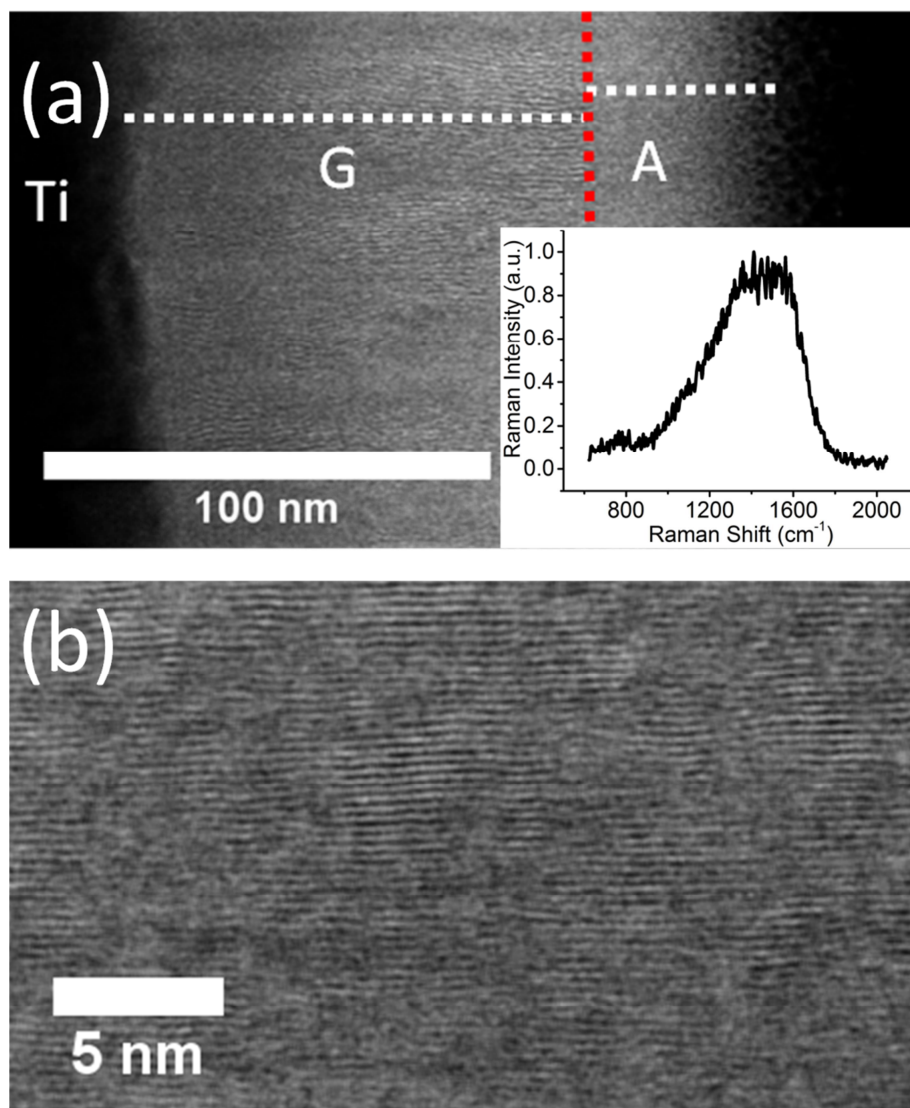


Figure 37 - TEM characterization of pristine vnc-G. (a) Dark-field STEM micrograph showing two sublayers within the un-annealed v-ncG film: a 40 nm-thick amorphous layer (“A”) on top of a 100 nm-thick graphitic layer (“G”). *Inset*: Raman spectrum of pristine vnc-G. (b) HR-STEM-Dark Field micrograph on a zoomed area from the graphitic “G” layer illustrating the parallel graphitic planes

Matter Removal and Amorphization at beam center

After characterization of the pristine film, we laser-anneal specific locations for short laser annealing duration and/or power in air. After this process, these specific locations feature single clear circular spots. For longer duration and/or larger power, a dark spot appears, that extends outward with duration and power, until a white inner disk appears at the center (Figure 38 (a)).

AFM and TEM imaging reveal the topology of these spots: they feature a center crater surrounded by a slight bulge (Figure 38 (b)). The depth and diameter of the craters both increase with annealing power and/or duration, clearly indicating that matter removal occurs. The increase in depth stops when the Ti layer is reached. The high reflectivity of the metallic Ti layer explains the white spot observed optically for high power or long duration exposure (Figure 39 (a)).

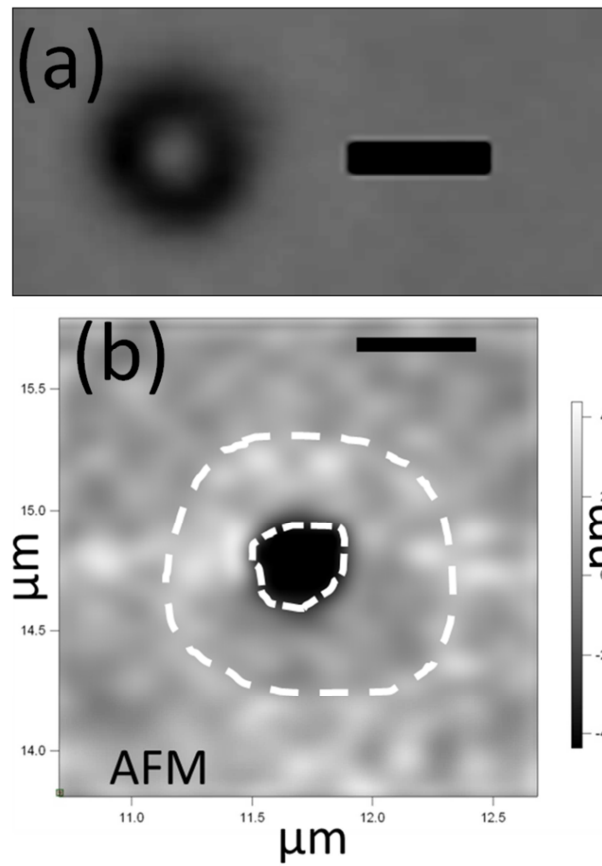


Figure 38 - Morphology of laser-annealed vnC-G. (a) Optical image (scale bar 1 μm) of a laser-annealed region with energy density $5.9 \cdot 10^6 \text{ J} \cdot \text{mm}^{-2}$ (b) AFM 2D height image showing a crater (black surrounded by a white dashed line) and a surrounding bulge (marked with a white dashed line) of a laser-annealed region with energy density $1.7 \cdot 10^7 \text{ J} \cdot \text{mm}^{-2}$

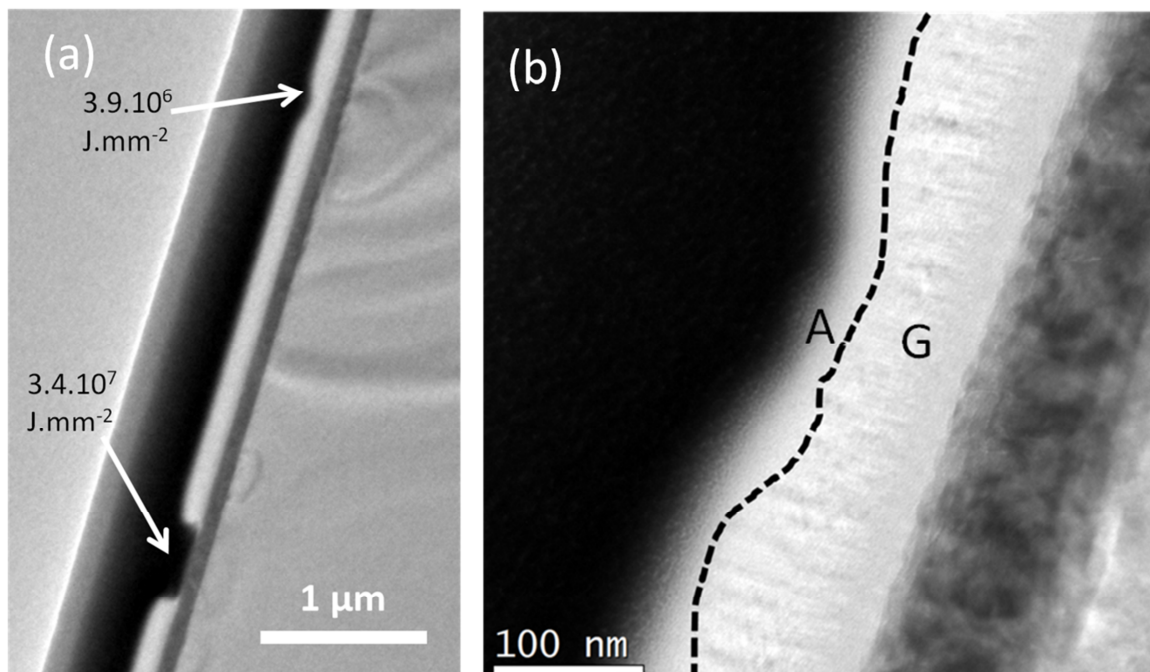


Figure 39 - (a) cross-sectional TEM micrograph showing the two craters created by laser-annealing corresponding to two different power densities and durations (b) TEM micrograph showing the structure of the crater created by annealing with energy density $3.9 \cdot 10^6 \text{ J} \cdot \text{mm}^{-2}$. The two "G" and "A" sublayers are visible

TEM images (Figure 39 (b)) show that, as the annealing energy increases and the matter loss progresses, the thickness of the “G” layer at the top of the substrate decreases while the thickness of the “A” layer remains roughly constant, so that overall the material becomes more amorphous. While CW lasers have been reported as efficient tools to turn amorphous carbon into graphitic carbon³⁰⁻³², their use as a tool to amorphize carbon has been reported only once³⁰, with minor discussion on the underlying mechanism.

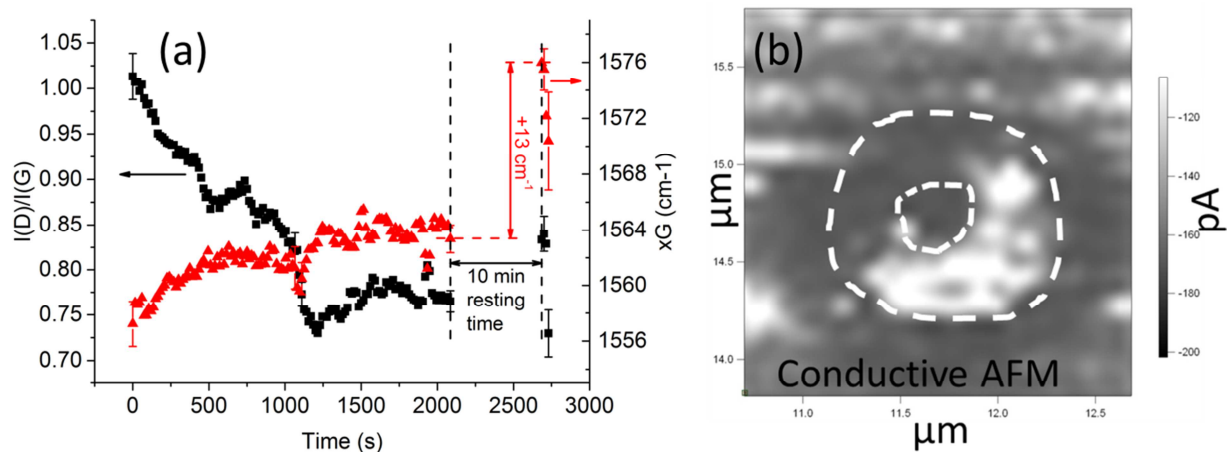


Figure 40 - Raman and c-AFM data suggest that sp^2 clustering takes place around the crater. (a) Evolution of the $I(D)/I(G)$ ratio (black squares) and G peak position values (red triangles) as a function of time for a film annealed at $16 \text{ kW}\cdot\text{mm}^{-2}$. The last four spectra (after 10 min resting time) were taken with much lower Raman power densities. (b) ($1.7\cdot 10^7 \text{ J}\cdot\text{mm}^{-2}$) c-AFM image of a laser-annealed crater showing that the highest conduction occurs at the location of the bulge surrounding the hole

To understand more finely the impact of annealing on the crystalline structure of the top carbon layer, we carry out *in-situ* Raman spectroscopy during laser annealing. The spectra are acquired directly from the back-scattered signal from the annealing laser. As each acquisition takes only 15 s, the acquisition time is negligible as compared to the timescale of the experiment (from 300 s to 2,100 s).

Representative results of the *in-situ* study are displayed in Figure 40 (a). It is found that, until 1,080 s, the $I(D)/I(G)$ ratio decreases, while the G peak width tends to increase slightly (Supplementary Information S2): both suggest a decrease of the average crystal size⁴⁰. This suggests that, while the amorphous “A” layer progresses toward the substrate, it also becomes more amorphous than the pristine material.

Graphitization at beam periphery

At 1,080 s, the G peak width undergoes a drastic reduction (Supplementary Information S2) correlated with a drastic increase in the Rayleigh (elastic) scattering (Supplementary Information S3). These drastic changes suggest that full removal of the carbon layer occurs at $\approx 1,080$ s, followed by elastic scattering on the naked titanium film (resulting in the drastic Rayleigh scattering increase) and Raman scattering by the more graphitic carbon on the sides of the hole (resulting in the drastic G peak width decrease). In the meantime, the $I(D)/I(G)$ keeps on decreasing until reaching a minimum at 1,025 s, which is unexpected considering the fact that the graphitic fraction rises drastically at 1,080 s (therefore the $I(D)/I(G)$ ratio should increase). However, we recall that the material is a mixture of the “G” and “A” layers, so this unexpected evolution may come from the complex

interplay of Raman signals coming from “G” and “A”. A way to un-ambiguously understand the structural changes is to study the evolution of the G peak width, which always increases when carbon follows an amorphization trajectory⁴¹.

After the drastic decrease of the G peak width at 1,080 s, its width keeps on decreasing more slowly (Supplementary Figure S2), suggesting a slight re-graphitization process after full removal of the carbon layer.

Because the carbon layer beneath the beam is fully removed, the Raman signal is attributed to the carbon material forming the periphery of the hole, which is exposed to a much lower power density. This result is consistent with the literature on CW laser annealing and thermal annealing, as graphitization²⁵⁻³² is frequently observed for low power density exposure.

Similarly, c-AFM data show that the circular bulge surrounding the crater is much more conductive than the pristine vnC-G film (Figure 40 (b)). It suggests that it is more graphitic than the crater. The topology of the area, forming a bulge, is also consistent with graphitization, as the density of graphitized carbon (2.09 - 2.23 g/cm³) is lower than the density of amorphous carbon. For FCVA deposition at a substrate potential of -300 V⁴² (2.86 - 3.17 g/cm³), it results in a dilation if amorphous carbon is graphitized, as also observed by Teo *et al.*⁴³ This enhanced graphitization compared to the pristine material is attributed to the low power annealing occurring at the periphery of the beam.

Let us remark that this feature is not observable either on the Raman spectra or on TEM images. Regarding to the Raman spectra, the graphitization concerns only the beam periphery which has a small effective cross-section: the corresponding signal is expected to be hidden by the main amorphization event occurring at the beam center.

Regarding to TEM images, no obvious graphitic planes may be observed at locations surrounding the crater (Figure 39 (b)). It suggests that the graphitization remains at the stage of formation of sp² clusters within the amorphous matrix, which may not be observed by TEM. sp² clustering is known to be enough to drastically enhance the electrical conductivity of carbon²⁸.

Amorphization and matter loss by oxidation

While the I(D)/I(G) values and the FWHM values in the Raman spectra are consistent with amorphization at the beam center, the G peak frequency increases significantly (Figure 40 (a)). It is unexpected from the usual framework for Raman spectroscopy interpretation^{40,41}, as it should decrease with amorphization. Other factors than the crystalline content may impact the G peak frequency. However, the temperature rise due to the annealing process cannot explain this unexpected G peak frequency increase as the G peak position is in fact expected to decrease, and not increase, with increasing temperature. The decrease is linear with a slope of -0.013 cm⁻¹/K⁴⁴⁻⁴⁶.

Hole doping is the other factor known to cause an upshift of the G peak. To verify its relevance here, a chemical characterization of the post-annealing material is carried out using energy dispersive spectroscopy (EDX) coupled with the scanning imaging mode of the electron microscope. Figure 41 presents the 2D EDX-STEM chemical maps obtained for the carbon K α -ionization edge (B) and oxygen K α -ionization edge (C) on two craters previously characterized by TEM (Figure 39 (a)).

Oxygen appears to be present in larger quantities at laser-annealed locations. As it is a strong hole dopant for carbon⁴⁷ materials, it explains the G peak position rise observed in the Raman data. The upshift still remains moderate because while the hole doping is increasing, the temperature in the material is simultaneously rising.

Moreover, higher oxygen concentrations are found at the highest power location, either on carbon or on titanium (when carbon is fully removed). The oxidation of titanium explains why no drastic conductivity rise is observed when the c-AFM tip is in direct contact with it at the center of the inner disk (Figure 40 (b)), as titanium oxide is an insulator.

Line scan analyses (Figure 41 (E)) show that the quantity of oxygen atoms increases considerably beneath the surface of laser-annealed carbon (from $\approx 5\%$ to $\approx 20\%$, see data on Figure 41 (E2)), down to ≈ 30 nm from the surface. These depths compare well to the amorphization depths observed by TEM (Figure 39 (b)). Overall, it suggests that the amorphization and matter removal processes are strongly related to oxidation in the annealed carbon layer.

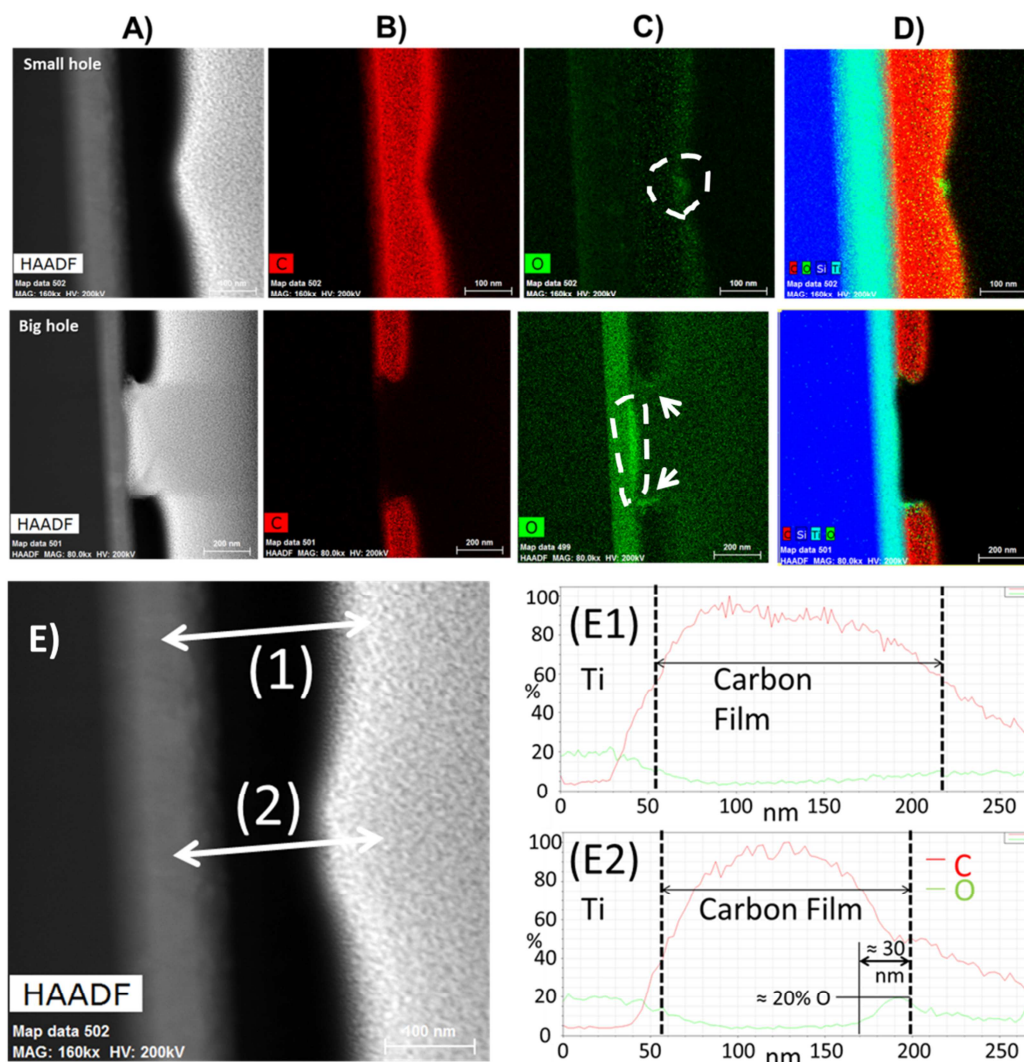


Figure 41 - EDX chemical mappings on two craters to study the oxygen concentration. Top row: $3.9 \cdot 10^6 \cdot \text{mm}^{-2}$. Bottom row: $3.4 \cdot 10^7 \cdot \text{mm}^{-2}$. A) HAADF-STEM micrographs. B) Carbon elemental map. C) Oxygen elemental map. D) Relative map showing the distribution of each element with the sample with carbon in red, silicon in dark blue, titanium in light blue and oxygen in green. E) EDX-STEM line scan analysis on two different positions, far and close to the beam center, for the

spot annealed with an energy density of $3.9 \cdot 10^6 \text{ J} \cdot \text{mm}^{-2}$ (E1) Carbon (in red) and oxygen (in green) concentrations recorded along the white arrow labeled (1). (E2) Carbon (in red) and oxygen (in green) concentrations recorded along the white arrow labeled (2).

To confirm this aspect, we derive an estimate of the temperature rise during annealing by monitoring the upshift of the G peak in the 10 minutes following annealing. While the temperature should decrease dramatically during those 10 minutes, the amount of doping should not change as much. Based on an upshift of 13 cm^{-1} (Figure 40 (a)), the expected temperature drop is $\approx 1,000 \text{ K}$, suggesting that the temperature reached at the end of the annealing process is around $1,300 \text{ K}$. This temperature estimate is confirmed by the fact that the Ti layer is found to be mostly un-damaged (Figure 39 (a)), while the melting temperature of Ti is $\approx 1,941 \text{ K}$.

This temperature range is way below the temperatures required for melting, sputtering or phase explosion of carbon (above $4,000 \text{ K}$ ⁴⁸). Additionally, the remaining matter does not display the major damages usually associated with processes occurring at the melting temperature: the roughness of the area surrounding the crater is below 1 nm .

On the contrary, the temperature is in the right range to enable carbon oxidation³⁸, which is known to cause amorphization by doping (introduction of larger oxygen atoms into sp^2 clusters leading to a loss of short and long range order⁴⁹) and matter loss by formation of gaseous CO and CO_2 ^{37,50}. Hence, we propose oxidation as the main mechanism for amorphization and matter removal. Figure 42 summarizes the phenomena occurring during laser annealing based on this interpretation.

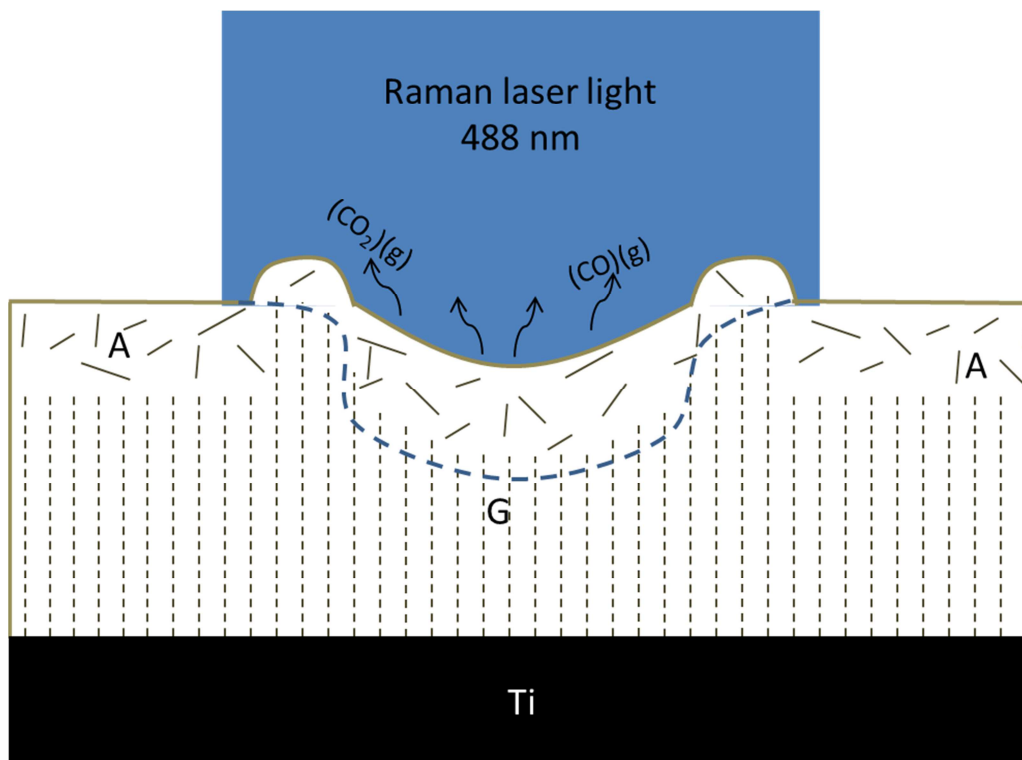


Figure 42 - Schematic cross-section of the carbon thin film, composed of the two layers “A” and “G”, during Raman laser annealing. It shows the matter loss process by oxidation in the center (formation of gas (CO) and CO_2)), the amorphization process by adsorption, the sp^2 clustering leading to a change in density. An arbitrary estimate of the region where most of the Raman information is collected is drawn in dashed blue. It highlights the importance of estimating the penetration depths of the photons when the characterized material is in-homogeneous along its depth

Post-annealing re-graphitization

During our *in-situ* study, we also monitor the Raman signal after 10 minutes of air-cooling (Figure 40 (a)). It is also found that the I(D)/I(G) increases. As, unlike the G peak frequency, it does not depend on the temperature, this increase suggests that re-graphitization takes place during the cooling phase, similarly to what happens during a thermal annealing process^{25-27,29}. Though here, the final material is still more amorphous than the initial material, this may explain why very few studies have been able to observe laser-induced amorphization of carbon thin films.

Application to continuous-wave laser writing

Based on this analysis of the mechanisms occurring during CW laser annealing, we demonstrate the writing capability of a CW laser. Figure 43 shows the acronym “NTU” drawn on a sample by applying a power density of $1.2\text{kW}\cdot\text{mm}^{-2}$ for 1s at each spot. The shape was achieved with a total of 154s exposure by using the line mapping capabilities of the Raman WITec system. This relatively low level of power and duration is expected to provide fine patterns with slightly graphitized and/or oxidized carbon. Figure 43 (b) shows that the surface morphology is only slightly modified by the writing. On the contrary, the electrical conductivity (Figure 43 (c)) is largely enhanced, suggesting the occurrence of sp^2 clustering. Though the time required for the patterning is rather long as compared to techniques based on nanosecond or femtosecond lasers, it can be achieved with relatively low-cost equipment and yields a material with a highly controlled surface state (roughness within the pattern and outside the pattern are both lower than 1 nm).

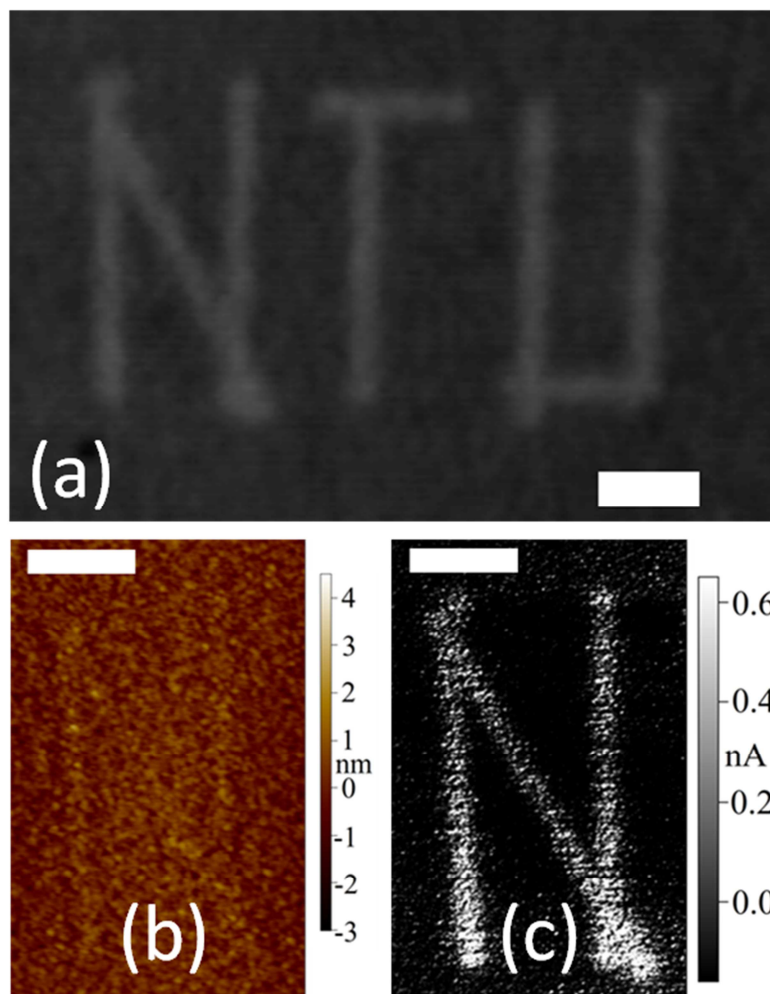


Figure 43 – Example of a pattern drawn on vertical nano-crystalline graphite using a CW 488 nm laser beam. (a) Optical image. (b) AFM image (contact mode) of the “N” showing the height of the features. (c) c-AFM image of the “N” showing the conductivity of the features. Scale bars: 2 μm

Conclusion

We have studied the annealing of vertical nano-crystalline graphite via CW laser and demonstrated the potential of this technique for laser writing. CW laser annealing results in amorphization and matter removal at the center of the beam, with an intensity controlled by the power density and duration of exposure. On the contrary, in the periphery of the beam, where exposure is less intense, sp^2 clustering is detected. Chemical analysis shows the strong presence of oxygen in the post-annealing material, suggesting that amorphization and matter removal are controlled by carbon oxidation. The simultaneous occurrence of amorphization and hole doping, which appears to be characteristic of this process, results in a unique evolution of the Raman spectra, with a decrease of the $I(\text{D})/I(\text{G})$ and an increase of the FWHM of the G peak, but an upshift of the G peak. Altogether, as the matter removal process is quite slow, the resulting annealed matter features very few macroscale defects. As a consequence, CW laser writing on vnC-G results in very clean structures with low surface roughness.

Methods

Film deposition

A ≈ 100 nm thick Ti layer is deposited on a clean Si substrate using electron-beam evaporation. The carbon layer is then deposited onto the Ti layer using a Filtered Cathodic Vacuum Arc⁵¹, with deposition time ≈ 3 min 58 s and vacuum pressure $\approx 5 \cdot 10^{-5}$ Torr. An arc current of 60 A is applied to the graphite target and an accelerating voltage of -300 V DC is applied to the substrate holder. The resulting film is 140 nm thick as evidenced by cross-sectional TEM.

In order to perform XPS analysis, a 10s Ar⁺ sputtering, at 0.2 nm/s etching rate (equivalent rate/Ta₂O₅ standard), was performed to remove adventitious carbon from the top of the sample. The film composition homogeneity in depth was also verified after a second Ar⁺ sputtering: 20s at 0.75 nm/s etching rate conditions (equivalent rate/Ta₂O₅ standard).

Annealing and Raman characterization

WITec 488 nm and 532 nm lasers are used for both annealing and Raman spectroscopy. The laser is fed into the x100 objective of a confocal microscope leading to a ≈ 1 μ m diameter spot at the proper working distance. The power density of the laser is measured with a THORLABS S121C photodiode connected to a THORLABS PM100D display. It is approximated by dividing the power by the area of a disk of 1 μ m diameter. The laser energy spread follows a Gaussian distribution along the radius with maximum power density at the center of the beam (see Supplementary Information S4). The surface of the vnC-G film is laser-annealed for varying durations (from 1 to 35 minutes) and power densities (from ≈ 13 to 28 kW.mm⁻²) at different locations of the film. During laser annealing, Raman spectra are collected every 15 s. Acquisition time varies between 300 and 2,100 s.

Typical Raman spectra of vnC-G consist of three broad peaks centered at ≈ 1060 cm⁻¹, ≈ 1350 cm⁻¹ and ≈ 1580 cm⁻¹ called the T, D and G peak, respectively^{40,52}. The T peak arises due to vibrations of the sp³ bonds, the G peak arises because of photon interactions with stretching vibrations of pairs of sp² C bonds, while the D peak appears in presence of defective graphitic rings. The D to G peak intensity ratio I(D)/I(G) is used to determine the amount of sp² crystalline content forming rings, and the size of sp² crystals can be estimated from it, using either the Tuinstra and Koenig (T-K) equation⁵³ or an equation derived by Ferrari et al.⁴¹, depending on the actual range of crystal sizes.

Using a program written in Scilab⁵⁴, we fit the Raman with three Lorentzian functions for the T (centered at *ca.* 1060 cm⁻¹), D (1350 cm⁻¹) and G (1580 cm⁻¹) peak. To estimate noise-related errors on the Raman spectra, we use the Bootstrap method (Supplementary Information S5): we find standard deviations values on I(D)/I(G) of ≈ 0.04 and $x_G \approx 4$ cm⁻¹. Some representative errors are calculated and the corresponding error bars are displayed on the figures.

Post-annealing characterization

For the TEM/STEM analysis, cross-sections are first prepared on selected regions of the film using a FIB-Scios dual beam microscope. The HR-TEM and STEM-EDX chemical analyses are performed using a Titan-Themis electron microscope operating at 200 kV, equipped with a Cs probe corrector and a SuperX detector. For the STEM-EDX analysis, several 1D EDX spectra are recorded at various locations

of the electron beam focused probe using a convergent angle α of about 25 mrad and a collection angle β of 30 mrad.

To obtain information on the surface morphology, we use an Asylum Research Cypher S AFM in tapping mode. We also characterize the through-film electrical properties in c-AFM mode by applying an electrical potential to the substrate and measuring the electrical current going through the tip and sample. For that method, we use Pt-coated silicon tips.

Acknowledgements

The authors are grateful to Dr. Jackie Vigneron and Mathieu Frégnaux for their kind help conducting the XPS characterization at the Centre d'Études et de Formation en Spectroscopies électroniques de Surfaces (CEFS2) of the Institut Lavoisier Versailles (UMR 8180 CNRS/UVSQ). L.L. acknowledges support from the SINGA scholarship. This work received support from the French state managed by the National Research Agency under the Investments for the Future program under the reference ANR-10-EQPX-50.

Author Contributions

L.L. did most of the experimental work except for the TEM and EDX characterization, which were conducted by I.F. B.L. and I.F. actively worked on the interpretation of the results along with L.L. B.L., C.S.C. and B.K.T. supervised the work.

Additional Information

The authors declare no competing financial interests.

References

- 1 Service, R. F. Is Silicon's Reign Nearing Its End? *Science* **323**, 1000-1002, doi:10.1126/science.323.5917.1000 (2009).
- 2 Geim, A. K. & Novoselov, K. S. The rise of graphene. *Nat Mater* **6**, 183-191 (2007).
- 3 Avouris, P., Chen, Z. & Perebeinos, V. Carbon-based electronics. *Nat Nano* **2**, 605-615 (2007).
- 4 Franklin, A. D. Nanomaterials in transistors: From high-performance to thin-film applications. *Science* **349**, doi:10.1126/science.aab2750 (2015).
- 5 Wagner, C. & Harned, N. EUV lithography: Lithography gets extreme. *Nat Photon* **4**, 24-26 (2010).
- 6 Dan, Y., Lu, Y., Kybert, N. J., Luo, Z. & Johnson, A. T. C. Intrinsic Response of Graphene Vapor Sensors. *Nano Letters* **9**, 1472-1475, doi:10.1021/nl8033637 (2009).
- 7 Cheng, Z. *et al.* Toward Intrinsic Graphene Surfaces: A Systematic Study on Thermal Annealing and Wet-Chemical Treatment of SiO₂-Supported Graphene Devices. *Nano Letters* **11**, 767-771, doi:10.1021/nl103977d (2011).
- 8 Fan, J. *et al.* Investigation of the influence on graphene by using electron-beam and photo-lithography. *Solid State Communications* **151**, 1574-1578, doi:<http://dx.doi.org/10.1016/j.ssc.2011.07.028> (2011).
- 9 Xu, N. *et al.* Electrical properties of textured carbon film formed by pulsed laser annealing. *Diamond and Related Materials* **23**, 135-139 (2012).

- 10 Shakerzadeh, M. *et al.* Field emission enhancement and microstructural changes of carbon films by single pulse laser irradiation. *Carbon* **49**, 1018-1024 (2011).
- 11 Abdelsayed, V. *et al.* Photothermal Deoxygenation of Graphite Oxide with Laser Excitation in Solution and Graphene-Aided Increase in Water Temperature. *The Journal of Physical Chemistry Letters* **1**, 2804-2809, doi:10.1021/jz1011143 (2010).
- 12 Huang, L. *et al.* Pulsed laser assisted reduction of graphene oxide. *Carbon* **49**, 2431-2436, doi:<http://dx.doi.org/10.1016/j.carbon.2011.01.067> (2011).
- 13 Zhang, Y. *et al.* Direct imprinting of microcircuits on graphene oxides film by femtosecond laser reduction. *Nano Today* **5**, 15-20, doi:<http://dx.doi.org/10.1016/j.nantod.2009.12.009> (2010).
- 14 Sokolov, D. A., Rouleau, C. M., Geohegan, D. B. & Orlando, T. M. Excimer laser reduction and patterning of graphite oxide. *Carbon* **53**, 81-89, doi:<http://dx.doi.org/10.1016/j.carbon.2012.10.034> (2013).
- 15 Sokolov, D. A., Shepperd, K. R. & Orlando, T. M. Formation of Graphene Features from Direct Laser-Induced Reduction of Graphite Oxide. *The Journal of Physical Chemistry Letters* **1**, 2633-2636, doi:10.1021/jz100790y (2010).
- 16 Yung, K. C. *et al.* Laser direct patterning of a reduced-graphene oxide transparent circuit on a graphene oxide thin film. *Journal of Applied Physics* **113**, 244903, doi:<http://dx.doi.org/10.1063/1.4812233> (2013).
- 17 Chen, H.-Y., Han, D., Tian, Y., Shao, R. & Wei, S. Mask-free and programmable patterning of graphene by ultrafast laser direct writing. *Chemical Physics* **430**, 13-17, doi:<http://dx.doi.org/10.1016/j.chemphys.2013.12.005> (2014).
- 18 Spanò, S. F., Isgro, G., Russo, P., Fragalà, M. E. & Compagnini, G. Tunable properties of graphene oxide reduced by laser irradiation. *Applied Physics A* **117**, 19-23, doi:10.1007/s00339-014-8508-y (2014).
- 19 Strong, V. *et al.* Patterning and Electronic Tuning of Laser Scribed Graphene for Flexible All-Carbon Devices. *ACS Nano* **6**, 1395-1403, doi:10.1021/nn204200w (2012).
- 20 Rios, C. *et al.* Integrated all-photonic non-volatile multi-level memory. *Nat Photon advance online publication*, doi:<http://www.nature.com/nphoton/journal/vaop/ncurrent/full/nphoton.2015.182.html> (2015).
- 21 Speck, J. S., Steinbeck, J. & Dresselhaus, M. Microstructural studies of laser irradiated graphite surfaces. *Journal of Materials Research* **5**, 980-988 (1990).
- 22 Miotello, A. & Kelly, R. Critical assessment of thermal models for laser sputtering at high fluences. *Applied Physics Letters* **67**, 3535-3537 (1995).
- 23 Miotello, A. & Kelly, R. Laser-induced phase explosion: new physical problems when a condensed phase approaches the thermodynamic critical temperature. *Applied Physics A* **69**, S67-S73 (1999).
- 24 Sundaram, S. & Mazur, E. Inducing and probing non-thermal transitions in semiconductors using femtosecond laser pulses. *Nature materials* **1**, 217-224 (2002).
- 25 Conway, N. M. J. *et al.* Defect and disorder reduction by annealing in hydrogenated tetrahedral amorphous carbon. *Diamond and Related Materials* **9**, 765-770, doi:[http://dx.doi.org/10.1016/S0925-9635\(99\)00271-X](http://dx.doi.org/10.1016/S0925-9635(99)00271-X) (2000).
- 26 Ferrari, A. C. *et al.* Stress reduction and bond stability during thermal annealing of tetrahedral amorphous carbon. *Journal of Applied Physics* **85**, 7191-7197, doi:<http://dx.doi.org/10.1063/1.370531> (1999).
- 27 McCulloch, D. G. *et al.* Mechanisms for the behavior of carbon films during annealing. *Physical Review B* **70**, 085406 (2004).

- 28 Orwa, J. O. *et al.* Thermally induced sp² clustering in tetrahedral amorphous carbon (ta-C) films. *Journal of Applied Physics* **96**, 6286-6297, doi:<http://dx.doi.org/10.1063/1.1808918> (2004).
- 29 Takai, K. *et al.* Structure and electronic properties of a nongraphitic disordered carbon system and its heat-treatment effects. *Physical Review B* **67**, 214202 (2003).
- 30 Lamberton, R. W., Morley, S. M., Maguire, P. D. & McLaughlin, J. A. Monitoring laser induced microstructural changes of thin film hydrogenated amorphous carbon (a-C:H) using Raman spectroscopy. *Thin Solid Films* **333**, 114-125, doi:[http://dx.doi.org/10.1016/S0040-6090\(98\)00848-7](http://dx.doi.org/10.1016/S0040-6090(98)00848-7) (1998).
- 31 Wan, J. Z., Pollak, F. H. & Dorfman, B. F. Micro Raman study of diamondlike atomic-scale composite films modified by continuous wave laser annealing. *Journal of Applied Physics* **81**, 6407-6414, doi:<http://dx.doi.org/10.1063/1.364421> (1997).
- 32 Bowden, M., Gardiner, D. J. & Southall, J. M. Raman analysis of laser annealed amorphous carbon films. *Journal of Applied Physics* **71**, 521-523, doi:<http://dx.doi.org/10.1063/1.350691> (1992).
- 33 Han, G. H. *et al.* Laser Thinning for Monolayer Graphene Formation: Heat Sink and Interference Effect. *ACS Nano* **5**, 263-268, doi:10.1021/nn1026438 (2011).
- 34 Rinzler, A. *et al.* Unraveling nanotubes: field emission from an atomic wire. *SCIENCE-NEW YORK THEN WASHINGTON*-, 1550-1550 (1995).
- 35 Shen, M. *et al.* High-Density Regular Arrays of Nanometer-Scale Rods Formed on Silicon Surfaces via Femtosecond Laser Irradiation in Water. *Nano Letters* **8**, 2087-2091, doi:10.1021/nl080291q (2008).
- 36 Ju, L. *et al.* Graphene plasmonics for tunable terahertz metamaterials. *Nat Nano* **6**, 630-634, doi:<http://www.nature.com/nano/journal/v6/n10/full/nnano.2011.146.html> (2011).
- 37 Liu, L. *et al.* Graphene Oxidation: Thickness-Dependent Etching and Strong Chemical Doping. *Nano Letters* **8**, 1965-1970, doi:10.1021/nl0808684 (2008).
- 38 Du, Z., Sarofim, A. F., Longwell, J. P. & Mims, C. A. Kinetic measurement and modeling of carbon oxidation. *Energy & Fuels* **5**, 214-221, doi:10.1021/ef00025a035 (1991).
- 39 Wang, D.-Y., Chang, C.-L. & Ho, W.-Y. Oxidation behavior of diamond-like carbon films. *Surface and Coatings Technology* **120-121**, 138-144, doi:[http://dx.doi.org/10.1016/S0257-8972\(99\)00350-3](http://dx.doi.org/10.1016/S0257-8972(99)00350-3) (1999).
- 40 Ferrari, A. C. & Robertson, J. Raman spectroscopy of amorphous, nanostructured, diamond like carbon, and nanodiamond. *Philosophical Transactions of the Royal Society of London. Series A: Mathematical, Physical and Engineering Sciences* **362**, 2477-2512 (2004).
- 41 Ferrari, A. C. & Robertson, J. Interpretation of Raman spectra of disordered and amorphous carbon. *Physical review B* **61**, 14095 (2000).
- 42 Ferrari, A. C. *et al.* Density, sp³ fraction, and cross-sectional structure of amorphous carbon films determined by x-ray reflectivity and electron energy-loss spectroscopy. *Physical Review B* **62**, 11089-11103 (2000).
- 43 Teo, E., Bolker, A., Kalish, R. & Saguy, C. Nano-patterning of through-film conductivity in anisotropic amorphous carbon induced using conductive atomic force microscopy. *Carbon* **49**, 2679-2682 (2011).
- 44 Fischbach, D. B. & Couzi, M. Temperature dependence of Raman scattering by disordered carbon materials. *Carbon* **24**, 365-369, doi:[http://dx.doi.org/10.1016/0008-6223\(86\)90239-3](http://dx.doi.org/10.1016/0008-6223(86)90239-3) (1986).

- 45 Huang, F. *et al.* Temperature dependence of the Raman spectra of carbon nanotubes. *Journal of Applied Physics* **84**, 4022-4024, doi:doi:<http://dx.doi.org/10.1063/1.368585> (1998).
- 46 Li, H. D. *et al.* Temperature dependence of the Raman spectra of single-wall carbon nanotubes. *Applied Physics Letters* **76**, 2053-2055, doi:doi:<http://dx.doi.org/10.1063/1.126252> (2000).
- 47 Ryu, S. *et al.* Atmospheric Oxygen Binding and Hole Doping in Deformed Graphene on a SiO₂ Substrate. *Nano Letters* **10**, 4944-4951, doi:10.1021/nl1029607 (2010).
- 48 Savvatimskiy, A. Measurements of the melting point of graphite and the properties of liquid carbon (a review for 1963-2003). *Carbon* **43**, 1115-1142 (2005).
- 49 Osswald, S., Havel, M. & Gogotsi, Y. Monitoring oxidation of multiwalled carbon nanotubes by Raman spectroscopy. *Journal of Raman Spectroscopy* **38**, 728-736, doi:10.1002/jrs.1686 (2007).
- 50 Li, C. & Brown, T. C. Carbon oxidation kinetics from evolved carbon oxide analysis during temperature-programmed oxidation. *Carbon* **39**, 725-732, doi:[http://dx.doi.org/10.1016/S0008-6223\(00\)00189-5](http://dx.doi.org/10.1016/S0008-6223(00)00189-5) (2001).
- 51 Tay, B. K., Zhao, Z. W. & Chua, D. H. C. Review of metal oxide films deposited by filtered cathodic vacuum arc technique. *Materials Science and Engineering R Reports* **52**, 1-48, doi:<http://dx.doi.org/10.1016/j.mser.2006.04.003> (2006).
- 52 Shakerzadeh, M. *et al.* Re ordering Chaotic Carbon: Origins and Application of Textured Carbon. *Advanced Materials* **24**, 4112-4123 (2012).
- 53 Tuinstra, F. & Koenig, J. L. Raman Spectrum of Graphite. *The Journal of Chemical Physics* **53**, 1126-1130, doi:doi:<http://dx.doi.org/10.1063/1.1674108> (1970).
- 54 Scilab : Logiciel open source gratuit de calcul numérique, (Windows 7, Version 5.5.0). <http://www.scilab.org> (2014).